SPATIAL REGULATION OF CELL DIVISION

BY THE NUCLEOID OCCLUSION PROTEIN SLMA IN ESCHERICHIA COLI

BY

Shishen Du

Submitted to the graduate degree program in Microbiology, Molecular Genetics and Immunology and the Graduate Faculty of the University of Kansas in partial fulfillment of the requirement for the degree of Doctor of Philosophy.

Dissertation Committee:

Joe Lutkenhaus, Ph.D., Chairman

Indranil Biswas, Ph.D.

Wolfram Zückert, Ph.D.

Thomas Yankee, Ph.D.

Liskin Swint-Kruse, Ph.D

Date defended: December 20th, 2013

The Dissertation Committee for Shishen Du

Certifies that this is the approved version of the following dissertation:

SPATIAL REGULATION OF CELL DIVISION

BY THE NUCLEOID OCCLUSION PROTEIN SLMA IN ESCHERICHIA COLI

Joe Lutkenhaus, Ph.D., Chairperson

Date approved: December 20th, 2013

Abstract

Spatial regulation of cell division in bacteria occurs at the stage of Z ring formation, a cytoskeletal element that bacterial cells employ for assembly of the cell division machinery. In the model organism *Escherichia coli*, spatial regulation of Z ring formation is dependent on two partially redundant negative regulatory systems, the Min system, which prevents Z ring formation near the cell poles, and Nucleoid Occlusion (NO), which prevents Z ring formation over the nucleoid. The effector of the Min system, MinC, prevents assembly of the Z ring in its vicinity by antagonizing FtsZ polymerization and membrane attachment, the two essential activities required for FtsZ to assemble into the Z ring. Previous studies have shown that the effector of the NO system, SlmA, is a DNA associated FtsZ inhibitor that is activated by binding to a SlmA binding sequence (SBS). The SlmA binding site on FtsZ has not been identified and how SBS bound SlmA prevents FtsZ assembly into the Z ring in its vicinity is controversial. In this study, we show that SBS bound SlmA acts in a similar manner to MinC, antagonizing FtsZ polymerization and membrane attachment.

In the first part of this thesis, two FtsZ mutants were isolated that are resistant to de-localized SBS bound SlmA, which has been shown to block Z ring formation throughout the cell and cause cell death. By characterizing these two FtsZ mutants, we found that SBS activated SlmA antagonizes FtsZ polymerization and the efficacy of SlmA to antagonize FtsZ polymerization depends upon the length of the DNA molecule containing the SBS. The longer the bound SBS DNA molecule (14-30 bp), the more efficiently SlmA disassembles FtsZ polymers; SlmA bound to the shorter SBS DNA molecule is missing several DNA contacts likely explaining the weaker impact on FtsZ polymerization. Even though the isolated *ftsZ* mutations conferred resistance to the action of SlmA *in vivo* and *in vitro*, they did not disrupt FtsZ-SlmA binding. One of the *ftsZ* mutations increased the bundling of FtsZ polymers *in vitro*, indicating that it provides resistance to SlmA by increasing FtsZ lateral interactions. The other *ftsZ* mutation alters a residue in the H7 helix of FtsZ. This helix mediates the conformational change between

the two sub-domains of FtsZ during assembly suggesting that SBS bound SlmA antagonizes FtsZ polymerization by reversing this conformational change and that the mutation is resistant to this affect.

In the second part of the project, we found that SlmA binds to FtsZ largely through the conserved C-terminal tail of FtsZ, a region critical for FtsZ-ZipA and FtsZ-FtsA interactions and therefore attachment of FtsZ filaments to the membrane. More importantly, we found that SlmA requires the presence of the conserved C-terminal tail of FtsZ to disassemble FtsZ polymers. As the conserved C-terminal tail of FtsZ is not required for FtsZ polymerization, this unexpected finding suggests that SlmA binding to the FtsZ tail allows it to bind to a secondary site in the globular domain of FtsZ to antagonize FtsZ polymerization. This two binding site model is consistent with the observation that SlmA forms a sandwich like complex with FtsZ truncations lacking the conserved C-terminal tail and our finding that *ftsZ* mutations in the globular domain of FtsZ confer resistance to the action of SlmA. Collectively, our results suggest that SlmA antagonizes Z ring formation in its vicinity in at least two ways: first, SBS bound SlmA competes with ZipA and FtsA for the conserved C-terminal tail of FtsZ preventing membrane attachment of FtsZ filaments; and, second, the binding to the conserved C-terminal tail of FtsZ brings the SBS-SlmA complexes close to FtsZ filaments such that SlmA can actively disassemble FtsZ polymers by reversing the conformational change occurring upon FtsZ assembly.

ZipA and FtsA promote Z ring assembly by tethering FtsZ filaments to the membrane through the conserved FtsZ tail. In contrast, MinC and SlmA promote Z ring disassembly by binding the tail because they also have an antagonistic effect on FtsZ polymers. Competition for the FtsZ tail between Z ring promoting factors and Z ring disassembling factors may be an important way to regulate Z ring formation. The remarkable similarity between MinC and SlmA also indicates that antagonizing FtsZ polymerization and FtsZ filaments membrane attachment simultaneously may be a universal mechanism for FtsZ spatial regulators to antagonize Z ring formation in their vicinity.

Acknowledgements

I would like to take this opportunity to thank my mentor Dr. Joe Lutkenhaus for his guidance and continuous support of my research all these years. His knowledge and scientific way of thinking are invaluable for my studies. Furthermore, his mentoring style makes it a very pleasant experience to work in the lab. I would also like to thank him for his patience with the progress of completing this study and his encouragement to test various hypotheses.

Thanks also go to the previous and current member of the Lutkenhaus lab for their help and support. I am deeply grateful to Dr. Bang Shen and Dr. Sebastian Pichoff, who teach me most of the techniques and always have great suggestions. Dr. Christina Hester and Dr. Kyung-Tae Park offered valuable advices and help throughout this study.

Drs. Indranil Biswas, Wolfram Zueckert, Thomas Yankee and Liskin Swint-Kruse also deserve gratitude for serving on my thesis committee and insightful advices. I am also grateful to Dr. Jianming Qiu for this help in getting me into the graduate school of KU Medical Center.

I would like to thank Dr. Thomas Bernhardt for sending me the SlmA anti-serum and Dr. William Margolin for sending me the *parC*^{ts} strain WM1033. Without their help, I would not be able to finish the study.

Lastly, I would like to extend my appreciation to my parents, my wife and my son for their support and encouragement throughout this work.

Table of Contents

List of figures

List of tables

Abbreviations

DNA: deoxyribonucleic acid

GFP: green fluorescent protein

IPTG: isopropyl-β-thiogalactopyranoside

LB: Luria-Bertani medium

OD: optical density

GDP: guanosine diphosphate

GTP: guanosine triphosphate

GMPCPP: guanosine-5'-[(alpha, beta)-methyleno] triphosphate

HEPES: N-(2-hydroxymethyl) piperazine-N'-(2-ethanesulfonic acid)

PAGE: polyacrylamide gel electrophoresis

SDS: sodium dodecyl sulfate

SBS: SlmA binding sequence

NO: Nucleoid Occlusion

PEP-K: mono-Potassium phosphoenolpyruvate

NADH: nicotinamide adenine dinucleotide

PK/LDH: pyruvate kinase/lactic dehydrogenase

Chapter I: Introduction

Bacterial cell division

One of the three statements of the cell theory developed by Theodor Schwann, Matthias Jakob Schleiden and Rudolf Virchow in 1893 is that "New cells are created by old cells dividing into two". This holds true for all living cells from the three domains of life, Archaea, Bacteria and Eukarya, even though cells do not always divide in the same way. Eukaryotic cells divide by processes known as "mitosis" or "meiosis", while archaeal and bacterial cells usually divide through a process called "binary fission", in which a septum is placed at a position called the division site in a cell to separate it into two daughter cells (Fig. 1). Central to this process is that each daughter cell receives an intact copy of the genome and other necessary components required for viability and functionality. Thus, this simple process has to be well coordinated with cell growth, chromosome duplication and segregation to avoid aberrant division. Furthermore, to separate the two daughter cells safely, a concerted action from the cytoplasm, cytoplasmic membrane to the peptidoglycan layer (as well as the outer membrane in the case of Gram-negative bacteria) is required.

Studies of bacterial cell division date back to the 1960s when a collection of *Escherichia coli* mutants were found to be specifically affected in the process of septation. These mutants are thermosensitive and form septum-less long filaments with normally distributed nucleoids when shifted to the non-permissive temperature (Hirota et al., 1968; Van De Putte et al., 1964). Characterization of these mutants and similar mutants isolated later led to the identification of a number of genes (designated *fts*, filamentation temperature sensitive) that are essential for bacterial cell division. However, due to their small size and lack of suitable genetic and imaging tools, it was not clear what roles these genes play in the process of division. For the same reason, division machinery analogous to the contractile ring used by eukaryotic cells was not observed during division in bacteria. Therefore, the cell division process was almost a black box until the 1980s when several important discoveries were made: 1) the *ftsZ* gene was

Fig. 1. Cell cycle and cell division in bacteria. A new born cell starts a new round of the cell division cycle by increasing its size and replicating and segregating the chromosome. Once chromosome segregation has reached about two third of the chromosome, the cells initiate division by forming the Z ring underneath the cytoplasmic membrane. The Z ring functions as a scaffold for the assembly of the complete cell division machinery (the divisome), which consists of many proteins involved in cell wall remodeling and membrane invagination. Once assembly of the divisome is completed, constriction starts generating two daughter cells, each with a copy of the chromosome.

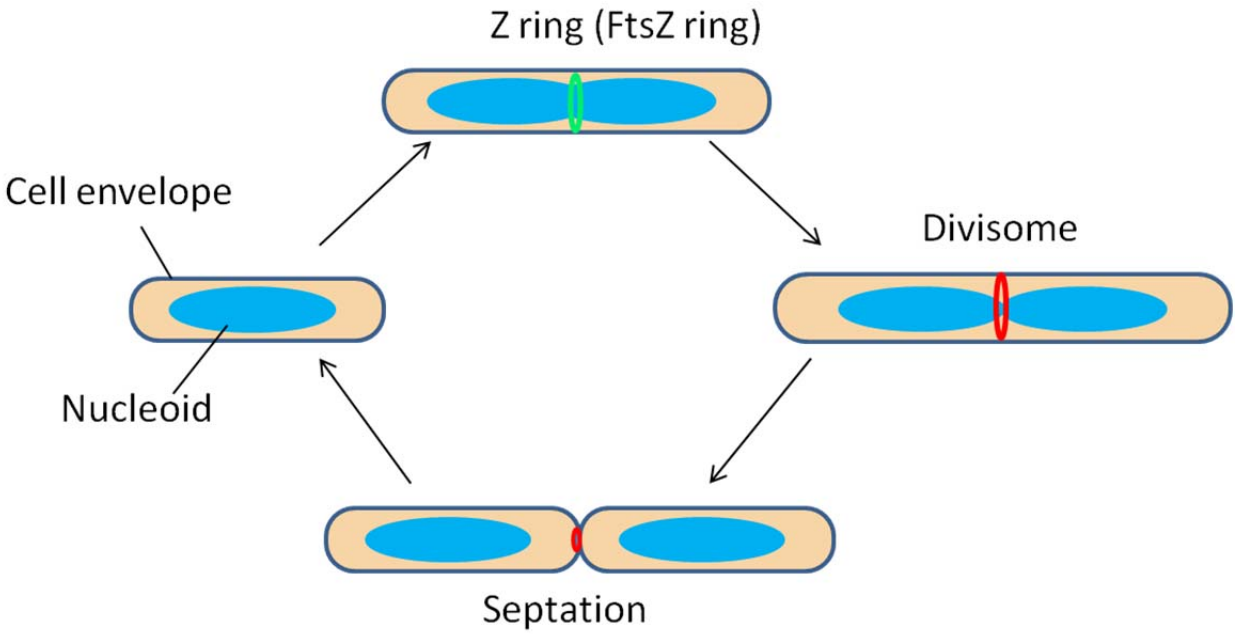
Z ring (FtsZ ring)
Cell envelope
Divisome
Nucleoid
Septation

identified and shown to be required for the earliest known step of septation (Begg and Donachie, 1985; Lutkenhaus et al., 1980; Taschner et al., 1988); 2) the level of FtsZ dictates the division frequency (Bi and Lutkenhaus, 1990b; Ward and Lutkenhaus, 1985); and 3) FtsZ is likely to be the target of two division inhibitors (Bi and Lutkenhaus, 1990a, c; de Boer et al., 1990; Lutkenhaus et al., 1986; Lutkenhaus, 1983; Maguin et al., 1986), SulA, which is induced in response to DNA damage (Huisman and D'Ari, 1981), and MinCD, which prevents cell division at the cell poles (de Boer et al., 1989). Employment of immuno-electron microscopy to study FtsZ localization led to the hallmark discovery that FtsZ self-assembles into a ring like structure, the Z ring, at the division site in *E. coli* (Bi and Lutkenhaus, 1991). Later analysis of FtsZ localization in other microorganisms, such as *Bacillus subtilis and Caulobacter cresentus* revealed the presence of the Z ring (Quardokus et al., 1996; Wang and Lutkenhaus, 1993), suggesting that it may be in all bacterial species. Studies of division inhibitors SulA, MinCD as well as others also revealed that most division regulatory pathways target FtsZ and regulate cell division at the stage of Z ring formation (Bernhardt and de Boer, 2005; Bi and Lutkenhaus, 1993; Thanbichler and Shapiro, 2006). The discovery of the Z ring also made it possible to define whether a protein is a component of the division machinery or a regulator of division. This discovery also led to the realization that bacteria, like larger eukaryotic cells, have dynamic internal structures to organize cellular events in time and space.

Studies of bacterial division have been primarily carried out in *Escherichia coli*, *Bacillus subtilis* and *Caulobacter cresentus*, but recently have been extended to many other bacteria. The picture emerging from these investigations is that the division process is highly organized and can be artificially divided into at least three steps (de Boer, 2010; Lutkenhaus et al., 2012)(Fig. 2). First, formation of the Z ring occurs underneath the cytoplasmic membrane through the aid of membrane-associated proteins. Second, the remaining cell division proteins are recruited to the Z ring to form the complete cell division machinery or divisome. Third, the divisome is activated to form the septum to separate the two daughter cells. A comparison of these bacteria has revealed the basic components of the division machinery that

are essential for viability and conserved in bacteria. However, except for these core components, the other parts of the divisome vary among bacteria, although in most cases they are functionally analogous.

In *E. coli*, more than two dozen proteins have been identified to be components of the divisome and the list is still growing. Dependency studies indicate that these division proteins localize to the Z ring in a linear hierarchy, but several of these proteins have been shown to exist in complexes even when they are not associated with the Z ring (Goehring et al., 2005; Lutkenhaus et al., 2012). Even though we do not understand the exact function of most of these proteins, they could participate in any one of the three steps mentioned above. Formation of the Z ring requires the presence of either one of the two membrane tethering proteins, ZipA and FtsA (Pichoff and Lutkenhaus, 2002). Both of them bind to the conserved C-terminal tail of FtsZ and thus bring the FtsZ polymers to the membrane (Din et al., 1998; Haney et al., 2001; Liu et al., 1999; Ma and Margolin, 1999; Mosyak et al., 2000; Szwedziak et al., 2012; Wang et al., 1997). Either one of them is sufficient for Z ring formation, but Z rings formed with only ZipA or FtsA are not capable of recruiting downstream cell division proteins (Hale and de Boer, 2002; Pichoff and Lutkenhaus, 2002), suggesting that they are also important for the second step.

During the first step, a number of FtsZ associated proteins (Zaps), including ZapA, ZapC and ZapD, are also recruited to the Z ring (Durand-Heredia et al., 2012; Durand-Heredia et al., 2011; Gueiros-Filho and Losick, 2002; Hale et al., 2011). These proteins are not essential for Z ring formation or later steps, but deletion of any one of them can lead to formation of "looser" Z rings and a delay in cell division. Deletion of two or all of the Zaps results in more dramatic delay in cell division, suggesting they work synergistically to promote the integrity of the Z ring. *In vitro* studies showed that all these Zap proteins can bundle or crosslink FtsZ proto-filaments, consistent with the "looser" Z ring phenotype observed in the deletion mutants. The bacterial actin homolog MreB, which is important for bacterial cell elongation and cell shape maintenance, is also recruited to the Z ring through a direct interaction with FtsZ (Fenton and Gerdes, 2013), but its role in division is not clear. It is proposed that the MreB-FtsZ

Fig. 2. Assembly of the Z ring and maturation of the divisome in *E. coli*. FtsZ first polymerizes into filaments (FtsZ [n]) which are tethered to the membrane by ZipA and FtsA, which leads to the formation of the Z ring. Although not absolutely required, several FtsZ interacting proteins named ZapA, ZapC and ZapD are recruited to the Z ring to promote the integrity of the Z ring (ZapB localizes to the Z ring through interaction with ZapA). The bacterial actin homolog, MreB, which organizes lateral cell wall biosynthesis, is also recruited to the Z ring by direct interaction with FtsZ. After an apparent lag, the other Fts proteins, including FtsEX, FtsK, FtsQLB, FtsW, FtsI and FtsN localize to the Z ring in a linear order. Arrival of FtsN triggers the start of constriction of the divisome, leading to synthesis of the septal peptidoglycan by PBP1b, its activator LpoB, and FtsI. Separation of the two daughter cells requires another set of proteins that split the septal cross wall and coordinate the invagination of the two membranes with cell wall synthesis. These include AmiB and AmiC, their activators EnvC and NlpD, respectively and the Tol-Pal complex.

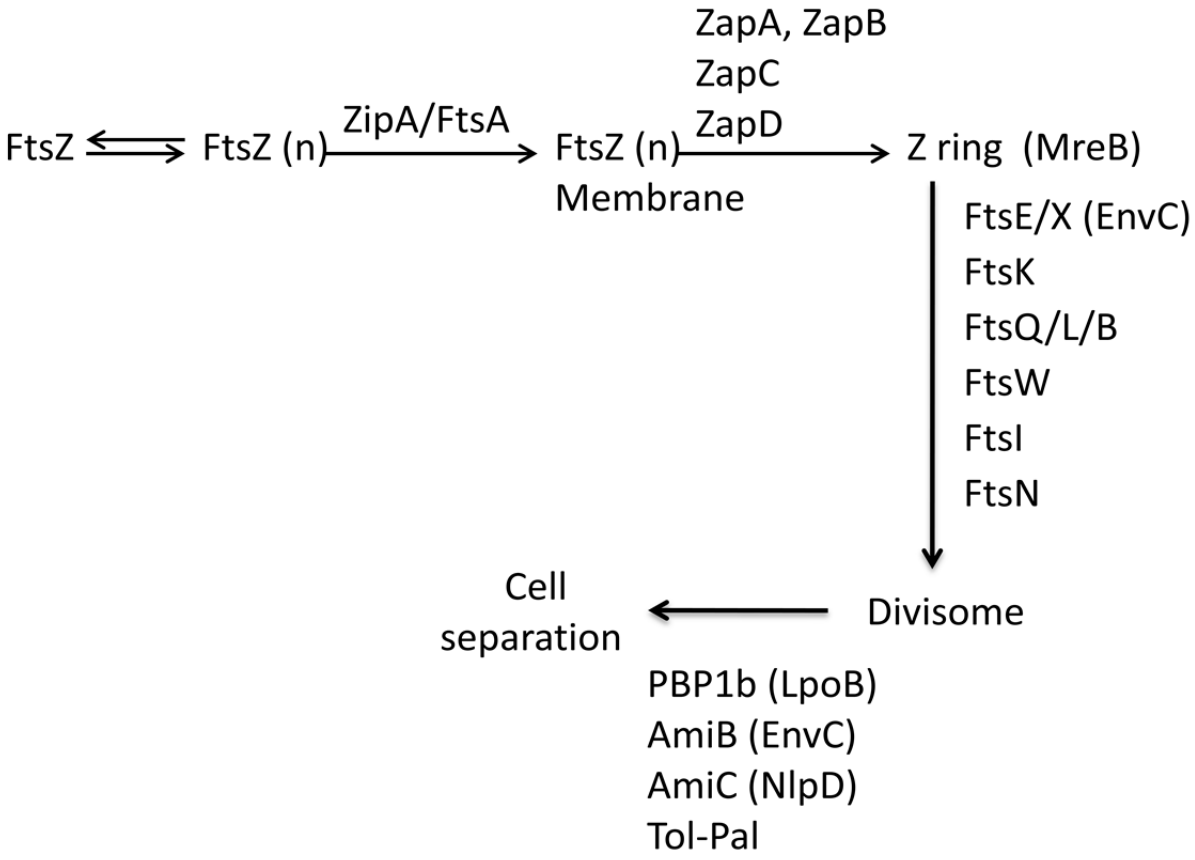
ZapA, ZapB
ZapC
ZapD
FtsZ
FtsZ (n)
ZipA/FtsA
FtsZ (n)
Membrane
Z ring (MreB)
FtsE/X (EnvC)
FtsK
FtsQ/L/B
FtsW
FtsI
FtsN
Divisome
Cell
separation
PBP1b (LpoB)
AmiB (EnvC)
AmiC (NlpD)
Tol-Pal

interaction transfers the cell-wall biosynthetic enzymes from the lateral wall to the divisome (Fenton and Gerdes, 2013), allowing cells to synthesize the septum. Even though MreB localizes early, the septum is not synthesized until the completion of the divisome assembly, suggesting the existence of temporal regulation of the transfer.

The second step occurs with an apparent lag after Z ring formation. The reason for this delay is not clear, but presumably allows more time for the cell to elongate/enlarge and segregate the chromosome before the last step. Also not clear is how the late cell division proteins are recruited to the Z ring, FtsA seems to play an important role as it interacts with many of the late division proteins and many *ftsA* alleles allow deletion of *zipA* (Busiek et al., 2012; Corbin et al., 2004; Geissler et al., 2003; Karimova et al., 2005; Pichoff et al., 2012), which is normally essential for recruitment of these proteins. Proteins recruited to the Z ring in this step include FtsEX, FtsK, FtsQLB, FtsW, FtsI and FtsN (Addinall et al., 1997; Buddelmeijer et al., 1998; Buddelmeijer and Beckwith, 2004; Schmidt et al., 2004; Wang et al., 1998; Wang and Lutkenhaus, 1998).

FtsE and FtsX constitute an ATP-binding cassette transporter: FtsX encodes the membrane component and FtsE encodes the ATPase(Schmidt et al., 2004). In medium of low osmotic strength, such as LB without NaCl, cells lacking FtsEX form smooth filaments with normally distributed Z rings which lack FtsK and other late cell division proteins(Schmidt et al., 2004). However, this division defect can be easily rescued by growing the cells at high osmotic conditions or overproduction of other division proteins (FtsZ, FtsN, or FtsP) (Reddy, 2007) such that the function of FtsEX in division has been obscure for a long time. Recently, it was shown that FtsEX recruits EnvC, an activator of a septal peptidoglycan amidase (AmiB), to the Z ring and regulates the amidase activation via EnvC and requiring ATP hydrolysis by FtsE (Yang et al., 2011). Thus, FtsEX couples amidase activity in the periplasm with the contraction of the Z ring in the cytoplasm.

FtsK is DNA translocase with a membrane domain containing four transmembrane spanning segments fused to the DNA translocase domain by a long linker (Begg et al., 1995). When located at the septum, this protein is able to translocate DNA away from the septum due to specific DNA sequence (KOPS) distributed throughout the chromosome, which give directionality to the movement of the DNA (Bigot et al., 2005). However, this DNA translocase activity is not necessary for division as the four transmembrane segments are able to complement the division defect of *ftsK* knock out cells (Wang and Lutkenhaus, 1998). An apparent function of FtsK is the recruitment of downstream division proteins, but it can also be bypassed under certain conditions (Chen and Beckwith, 2001; Geissler and Margolin, 2005), raising a question about its exact function in division.

FtsQ, FtsL and FtsB are membrane proteins with a single transmembrane segment and a large periplasmic domain (Goehring et al., 2005). They localize to the Z ring simultaneously and form a complex even when they are not at the Z ring (Goehring et al., 2005). None of the three has known enzymactic activity, but they are believed to function as a link between the Z ring and the peptidoglycan biosynthetic machinery.

FtsW is an essential division protein with 10 predicted transmembrane segments and belongs to the SEADS (shape, elongation, division and sporulation) family. Recently, FtsW has been shown to be a transporter of the lipid-linked peptidoglycan precursors (Lipid II flippase) (Mohammadi et al., 2011). As FtsW localizes to the division site, it may be dedicated for Lipid II flipping during septation, while its orthologue RodA may be dedicated for Lipid II transport across the membrane during cell elongation (Mohammadi et al., 2011).

FtsI (PBP3) is a peptidoglycan transpeptidase dedicated for septation and it is believed that its activity is stimulated by presence of FtsN (Gerding et al., 2009; Goehring et al., 2005), the last essential division protein to arrive at the ring and a trigger for septation. FtsN is a bitopic protein with a short cytoplasmic region connected to a larger periplasmic region by a single transmembrane domain (Dai et

al., 1993). The most conserved region of FtsN lies at the C-terminus (SPOR domain) and binds a form of peptidoglycan which is only present at the septum (Gerding et al., 2009). However, this domain is not essential, and a short fragment in the periplasm contains the essential function in division. Even though not essential, the cytoplasmic domain and transmembrane segment of FtsN increase the efficiency of the essential domain to complement (Gerding et al., 2009), presumably due to the interaction of the cytoplasmic domain with FtsA. FtsN is also required for the recruitment of a number of downstream proteins involved in cell wall biosynthesis whose functions are partially redundant (Lutkenhaus et al., 2012). It is unlikely that this recruitment is dependent on direct interaction with FtsN, but may rely on a specific form of peptidoglycan synthesized after FtsN triggers septation.

Upon arrival of FtsN, the third step is triggered leading to the synthesis of the septum and splitting of the two daughter cells. This step is under complex topological control so that cell wall degrading enzymes work in concert with cell wall synthesizing enzymes. FtsN signals the completion of divisiome assembly and activates FtsI. Along with PBP1b, FtsI starts to synthesize septal specific peptidoglycan which in turn leads to recruitment of additional proteins that metabolize the peptidoglycan and invaginate the outer membrane (Lutkenhaus et al., 2012). *In E. coli*, three additional proteins localize to the septum by a conserved SPOR domain which recognizes septal specific peptidoglycan (Gerding et al., 2009). The localization of the SPOR domain containing proteins at the septum depends on the essential domain of FtsN as well as peptidoglycan amidase activity, suggesting that this septal specific peptidoglycan consists of glycan strands that have been metabolized by the amidases (Gerding et al., 2009).

Amidases are peptidoglycan hydrolyases that remove the stem peptide from the glycan strand and thus break cross-links in the peptideglycan network. *E. coli* contains three amidases, AmiA, AmiB and AmiC, all of which contain a LytC type amidase domains and are important for cell separation (Uehara and Bernhardt, 2011). The working mechanism of these amidases has been revealed recently by elegant

genetic and biochemical studies. In the absence of an activator, the active site of these cell separation amidases is occluded by a conserved alpha helix thus suppressing their activity by an autoinhibition mechanism (Yang et al., 2012). Binding of a cognate activator removes the inhibitory alpha helix from the active site such that the active site is exposed and allowed to bind to peptidoglycan (Yang et al., 2012). The activity of these amidases overlap and the presence of any one of them ensures survival, however, they normally execute their functions in different locations. AmiB and AmiC primarily localize to the septum while AmiA localizes throughout the cell (Peters et al., 2011). To separate the two daughter cells at the right time, the activation of these amidases is coupled with the assembly of the cytokinetic ring. As mentioned above, the FtsEX ABC transporter and EnvC localize to the Z ring early, but they only switch on AmiB after FtsN has triggered septation (Yang et al., 2011). AmiC and its cognate activator NlpD both require FtsN for septa localization (Uehara and Bernhardt, 2011). Even though AmiA does not localize to the septum, it can also be stimulated to split septal peptidoglycan by the localized EnvC in the absence of AmiB and AmiC. Separation of the two daughter cells also requires a concerted invagination of the outer membrane during septal peptidoglycan synthesis. The trans-envelope Tol-Pal complex has been shown to localize to the septum and is believed to play an important role in the timely and efficient constriction of the outer membrane (Gerding et al., 2007). Lastly, the invaginated membrane has to be fused at the end of constriction. So far, no protein has been shown to execute such a function, but the transmembrane segments of FtsK are believed to play a role (Fleming et al., 2010). It is very likely the transmembrane segments of the other division proteins also participate in membrane fusion.

In *E. coli* and *B. subtilis*, new Z rings start to assemble at the quarter positions to initiate another division cycle before the completion of the ongoing constrictions under some conditions. However, in *C. cresentus* FtsZ, and probably also other components of the divisome, are retained at the new pole until the arrivial of the spatial regulator MipZ (Quardokus et al., 1996; Thanbichler and Shapiro, 2006), which dislodges it and drives it to midcell. In other slow growing bacteria like *Agrobacterium* the components of the divisome are retained at the new pole to direct the growth of the cell until signals arise to initiate

another division cycle (Zupan et al., 2013). Despite these differences, once the Z ring assembles, the following steps are pretty much the same as in *E. coli*, and the principles underlying the maturation of the divisome and septation can be applied to any bacteria.

FtsZ

FtsZ is required for division in most bacteria, chloroplasts in plant cells and many archaea. It assembles into the Z ring under the membrane at the center of the cell (sometimes asymmetrically for certain bacteria) and then functions as a scaffold for the assembly of the divisome (Erickson et al., 2010). FtsZ is also believed to be the force generator during septation. Because of its importance in division, FtsZ has been studied extensively and many interesting properties of FtsZ have been revealed.

One of the most astounding findings about FtsZ is that it is similar to eukaryotic tubulin in many ways despite limited sequence identity (Lowe and Amos, 1998; Nogales et al., 1998a; Nogales et al., 1998b) (Fig. 3A). Overall the amino acid sequence identity between FtsZ and tubulin is less than 10%, but motifs required for GTP binding and hydrolysis are highly conserved (Erickson, 2007). Both of them contain the FtsZ/tubulin signature loop (GGGTG[S/T]G), which is required for GTP binding, and the synergy loop (NxDxx[D/E]), which is required for GTP hydrolysis. Furthermore, FtsZ and tubulin hydrolyze GTP using a similar mechanism. GTP is bound on one end of an FtsZ/tubulin (the + end) subunit with the aid of the FtsZ/tubulin signature loop. When FtsZ/tubulin assembles into filaments, the GTPase catalytic site is formed with the addition of the synergy loop from the incoming subunit (Michie and Lowe, 2006). Thus, the GTPase activity of FtsZ/tubulin is coupled to polymerization. In addition, the structures of the monomer and filament of FtsZ are similar to those of tubulin (Elsen et al., 2012; Li et al., 2013; Lowe and Amos, 1998; Matsui et al., 2012; Nogales et al., 1998b) , suggesting that they are evolutionarily related.

FtsZ from any bacterial species or from chloroplast and archaea has the same arrangement of domains: a conserved globular domain and a conserved C-terminal tail connected by a linker region

(Erickson et al., 2010) (Fig. 3B). The globular domain of FtsZ is responsible for FtsZ polymerization and is separated by the H7 helix into two subdomains, which can be expressed separately and fold independently (Oliva et al., 2004; Osawa and Erickson, 2005). The N terminal sub-domain contains the GTP binding site and the entire lower side of the interface of the longitudinal proto-filament bond. The C-terminal sub-domain contains the synergy loop (T7 loop) and the upper side of the interface between subunits in the filaments. The two sub-domains undergo prominent rotation as FtsZ assembles into filaments. It is believed that the H7 helix transmits the conformational change from the N terminal to the C terminal sub-domain when assembly or disassembly occurs (Elsen et al., 2012).

The linker shows no sequence conservation and is generally considered to be intrinsically disordered. Two recent studies confirmed this and found that the linker of *E. coli* FtsZ and *B. subtilis* FtsZ could be replaced by other sequences of similar length as long as the inserted sequence is intrinsically disordered (Buske and Levin, 2013; Gardner et al., 2013). The length of the linker is normally about 50 amino acids for most bacterial FtsZs, but some have an extraordinary long linker, for example, the linker region of *C. cresentus* FtsZ is about 179 amino acids. In E. coli and B. subtilis, the linker has to be within a certain length to complement (Buske and Levin, 2013; Gardner et al., 2013), but the reason for this requirement is not clear. Evidence shows that the linker is not necessary for polymerization *in vitro* or Z ring formation *in vivo*. Thus, it has been proposed that the linker functions as a stiff entropic spring linking the proto-filaments to the membrane while simultaneously allowing FtsZ to interact with itself and modulatory proteins (Buske and Levin, 2013; Gardner et al., 2013).

Similar to the linker, the conserved C-terminal tail of FtsZ is not necessary for polymerization in *vitro* (Wang et al., 1997), but it is absolutely required for Z ring formation *in vivo* because it is the primary binding site for the membrane anchors of FtsZ (ZipA and FtsA in *E. coli,* FtsA, SepF and EzrA in *B. subtilis*) (Krol et al., 2012; Mosyak et al., 2000; Singh et al., 2007, 2008; Szwedziak et al., 2012). Several other division proteins also bind to the tail of FtsZ, such as ZapD, MinC and ClpX

Fig. 3. A) The structure of FtsZ and the α/β tubulin heterodimer. The signature loop (GGGTG [S/T] G) and the synergy loop (NxDxx [D/E]) shared by FtsZ (PDB #2VAW) and α/β tubulin (PDB # 1 TUB) are colored in blue and magenta, respectively. The signature loop is required for GTP (colored cyan) binding and the synergy loop is required for GTP hydrolysis. B) Domain arrangement of FtsZ (PDB #2VAW) with linker region and the conserved C terminal tail. GDP is colored red, the N terminal and C terminal sub-domains of the globular domain of FtsZ are colored green and cyan respectively. The H7 helix connecting the two sub-domains is colored blue and the instrinsic disordered linker is colored magenta. The C terminal tail of FtsZ that binds to many FtsZ interacting proteins is an α-helix at the end of the linker region.

A.

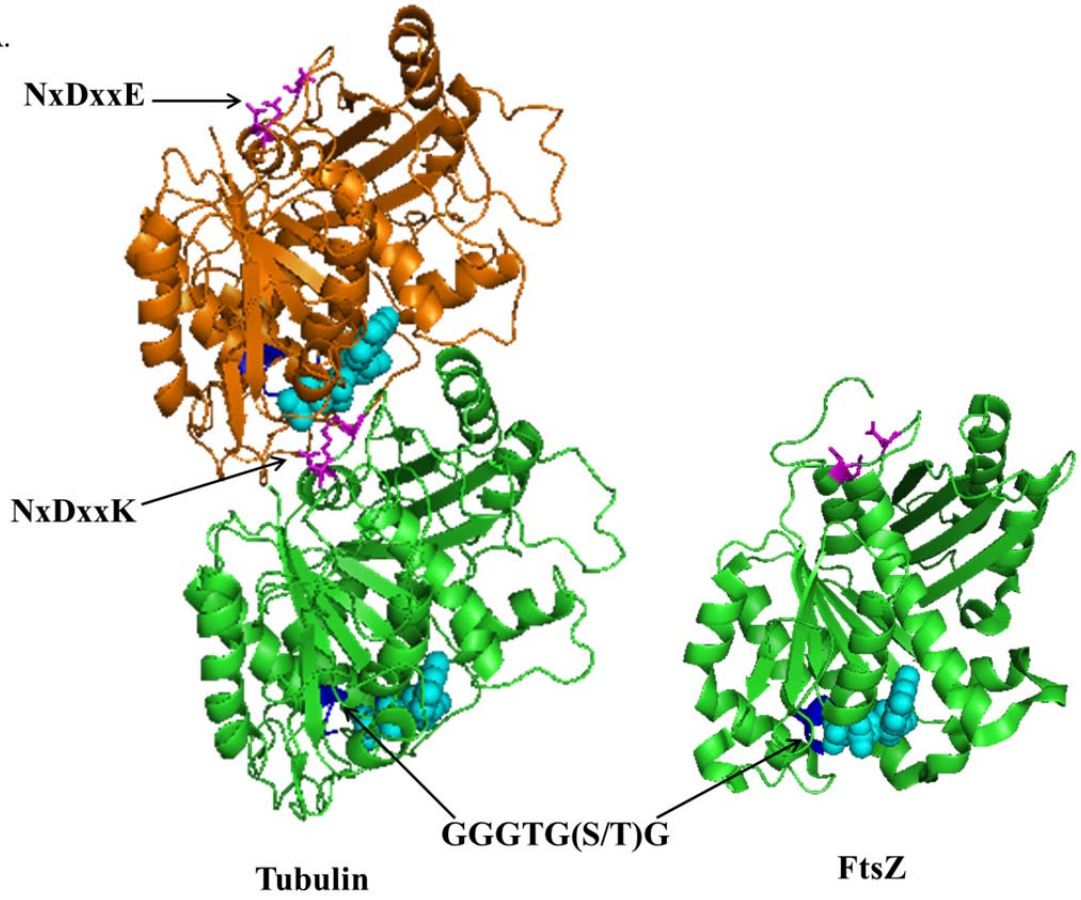

B.

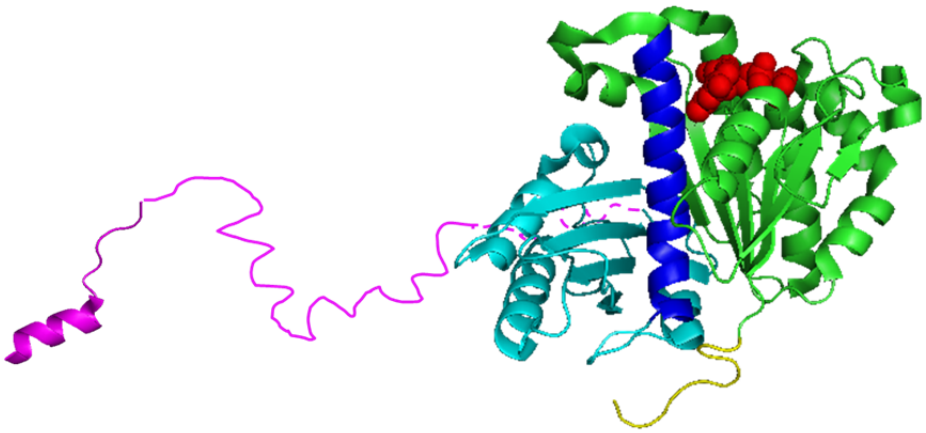

(Camberg et al., 2009; Durand-Heredia et al., 2012; Shen and Lutkenhaus, 2009). The sequence of the FtsZ tail is highly conserved across bacterial species, consistent with its importance for Z ring formation and regulation.

In the presence of GTP, FtsZ polymerizes into dynamic filaments that are structurally similar to the proto-filaments in a microtubule formed by eukaryotic tubulin (Lowe and Amos, 1999; Mukherjee and Lutkenhaus, 1998a). Depending on the buffer conditions, the FtsZ filaments readily associate into bigger structures such as bundles or sheets, but there is controversy about the nature of lateral bonds between the filaments. Under conditions that mimic the physiological situation, the filaments are single-stranded with about 30 subunits on average (Chen and Erickson, 2009). Assembly results in GTP hydrolysis, converting FtsZ-GTP to FtsZ-GDP (Mukherjee and Lutkenhaus, 1998a; Yu and Margolin, 1997). Therefore, FtsZ filaments assembled with GTP are actually an array of FtsZ-GDP and FtsZ-GTP molecules. The half life time of subunit exchange in an FtsZ filament is about 10 s (Chen and Erickson, 2009), but how disassembly of filaments occurs is not clear. FtsZ can also assemble into filaments with GDP, but it does it much more weakly than with GTP (Erickson et al., 1996; Mukherjee and Lutkenhaus, 1994). Addition of GDP strongly destabilizes FtsZ polymers formed with GTP, suggesting that the role of GTP in FtsZ assembly is to provide a way for destabilizing the polymers following hydrolysis. Consistent with this idea, FtsZ filaments formed with a non-hydrolyzable GTP analog GMPCPP are stable (Lu et al., 2000).

An enduring enigma about FtsZ assembly is that it displays a critical concentration of 1 μM, remarkably similar to tubulin, even though it assembles into a single-stranded filament with features of cooperative assembly (Chen and Erickson, 2005; Mukherjee and Lutkenhaus, 1998a). Three different groups suggest that this cooperative behavior of FtsZ could be explained by having FtsZ exist in two different states, an assembly incompetent state and an assembly competent state (Dajkovic et al., 2008b; Huecas et al., 2008; Miraldi et al., 2008) (Fig. 4). Below the critical concentration, the amount of

Fig. 4. Straight and curved conformation of the FtsZ filament. Structure comparison of FtsZ in the assembly competent form (*Staphylococcus aureus* FtsZ-GDP-PC190723, PDB # 3VOB, colored green) and assembly incompetent form (Bacillus subtilis FtsZ-GDP, PDB # 2RHL, colored magenta) as well as the straight and curved FtsZ filament. PC190723 is colored gray, GDP is colored yellow in the assembly competent form but red in the assembly incompetent form. Note that the guanine in the GDP molecule is more twisted in the assembly incompetent form compared to that in the assembly competent form. The C-terminal sub-domain of FtsZ is also pushed away from the H7 helix by the PC190723 molecule in the assembly competent form. The straight FtsZ filament is built with the FtsZ-GDP-PC190723 structure while the curved FtsZ filament comes from Mycobacterium tuberculosis FtsZ-GDP (PDB #4KWE). The H10 helix which forms the bottom interface in FtsZ filament is colored blue while the T7 loop is colored magenta. The T3 loop required to stabilize FtsZ straight filaments is colored brown and in the curved structure the T3 loop no longer contacts the T7 loop, generating the curvature.

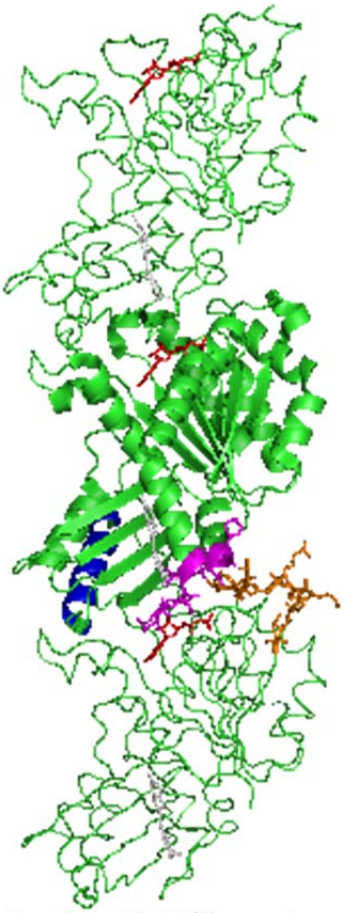

Straight FtsZ filament

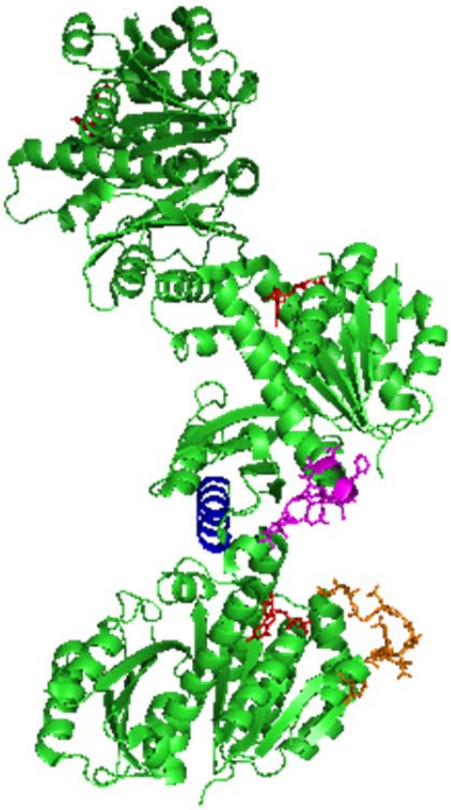

Curved FtsZ filament

assembly competent FtsZ molecules is too low to interact with each other to assemble; above the critical concentration, the level of assembly competent FtsZ interacts productively, producing filaments. Consistent with this model, the structure of FtsZ with GDP, representing the assembly incompetent form, shows dramatic conformational differences to that of FtsZ with GDP and an inhibitor (FtsZ-PC190723-GDP), representing the assembly competent form (Elsen et al., 2012; Matsui et al., 2012). Prominently, in the FtsZ-PC190723-GDP complex, the entire C terminal sub-domain rotates away from the H7 helix, creating a groove for PC190723 to bind. At the same time, the entire H7 helix rotates down one helical turn relative to the N terminal sub-domain, allowing the T7 loop to make contacts with the GTP binding site of the adjacent subunit. This conformational change induced by PC190273 switches the assembly incompetent FtsZ to the assembly competent form (Elsen et al., 2012; Matsui et al., 2012).

FtsZ filaments display different degrees of curvature depending on the nucleotide (Lu et al., 2000). With GDP, the filaments are highly curved with a diameter about 24 nm. With GTP, the filaments are straight, but accumulating evidence suggests that the FtsZ-GTP filaments also have an intermediate curvature. This intermediate curvature is not dependent on GTP hydrolysis as FtsZ filaments formed with non-hydrolyzable GTP analog also exhibit such a curvature (Mingorance et al., 2005). However, the strong curvature associated with FtsZ-GDP filaments is believed to stem from GTP hydrolysis. Comparison of FtsZ structure in a straight filament with that of highly curved filaments supports such a model (Fig. 4). In the straight filament, the T3 loop is stabilized by the GTP ɣ-phosphate in a compact state and interacts extensively with the T7 loop of the top subunit, stabilizing the filaments in the straight conformation(Li et al., 2013). However, in the curved filaments the T3 loop adopts a relaxed conformation due to the absence of ɣ-phosphate and loses contacts with the T7 loop of the top subunit. This lost in contacts between subunits results in the weakening of longitudinal interactions between adjacent subunits, resulting in a hinge-opening motion that pivots around one side of the intersubunit interface (Li et al., 2013). This hydrolysis mediated straight-to-curved conformational change is believed to facilitate turnover as well as to generate mechanical force for cell division. In support of this

hypothesis, *in vitro* reconstitution of the division process in liposomes with a simplified division machinery containing only FtsZ and FtsA found that only GTP, and not GMPCPP (a nonhydrolyzable GTP analog) could promote successful division (Osawa and Erickson, 2013).

Z ring

Using immunoelectron microscopy to visualize FtsZ localization in *E. coli* cells, Bi and Lutkenhaus made the hallmark discovery that FtsZ localizes as a ring-like structure (the Z ring) associated with constriction sites (Bi and Lutkenhaus, 1991). Subsequent employment of immunofluorescence microscopy confirmed the Z ring and found that Z rings were present at the centers of almost all cells, not just the dividing ones (Addinall et al., 1996; Levin and Losick, 1996). This suggests that FtsZ assembles into the Z ring very early in the cell cycle and remains assembled for most of the cell cycle. Nowadays, the most commonly used technique to visualize Z rings is green fluorescence protein (GFP) fusions (Ma et al., 1996). Even though GFP-FtsZ is not fully functional, if expressed at less than 25% of the chromosomal level, it works as a dilute label of WT FtsZ without causing any observable defects in division (Inoue et al., 2009). Not just FtsZ, but any component of the divisome can be tagged with GFP and localizes as a band at the midcell. Detailed examination of the localization of GFP-FtsZ in living cells revealed that FtsZ initially assembles as loosely organized helices at the midcell before eventually coalescing into a sharp ring (Inoue et al., 2009). This transition is largely dependent on FtsZ itself, but the Zap proteins are believed to facilitate this transition as deletion of any one of them results in the formation of "looser" Z rings (Buss et al., 2013; Durand-Heredia et al., 2011). As a Z ring constricts, it disassembles with FtsZ helices emanating from the constricting ring.

GFP fusion labeling also makes it possible to quantify the amount of FtsZ in the Z ring versus that in the cytoplasmic pool. It is estimated that only 30 to 40% of the FtsZ molecules in the cell are in the Z ring (Anderson et al., 2004; Geissler et al., 2007). This suggests that the amount of FtsZ outside of the ring is much higher than the critical concentration of 1 μM, but FtsZ filaments outside of the Z ring are

Fig. 5. Formation of the Z ring occurs in two steps. First, FtsZ polymerizes into head to tail linear filaments, through its globular domain. Second, FtsZ filaments are tethered to the membrane by ZipA and FtsA, both of which bind to the conserved C-terminal tail of FtsZ. Note that the FtsZ tail adopts different conformations when bound to ZipA versus FtsA. Both ZipA and FtsA are tethered to the membrane by their own membrane binding domains connected to the main body of the protein by a flexible linker.

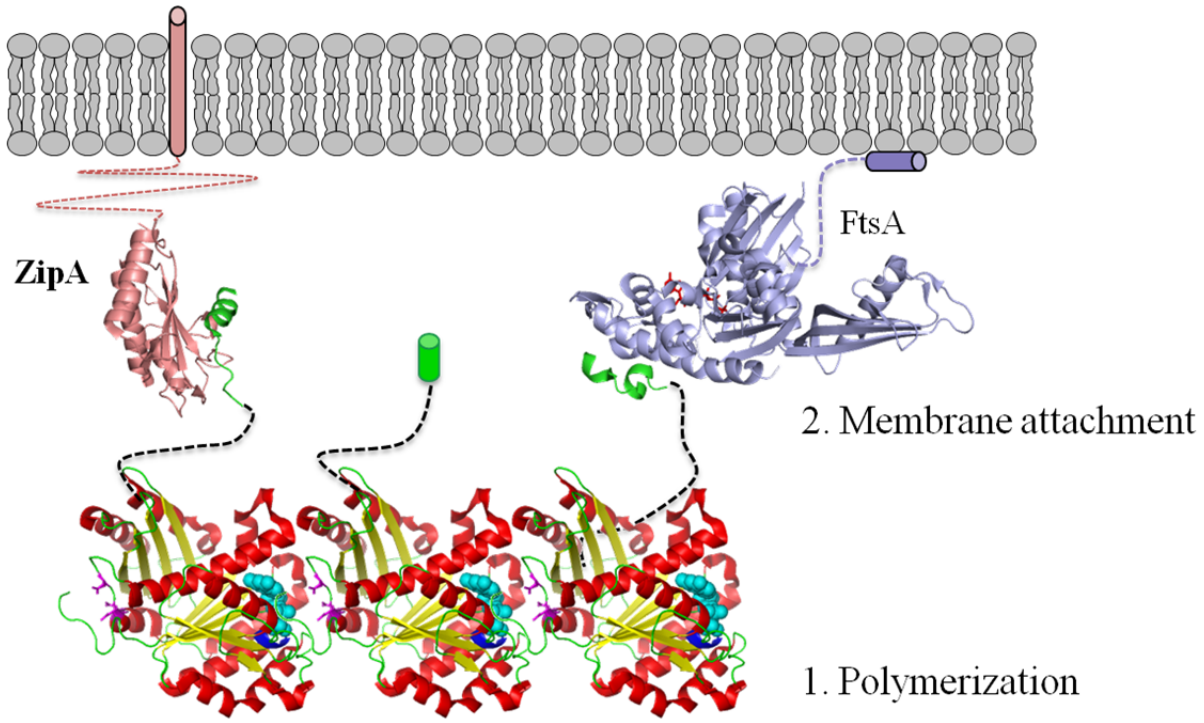
ZipA
FtsA
2. Membrane attachment
1. Polymerization

not readily observed, indicating that cytoplasmic FtsZ either exists as monomers or as short oligomers that turnover too fast to be seen. In agreement with this, studies of fluorescence recovery after photobleaching (FRAP) showed that the subunits in the Z rings are turning over rapidly with a half life time of 10 s (Erickson et al., 2010; Stricker et al., 2002). It is amazing that Z rings remain at the division site for at least 80% of the cell cycle but the FtsZ molecules in the ring have such a short half-life.

To form a Z ring, FtsZ has to polymerize into filaments and be attached to the membrane (Fig. 5). It is very likely these activities occur simultaneously, but to simplify the assembly process, we artificially separate them into two steps. It is well accepted that Z rings consist of FtsZ filaments, but it is not clear how the FtsZ filaments are organized into a ring-like structure. Overexpression of FtsZ results in the formation of extra Z rings at other positions rather than a thickening of the existing midcell Z ring, suggesting that the Z ring has a defined structure (Bi and Lutkenhaus, 1990b; Quardokus et al., 2001; Weart and Levin, 2003; Yu and Margolin, 1999). However, efforts to visualize the Z ring by electron microscopy have been unsuccessful due to the dense cytoplasm of bacterial cells. Two different models have been proposed for the organization of FtsZ filaments in the Z ring (Erickson et al., 2010). In one model, Z rings are composed of short FtsZ filaments arranged in a discontinuous manner without strong lateral interactions. In the other model, short FtsZ filaments are annealed into a long continuous filament encircling the midcell two to three times with strong lateral interactions. Studies from super resolution microscopy favor the first model. In one study, the Z ring of *E. coli* appears to be composed of a loose bundle of FtsZ filaments running in both longitudinal and radial directions (Fu et al., 2010). In another study, FtsZ was found to be distributed heterogeneously with apparent gaps in the Z ring of both *B. subtilis* and *S. aureus*, suggesting a "bean on a string" like model (Strauss et al., 2012). However, *in vitro* reconstitution of Z rings using FtsZ containing a membrane targeting sequence on membrane tubules showed that the reconstituted Z rings appear as a ribbon of filaments packed side by side with virtually no space between the filaments (Milam et al., 2012), in support of the second model. It could be envisioned

that the debate about the structure of the Z ring is going to last until new evidence is provided for either model.

Membrane attachment of FtsZ filaments relies on the interaction of the conserved C-terminal tail with membrane anchors (Fig 5). In *E. coli*, the presence of either one of the two membrane-associated proteins, ZipA and FtsA, is sufficient to form a Z ring at the membrane, but both proteins are required to recruit the late cell division proteins to form the complete divisome (Pichoff and Lutkenhaus, 2002). ZipA has a transmembrane segment attached by a long flexible linker to the FtsZ binding domain and FtsA binds to the membrane through a C terminal amphipathic helix that is connected to the main body of FtsA by a linker (Hale and de Boer, 1997; Pichoff and Lutkenhaus, 2005). Even though both proteins bind to the conserved C-terminal tail of FtsZ, genetic analysis of their interactions with FtsZ suggests that they interact with the tail differently (Haney et al., 2001). This was confirmed by the crystal structures of ZipA and FtsA in complex with the C terminal tail of FtsZ (Mosyak et al., 2000; Szwedziak et al., 2012). In the ZipA-Ztail complex, the tail occupies a hydrophobic cavity in ZipA and binds as an extended β-strand followed by an α helix, while in the FtsA-Ztail complex, the tail forms salt bridges with FtsA and appears as two short α helixes (Mosyak et al., 2000; Szwedziak et al., 2012). This difference suggests that tail of FtsZ cannot bind to ZipA and FtsA simultaneously. FtsA is a bacterial actin and forms actin-like proto-filaments, thus it has been proposed that the Z ring may be tethered to the membrane by an FtsA-ring made of FtsA polymers (Szwedziak et al., 2012).

The C-terminal tail of FtsZ is highly conserved even in bacteria without ZipA and FtsA, suggesting that functionally analogous membrane anchors must exist to perform the same task as ZipA and FtsA. Indeed, in *B. subtilis*, SepF which binds to membrane through an amphipathic helix, and EzrA, which has a topology similar to ZipA, bind to the tail of FtsZ (Krol et al., 2012; Singh et al., 2007, 2008). Deletion of FtsA or SepF impairs Z ring formation, but deletion of EzrA results in the formation of extra Z rings at the poles rather than a delay in Z ring formation, suggesting that it has additional roles at the Z

ring besides attaching FtsZ filaments to the membrane (Levin et al., 1999). The fact that different bacteria employ distinct membrane anchors for Z ring formation indicates that formation of a Z ring is largely a self-organization of membrane tethered FtsZ filaments. This concept is reinforced by the successful reconstitution of Z rings *in vitro* using FtsZ containing a membrane targeting sequence (MTS) and phospholipid tubules (Osawa et al., 2008). As FtsZ with a MTS is sufficient to form Z rings at the membrane, it is surprising that bacteria do not evolve an FtsZ with MTS but instead rely on membrane anchors that bind to its conserved tail. One possible explanation is that having an additional protein provides an extra step for regulation, which appears to be a targeting step for FtsZ spatial regulators. But more importantly, this arrangement allows the cell to coordinate the invagination of the cytoplasm with its cell envelope. Invagination of the cell envelope requires a concerted action through the cytoplasmic membrane to the peptidoglycan layer, and the membrane anchors provide a platform for assembly of the complex to execute this function. Consistent with this, FtsA has been showed to interact with many of the membrane associated late cell division proteins involved in cell wall remodeling (Karimova et al., 2005).

FtsZ binds to membrane anchors with very high affinity, but peptide representing the FtsZ tail displays very weak binding affinity for membrane anchors. For example, ZipA binds full length FtsZ with a Kd of about 200 nM, but its affinity for a 17 amino acid peptide with the sequence of the tail of FtsZ is about 20 μM (Haney et al., 2001; Mosyak et al., 2000). Similarly, full length FtsZ binds to EzrA with a Kd about 4.3 μM, but a 17 amino acid FtsZ tail peptide only binds EzrA weakly, with a Kd about 100 μM (Singh et al., 2007). One explanation for this 100-fold difference in affinity is that the tail adopts a slightly different conformation when attached with the rest of the protein, which binds ZipA/EzrA better. Another more likely possibility is that there is a secondary binding site in the main body of FtsZ, which can bind cooperatively to ZipA/EzrA when the tail is bound.

Cell division regulation in bacteria

A fundamental question in bacterial cell division is how division is coordinated with bacterial cell growth, DNA replication and chromosome segregation. Studies from *E. coli*, *B. subtilis* and *C. cresentus* suggest that cell division is coupled with growth rate and under strict spatial and temporal regulation. Studies in these bacteria also reveal that cell division regulators target FtsZ directly and control cell division at the stage of Z ring formation, the first step of cell division.

Growth rate regulation of Z ring formation

Bacteria have a remarkable ability to adjust their cell size with growth rate and nutrient availability. For example, fast growing cells of *E. coli* and *B. subtilis* are 25% to 30% longer/larger than their slow growing counterparts (Hill et al., 2012; Lu and Kleckner, 1994; Weart et al., 2007). This ability to adjust cell size with nutrient status stems from the ability to modulate maturation of the Z ring according to the nutrient status. Both *E. coli* and *B. subtilis* encode metabolic sensors (OpgH for *E. coli* and UgtP for *B. subtilis*) that can delay cell division under nutrient rich conditions (Hill et al., 2013; Weart et al., 2007) (Fig. 6). Both OpgH and UgtP are FtsZ inhibitors that sense UDP-glucose, the level of which indicates the nutrient availability of the cell. OpgH localizes to the Z ring in nutrient-rich conditions in a UDP-glucose independent manner, but only delays cell division in the presence of UDP-glucose (Hill et al., 2013). Under nutrient-poor conditions, UDP-glucose is less abundant and OpgH is not localized to the Z ring such that Z ring matures earlier and cells are smaller. However, in a rich medium, OpgH is activated by UDP-glucose so that it can bind to FtsZ and delay the maturation of the Z ring (Hill et al., 2013). Slightly different, UgtP localizes to the Z ring under nutrient rich conditions in a UDP-glucose dependent manner (Weart et al., 2007). UgtP tends to oligomerize, but UDP-glucose reduces its potential to oligomerize and increases its affinity for FtsZ such that it can localize to the Z ring and delay cell division in rich medium (Chien et al., 2012).

Although both OpgH and UgtP antagonize FtsZ polymerization, they act by different mechanism. OpgH increases the critical concentration of FtsZ for GTP hydrolysis, suggesting that it antagonizes FtsZ

Fig. 6. Growth rate regulation of Z ring formation in *E. coli* and *B. subtilis*. Under nutrient poor conditions, the level of UDP-glucose is low and OpgH (*E. coli*) and UgtP (*B. subtilis*) are inactive and FtsZ can assemble into the Z ring at the future division site at a smaller cell size. Under nutrient rich conditions, accumulation of UDP-glucose leads to the activation of OpgH and UgtP, which antagonize FtsZ polymerization by sequestering FtsZ molecules and severing the FtsZ polymers, respectively. As a result the cells have to grow to a larger size for enough FtsZ molecules to accumulate to overcome the inhibition by OpgH and UgtP.

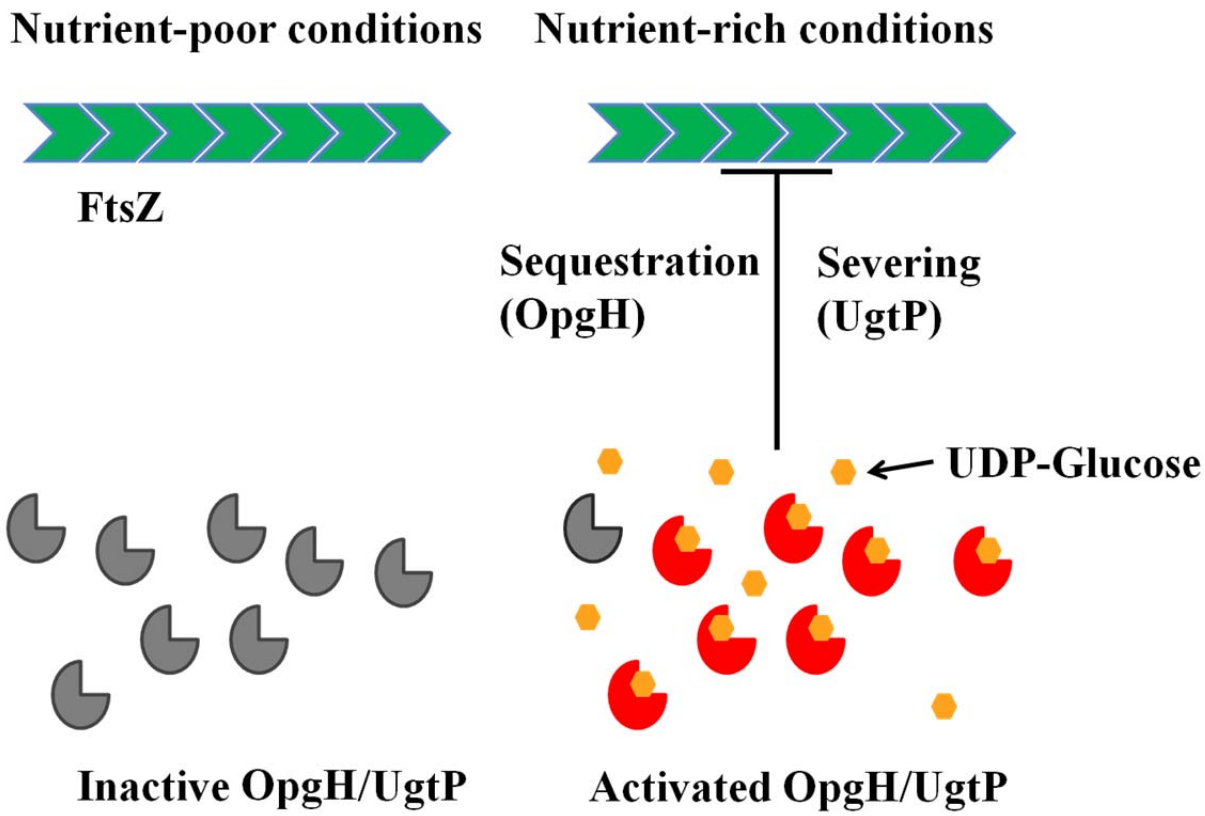
Nutrient-poor conditions
Nutrient-rich conditions
FtsZ
Sequestration (OpgH)
Severing (UgtP)
UDP-Glucose
Inactive OpgH/UgtP
Activated OpgH/UgtP

assembly by sequestration (Hill et al., 2013). In contrast, UgtP is thought to antagonize FtsZ polymerization by inhibiting single-filament formation (Chien et al., 2012). The exact working mechanisms of OpgH and UgtP still require further study, but the usage of UDP-glucose as a proxy for nutrient status to activate division inhibitors in two distantly related bacteria suggest that linking central metabolism with maturation of the cytokinetic machinery by "moonlighting" enzymes may be a widely conserved mechanism to control cell size in bacteria.

Spatial and temporal regulation of Z ring formation

Spatial and temporal regulation of cell division has been extensively studied in three divergent rod-shape bacteria, *E. coli, B subtilis* and *C. cresentus*, all of which divide near the middle of the long axis of the cell (Lutkenhaus et al., 2012). Both *E. coli* and *B. subtilis* employ two partially redundant negative regulatory systems to ensure Z ring forms precisely at midcell: Min (Minicell) and NO (nucleoid occlusion) (Lutkenhaus, 2007) (Fig. 7). Deletion of the Min system results in the formation of the Z ring at the cell poles and thus minicell formation (de Boer et al., 1989). In contrast, deletion of the NO system does not have any observable effect in exponential cells but leads to Z ring assembly over the nucleoids when the DNA replication initiator DnaA is depleted (Bernhardt and de Boer, 2005; Wu and Errington, 2004). Deletion of both the Min and NO systems leads to assembly of aberrant FtsZ structures throughout the cell which cannot mature into functional Z rings. Thus, cells become filamentous and die in the absence of both the Min and NO systems (Bernhardt and de Boer, 2005; Wu and Errington, 2004).

C. cresentus does not encode the effectors of the Min and NO systems found in *E. coli* and *B. subtilis*, but employs a protein called MipZ to ensure Z rings form at midcell (Thanbichler and Shapiro, 2006) (Fig. 7). MipZ is an essential gene and depletion results in the formation of aberrant FtsZ structures throughout the cell and cell filamentation, a phenotype similar to the deletion of Min and NO in *E. coli* and *B. subtilis* (Thanbichler and Shapiro, 2006).

A theme emerging from studies of these FtsZ spatial regulators is that spatial regulation of Z ring formation is negatively controlled and Z rings assemble in the area of least FtsZ inhibition (Lutkenhaus, 2007). Recent studies, however, of the bacteria *Streptomyces coelicolor* and *Myxococcus xanthus*, which lack the known negative regulatory systems found in *E. coli*, *B subtilis* and *C. cresentus*, indicate that Z ring formation in these bacteria is positively regulated (Treuner-Lange et al., 2013; Willemse et al., 2011). While the mechanism of the effectors of positive regulatory systems is largely unknown, the mechanisms of the negative regulators have been studied *in vivo* and *in vitro*. These negative regulators form gradients that originate from the cell pole or regions occupied by the origin region of the chromosome that extend toward midcell where their concentration is lowest (Lutkenhaus, 2007). Two of the three known spatial regulators have been characterized *in vitro*, MinC and MipZ, act in a similar manner to prevent Z ring formation by antagonizing FtsZ polymerization (Hu et al., 1999; Thanbichler and Shapiro, 2006). MinC also binds to the conserved C-terminal tail of FtsZ, competing with its binding to membrane anchors that promote Z ring formation (Shen and Lutkenhaus, 2009). Since formation of Z rings requires FtsZ polymerization and membrane attachment, the MinC mechanism suggests that targeting negative regulators to the conserved C-terminal tail of FtsZ might be the most efficient way to prevent Z ring formation.

Min system

The Min system prevents Z ring formation near the cell poles through the spatial regulation of the FtsZ assembly antagonist MinC (Lutkenhaus, 2007). MinC contains two domains, an N terminal domain and a C terminal domain, both of which can bind to FtsZ (Hu and Lutkenhaus, 2000; Shiomi and Margolin, 2007). MinD, a membrane associated ATPase, binds to the C terminal domain of MinC, recruiting MinC to the membrane and enhancing MinC's activity to bind to the conserved C terminal tail of FtsZ (de Boer et al., 1991; Johnson et al., 2002; Shen and Lutkenhaus, 2009). This binding to the tail of FtsZ, on the one hand reduces the tail binding to membrane anchors (in *E. coli*, FtsA and ZipA), and on

Fig. 7. Spatial regulation of Z ring formation. In *E. coli* and *B. subtilis*, Z ring formation is limited to midcell by the Min system and Nucleoid occlusion (NO). NO is mediated by SlmA in *E. coli* and by Noc in *B. subtilis*. Both SlmA and Noc bind to their specific DNA sequences (SBSs/NBSs, SlmA binding sequences/Noc binding sequences) that are mainly distributed in the origin 2/3 of the chromosome. In newborn cells the organization of the chromosome causes SlmA or Noc to be relatively homogeneous on the nucleoid which blocks Z ring formation over the nucleoid. As chromosome segregation moves the origin of replication toward the poles, SlmA or Noc forms a gradient on the nucleoid that originates from the origin of replication and extends toward midcell such where the SlmA/Noc concentration is lowest. The Min system prevents Z ring formation near the cell poles. MinC and MinD form a complex at the membrane that antagonizes FtsZ polymerization and membrane attachment by Z ring promotoing proteins. In *E. coli* MinCD is spatially regulated by MinE, which in complex with MinD continuously oscillates from one pole to the other such that the average concentration of MinCD is lowest at midcell and highest at the cell poles. In *B. subtilis*, MinCD is retained at the cell poles by binding to MinJ, which is anchored at the pole by the membrane curvature sensing protein DivIVA. In constricting cells, MinCD is recruited to the nascent septa by MinJ and DivIVA. In *C. cresentus*, Z ring positioning is regulated by MipZ, which forms a gradient on the nucleoid. The gradient orginates from its partner ParB which binds to specific DNA sequences near the origin of replication which is anchored to the stalked pole by PopZ. As chromosome segregation starts, one of the two origin-ParB complexes stays at the stalked pole while the other migrates to the opposite pole such that MipZ forms a bipolar gradient emanating from its partner ParB. FtsZ released from the opposite pole by the arriving MipZ migrates to midcell to assemble into the Z ring along with newly synthesized FtsZ.

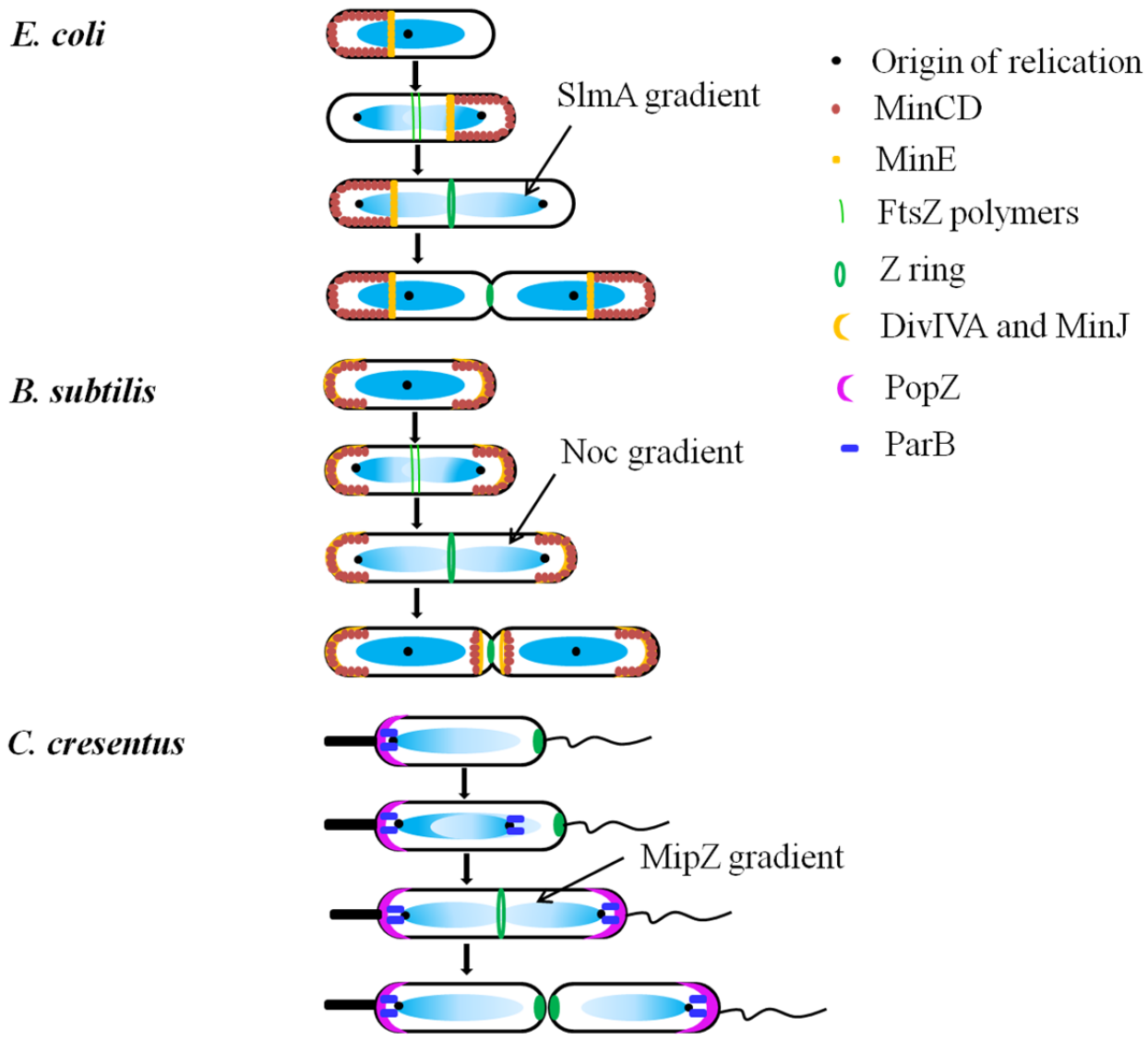
E. coli
SlmA gradient
B. subtilis
Noc gradient
C. cresentus
MipZ gradient
Origin of relication
MinCD
MinE
FtsZ polymers
Z ring
DivIVA and MinJ
PopZ
ParB

the other hand positions the N terminal domain of MinC close to the FtsZ filaments so that it can break FtsZ filaments at the interface of two subunits following GTP hydrolysis (Shen and Lutkenhaus, 2010) (Fig. 8). Working together, the C-terminal and N-terminal domains of MinC compete with positive factors and prevent FtsZ polymerization, the two critical activities required for Z ring formation.

The activity of MinCD is directed towards the poles of the cell. In *E. coli*, and most Gram-negative bacteria, MinCD are topologically regulated by MinE, which undergoes a coupled oscillation along with MinCD between the poles of the cell (Fu et al., 2001; Hale et al., 2001; Hu and Lutkenhaus, 1999; Raskin and de Boer, 1999b) (Fig. 7). The oscillation of MinC causes its time-averaged concentration to be highest at the cell poles and lowest at midcell, where the Z ring forms. Deletion of MinE disrupts the oscillation and leads to an even distribution of MinCD on the membrane, which blocks Z ring formation all over the cell (Bi and Lutkenhaus, 1993; de Boer et al., 1989; Hu and Lutkenhaus, 1999; Pichoff and Lutkenhaus, 2001; Raskin and de Boer, 1999a). Deletion of MinC leads to formation of Z rings at the cell poles but does not affect the oscillation of MinDE, suggesting that MinC is just a passenger in this oscillation (Hu and Lutkenhaus, 1999; Raskin and de Boer, 1999a, b). Consistent with this, MinD and MinE are able to self-organize into waves on a lipid bilayer *in vitro*, with the MinE wave chasing the MinD wave (Loose et al., 2008). The details of MinDE driven oscillation has been studied and modeled extensively. MinE is a dimer and an activator of the membrane bound MinD ATPase (Hu and Lutkenhaus, 2001). When MinE encounters MinD, MinE undergoes a conformational change so that it can bind to MinD and the membrane at the same time (Park et al., 2011). This active form of MinE stimulates the ATPase activity of MinD, causing release of MinD, and thus MinC from the membrane. Since MinE is transiently bound to the membrane after it knocks MinD off the membrane, it is either released from the membrane or it can swing to another MinD. This Tarzan of the Jungle like movement of MinE between membrane bound MinDs within a geometrical confined environment such as a cell, is necessary for a robust oscillation (Park et al., 2011; Schweizer et al., 2012).

In contrast to *E. coli*, *B. subtilis* generates a static gradient of MinCD that extends from the pole to midcell by anchoring MinCD to areas of membrane curvature by a protein called DivIVA (Marston et al., 1998) (Fig. 7). This anchoring also requires an intermediary designated MinJ that bridges DivIVA and MinD (Bramkamp et al., 2008; Patrick and Kearns, 2008). DivIVA localizes to the incipient septum as well as cell poles, where membrane curvature is the highest (Eswaramoorthy et al., 2011). As constriction is initiated, DivIVA is quickly recruited to the constriction site, forming a ring like structure on each side of the constriction. This DivIVA ring, further recruits MinCD through MinJ to prevent FtsZ released from the constricting Z ring from reforming a ring at the newly forming poles (Gregory et al., 2008). As septation is completed MinCD is retained at the poles by interaction with DivIVA and MinJ.

MipZ gradient formation

Unlike *E. coli* and *B. subtilis*, in which chromosome segregation and cell division can occur independently of each other, these two events are tightly coupled in *C. cresentus* as disruption of either event results in impairment of the other. MipZ is key factor that couples these two events (Thanbichler and Shapiro, 2006). It forms a bipolar gradient in predivisional cells dependent on the bipolarly localized ParB (Fig. 7), a component of the origin of replication segregation machinery that recognizes a cluster of centromere-like sites located near the origin. ParB is anchored at one cell pole along with the origin of replication. As DNA replication starts, one of the two duplicated origins is segregated to the other pole by ParB and ParA, a MinD like ATPase (Bowman et al., 2008). MipZ monomers are recruited to poles of the cell by interaction with ParB, where ParB promotes its dimerization (Kiekebusch et al., 2012). MipZ dimers, the form that antagonizes FtsZ assembly, diffuse away from ParB and bind nonspecifically to the DNA. This binding is transient as the intrinsic ATPase of MipZ causes its release from the DNA. Repeated cycling of MipZ between the bound ParB and the DNA leads to the formation of a gradient of MipZ that originates from ParB and extends toward the cell center (Kiekebusch et al., 2012). Duplication and segregation of the origin leads to a bipolar gradient of MipZ with the low point near midcell where

Fig. 8. Current model for how MinCD antagonizes FtsZ assembly into the Z ring. The C terminal domain of MinC binds to the conserved C-terminal tail of FtsZ. This binding reduces the FtsZ tail binding to the membrane anchors ZipA and FtsA, interfering with FtsZ membrane attachment, and positions the N terminal domain of MinC close to the FtsZ filaments such that it can antagonize FtsZ polymerization by binding to the interface between FtsZ subunits.

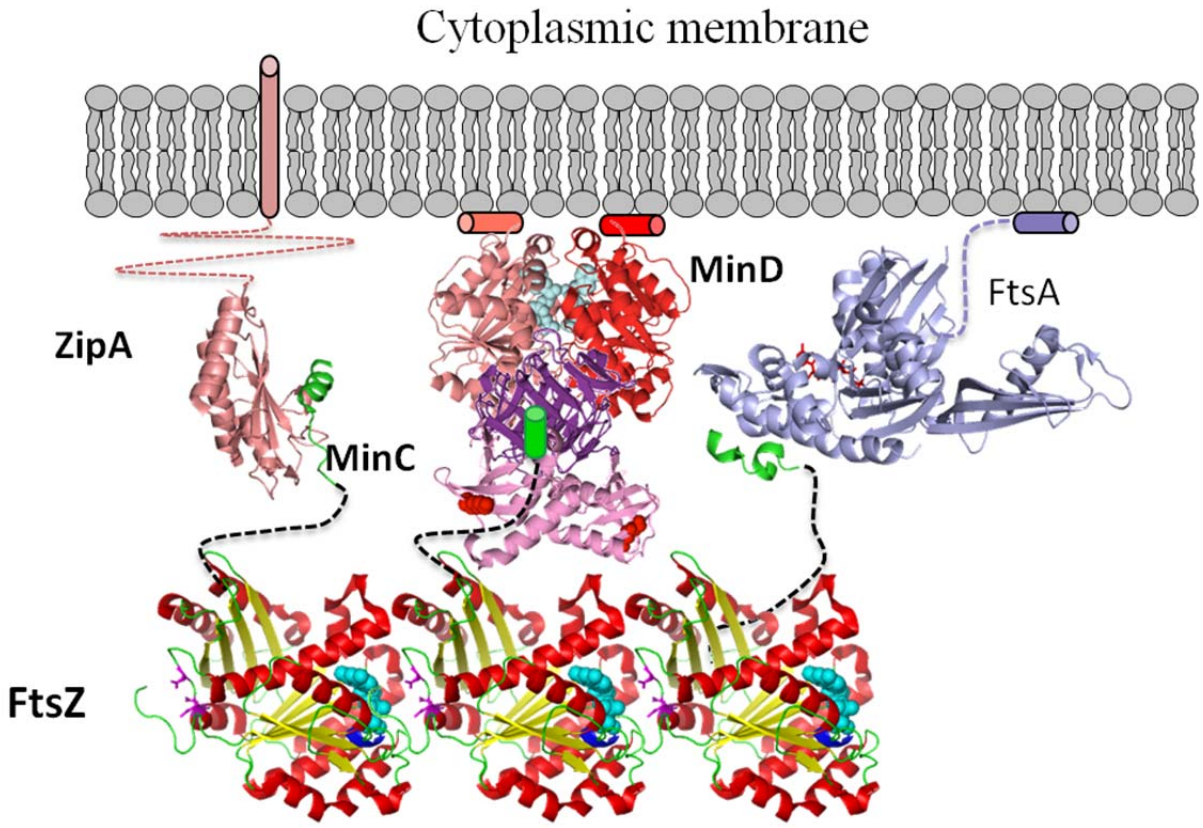
Cytoplasmic membrane
MinD
FtsA
ZipA
MinC
FtsZ

the Z ring forms (Thanbichler and Shapiro, 2006). The interplay among ParB, MipZ and FtsZ thus links chromosome segregation and cell division together. A defect in chromosome segregation results in the failure to form a bipolar MipZ gradient, whereas a division block results in the failure to form new poles; the ParB-origin complex cannot be anchored and a MipZ bipolar gradient is not formed, which in turn block blocks cell division.

Nucleoid Occlusion

Early studies of division site positioning in *E. coli* found that divisions rarely occur over the nucleoid in cells with DNA replication or segregation defects. These findings led to the nucleoid occlusion model (NO system) in which the nucleoid negatively controls the positioning of the division site (Mulder and Woldringh, 1989; Woldringh et al., 1990). According to this model, all positions along the cell length are competent for cell division, but cell division is prevented at positions occupied by nuceloids. As nucleoid segregation nears completion, this nucleoid-mediated inhibition is released, allowing division to occur between the nucleoids. Support for this model came from examining Z ring positioning in chromosome partition mutants; Z rings formed in nucleoid free regions but were occluded over the nucleoids in filamentous cells with unsegregated nucleoids (Yu and Margolin, 1999).

Effectors of the NO system in *E. coli* and *B. subtilis* have been identified, as SlmA and Noc respectively (Bernhardt and de Boer, 2005; Wu and Errington, 2004). SlmA is a TetR family DNA binding protein, while Noc is ParB like DNA binding protein. Even though these two proteins share no sequence homology or structural similarity, they act in a remarkably similar manner. Both proteins associate with the nucleoid through DNA binding domains that recognize specific DNA sequences (NBS/SBS, Noc binding site/SlmA binding site) that are enriched in origin-proximal regions of the chromosome (Bernhardt and de Boer, 2005; Cho et al., 2011; Tonthat et al., 2011; Wu and Errington, 2004; Wu et al., 2009). As the chromosome is replicated, Noc/SlmA associated with the two origins is segregated away from midcell and an inhibitor free zone is generated where the Z ring forms. Thus,

segregation of the origin and the surrounding NBS/SBS sites imparts spatial and temporal regulation of Noc and SlmA. Introduction of NBS/SBS sites in the terminus region of the chromosome, which occupies the middle of the cell, delays cell division significantly (Cho et al., 2011; Wu et al., 2009). If binding sites are introduced on multicopy plasmids (which are randomly distributed in the cytoplasm) division is inhibited because the division inhibitors NBS-Noc/SBS-SlmA are delocalized from their normal chromosomal location (Cho et al., 2011; Wu et al., 2009). Thus, the NO systems seem ideally suited to couple chromosome segregation to formation of the Z ring. The target for Noc in *B. subtilis* is currently unknown, but SlmA inhibits Z-ring formation over the DNA by a direct interaction with FtsZ (Bernhardt and de Boer, 2005).

SlmA mediated NO

SlmA was identified as a synthetic lethal knockout with the *min* deletion, but elimination of SlmA had no division defect in exponential growing cells (Bernhardt and de Boer, 2005), presumably because of the dominant role of the Min system in positioning the Z ring. However, when the DNA replication initiator DnaA is depleted in the absence of SlmA, division occurs on top of the nonreplicating nucleoid confirming the NO function of SlmA (Bernhardt and de Boer, 2005). Like other TetR family proteins, SlmA can be divided into two domains, a small conserved N-terminal domain (1-53) containing a canonical HTH motif and a less conserved large C-terminal domain (54-198) (Bernhardt and de Boer, 2005; Tonthat et al., 2011). The N-terminal domain is responsible for DNA binding and the large C-terminal domain nucleoid occupied by the origin region of the chromosome. In newborn cells with a single nucleoid and the origin at midcell, the GFP signal localizes as a cloud over the nucleoid. As the cell cycle proceeds, the duplicated origins segregate and the GFP-SlmA becomes bilobed (Bernhardt and de Boer, 2005). This dynamic localization of GFP-SlmA correlates with the timing of Z ring formation at midcell.

Fig. 9. Location of SlmA binding sites (SBS) and comparison SlmA structures with or without SBS DNA (PDB#3NXC and #4GCL). A) Cicular diagram of the *E. coli* chromosome with approximate locations of SBSs shown as blue lines. Green, red, dark- and light-orange colored regions represent the Ori, Ter, Left and Right macrodomains of the chromosome. B) Sequence logo of the consensus SlmA binding sequence is shown below the circular diagram of the chromosome. C) SlmA forms a homodimer in the absence of SBS DNA but forms an oriented dimer-of-dimer in the presence of SBS DNA. Arrows point to the residues that are important for DNA binding (T33A, colored as cyan) and interaction with FtsZ (F65, R73, L94, G97, R101 and N102, colored as yellow). Binding to DNA causes movement of the DNA binding domain such that F65 is no longer occluded.

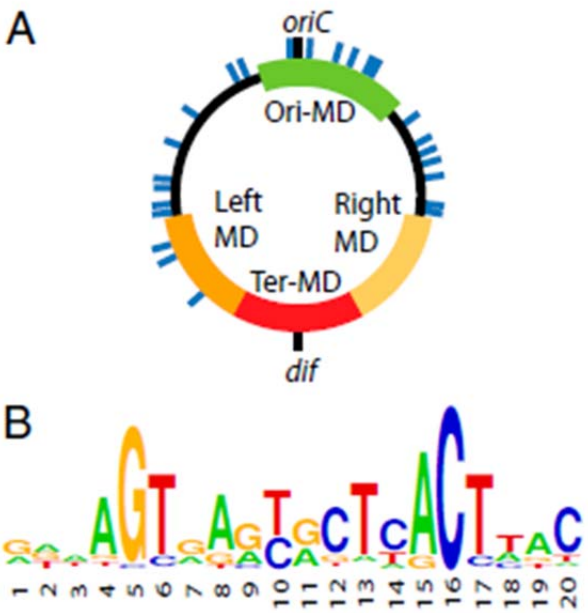

Cho & Bernhardt TG, et al. 2011

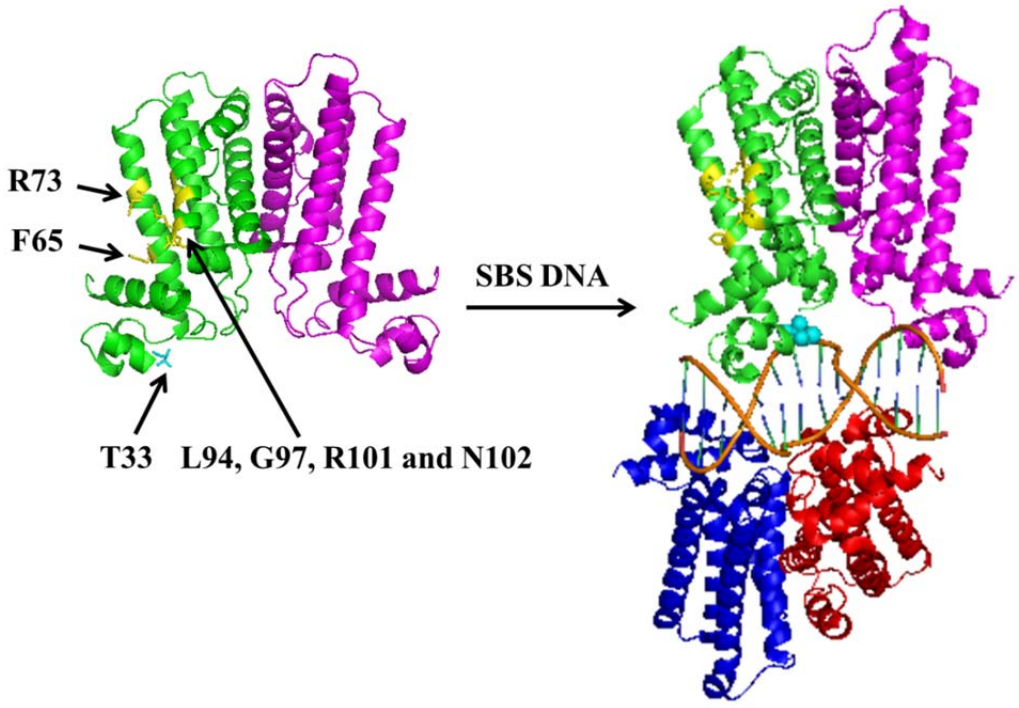

A single substitution in the HTH motif, SlmA-T33A, abolishes DNA binding and renders SlmA defective in NO (Cho et al., 2011). Initial analysis indicated that the SlmA-T33A mutant is defective in self-interaction and interaction with FtsZ, suggesting that SlmA may exist as monomers and the role of SBS DNA is to promote dimerization. Consistent with this, SlmA was monmeric at low concentrations but formed dimers at high concentrations (Cho et al., 2011). However, SlmA was subsequenstly crystallized without DNA and was a dimer with a highly hydrophobic dimer interface, arguing that SlmA exists as dimers in the absence of SBS DNA (Tonthat et al., 2011). Nonetheless, overproduction of SlmA-T33A still blocks Z ring formation but is much less effcieint, indicating that in the absence of DNA binding SlmA interacts weakly with FtsZ (Cho et al., 2011).

Inhibition of FtsZ polymerization by SBS-SlmA requires the GTPase activity of FtsZ as a catalytic mutant of FtsZ, FtsZ-D212N, is resistant to the activity of SBS-SlmA (Cho et al., 2011). Consistent with this, SBS-SlmA is able to pull down FtsZ-D212N filaments but not filaments formed with wild type FtsZ (Cho et al., 2011). SBS-SlmA was also found to increase the GTPase activity of FtsZ, suggesting that it stimulates FtsZ-GDP formation within the polymers to promote the breakdown of the FtsZ proto-filaments (Cho et al., 2011). Therefore, it is believed that once bound to SBS DNA, SlmA induces breaks in FtsZ filaments at positions where the GTP has been hydrolyzed to GDP in a manner similar to that proposed for MinC (Cho et al., 2011).

Examining the effect of SlmA on FtsZ polymerization with or without SBS DNA showed that SBS bound SlmA disassembles FtsZ proto-filaments about 40 fold more efficiently than DNA free SlmA, indicating that SBS binding activates SlmA to antagonize FtsZ polymerization (Cho et al., 2011). A number of substitutions, F65I/A, R73D, L94Q, G97D, R101D and N102S, of SlmA eliminate or reduce FtsZ binding and the ability of SlmA to antagonize FtsZ polymerization (Cho and Bernhardt, 2013). These residues likely constitue the binding site for FtsZ. Intriguingly, all of these residues cluster in a region of SlmA, which in the DNA-free SlmA structure is partially occluded by the DNA binding

Fig. 10. Current models for FtsZ regulation by SlmA. SlmA forms oriented dimer-of-dimer on SBS DNA, which can spread to the adjacent DNA (for simplicity, spreading is not shown). In one model, the SBS bound SlmA is activated to interact with FtsZ and sever the FtsZ polymers at interfaces where the GTP has been hydrolyzed to GDP. In the other model, SBS bound SlmA does not antagonize FtsZ polymerization but sequesters FtsZ polymers to the SlmA-DNA complex such that fewer FtsZ polymers would be on the membrane for Z ring formation.

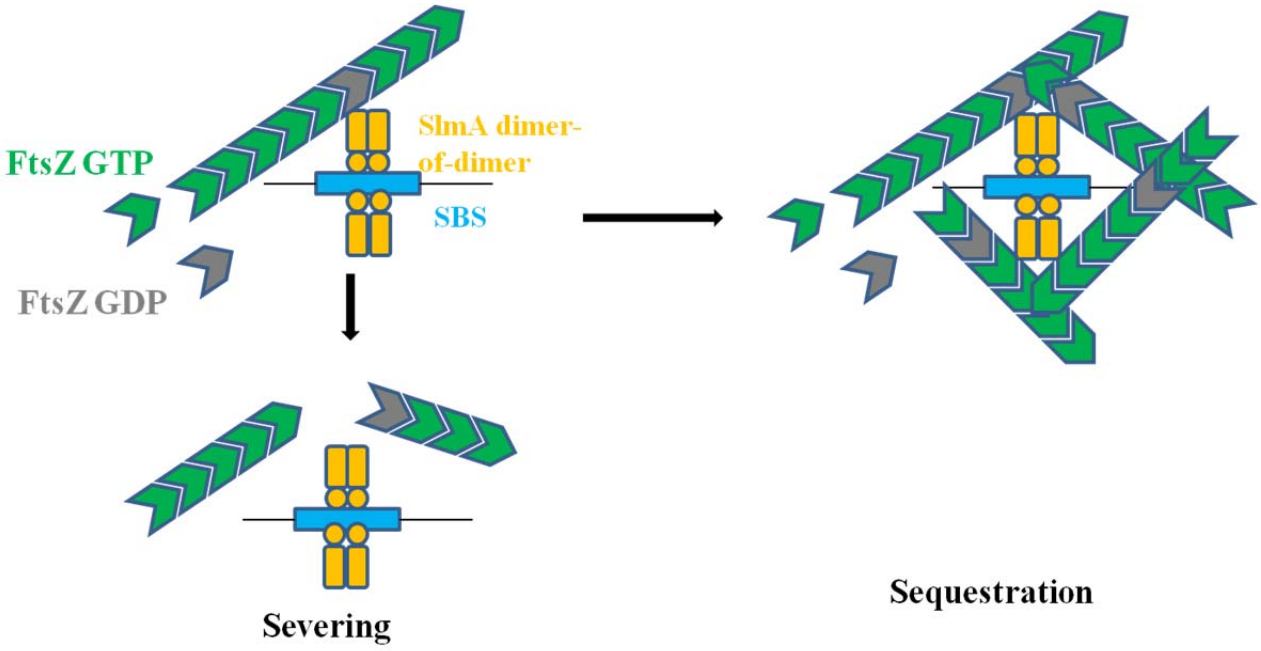
FtsZ GTP
SlmA dimer-
of-dimer
SBS
FtsZ GDP
Severing
Sequestration

domains (Cho and Bernhardt, 2013; Tonthat et al., 2013) (Fig. 9C). Thus, the binding to an SBS is proposed to stabilize SlmA in a conformation with a fully exposed FtsZ binding site so that it can bind FtsZ (Cho and Bernhardt, 2013).

SlmA forms an oriented dimer of dimers on the SBS DNA (Tonthat et al., 2013). Formation of the SlmA dimer of dimers requires only the consensus SBS sequence **GTgAGtaCTcAC**, but if longer SBS DNA molecules are used, additional contacts with nucleotides outside of the consensus sequence are observed (Tonthat et al., 2013). In addition, SlmA dimers spread on the DNA. Comparison of the DNA free and the SBS DNA bound SlmA structures indeed shows dramatic conformational differences in the SlmA dimers (Tonthat et al., 2013). Insertion of the DNA binding domain of SlmA into the groove of the DNA molecule results in the exposure of the region that is predicted to be the binding site for FtsZ, which is occluded in the DNA-free structure. Thus, in addition to regulating SlmA spatially, SBS binding activates SlmA by stabilizing a conformation that interacts with FtsZ. The role of SlmA dimer-of-dimers on the SBS and possibly further oligomerization on the DNA *in vivo* is unknown.

Although this group originally found that SlmA bound to the SBS affected FtsZ polymerization by forcing the FtsZ proto-filaments into some short anti-parallel higher order structures, they more recently found that SBS-SlmA does not affect FtsZ proto-filament formation (Tonthat et al., 2011; Tonthat et al., 2013). They also found that SBS-SlmA does not affect the GTPase activity of FtsZ (Tonthat et al., 2013). Furthermore, SAXS analysis of an SBS-SlmA-FtsZ complex showed that four FtsZ molecules associated with the SlmA dimer of dimers on their lateral side rather than the regions that would form the longitudinal interface in proto-filaments, suggesting these associated FtsZ molecules are likely able to polymerize (Tonthat et al., 2013). It was proposed that SBS bound SlmA prevents Z ring formation over the nucleoid by sequestration of proto-filaments on the DNA and inhibiting their further gtowth and lateral interactions to form a Z ring (Tonthat et al., 2013).

In this thesis, I studied the interaction between SlmA and FtsZ and tried to understand the molecular mechanism by which SlmA inhibits Z ring formation. Using a genetic approach, I isolated FtsZ mutants that are resistant to the NO function of SlmA. Analysis of these FtsZ mutants suggests that although they are resistant to the action of SlmA, they are not directly involved in SlmA binding. SlmA bound to the SBS DNA indeed antagonizes FtsZ protofilament formation and the different observations by the above two groups are likely due to the different SBS DNA molecules used in their studies. Unexpectedly, we found that SlmA binds to the conserved C-terminal tail of FtsZ and inhibition of FtsZ polymerization by SlmA requires the presence of FtsZ tail. As the conserved C terminal tail of FtsZ is not involved in polymerization and the resistant mutations reside in the globular domain of FtsZ, our data thus suggest that SBS-SlmA binds to the C-terminal tail of FtsZ and this binding stimulates its binding to a secondary binding site in the globular domain of FtsZ, allowing it to break the FtsZ filaments. Therefore, SlmA, similar to MinC, prevents Z ring formation by antagonizing FtsZ polymerization and membrane attachment simultaneously. This similarity between MinC and SlmA suggest that competing with membrane anchors and breaking the FtsZ filaments might be a universal mechanism for FtsZ spatial regulators.

Chapter II: Materials and Methods

Bacterial strains, plasmids and growth conditions

Strains and plasmids used in this study are listed in Tables 1 and 2, respectively. Cells were grown in LB medium at 37°C unless otherwise indicated. When needed, antibiotics were used at the following concentrations: ampicillin= 100 µg/ml; spectinomycin= 25 µg/ml; kanamycin= 25 µg/ml; tetracycline= 25 µg/ml; and chloramphenicol= 20 µg/ml.

The strain PS1603 (W3110 *slmA::cat)* was generated by *S. Pichoff* (unpublished) in which most of the *slmA* coding sequence was replaced by the *cat* gene expressing chloramphenicol resistance.

The Δ*min*Δ*slmA* double mutant strain DU5 (*W3110 min::kan*, *slmA::cat*) was generated by P1 transducing *slmA::cat* (from PS1603) into the strain *W3110 min::kan*. Chloramphenicol and kanamycin resistant transductants were selected at 42°C.

Strain DU11 (*W3110 ftsZ^0 slmA<frt> recA::Tn10*)/pKD3C was constructed in several steps. First strain S3 (*W3110 leu::Tn10*) was transduced with P1 grown on TB85 (*MG1655, slmA::kan*) (Bernhardt and de Boer, 2005) and kanamycin resistant transductants were selected. The purified transuductant was named DU8 (*W3110 leu::Tn10 slmA::kan*) and transformed with plasmid pCP20 by selecting ampicillin resistance at 30°C. The transformants were then streaked on LB plates with tetracycline and incubated at 42°C to get rid of the *kan* gene and plasmid pCP20. The resultant strain was named DU9 (*W3110 leu::Tn10 slmA<frt>*) and tested by PCR using primers flanking the deleted region to confirm that the *kan* gene had been removed. Plasmid pKD3C was then transformed into DU9 and a purified transformant DU9/pKD3C was transduced with P1 grown on PB143 (*leu+ ftsZ^0 recA::Tn10*) by selecting for Leu+ at 30° on M9 minimum medium. The resultant transductants were checked for temperature sensitivity and tetracycline resistance and the desired transductants (DU10/pKD3C) should have a genotype *leu+ ftsZ^0 slmA<frt>* with plasmid pKD3C providing FtsZ. Finally, the *recA::Tn10* allele from PB143 was transduced into DU10/pKD3C by selecting for tetracycline resistance on LB plate at 30°C.

Table 1. Strains used in this study

Strain	Description	Source/reference
JS238	MC1061 *malPp::lacI^q srlC::Tn10 recA1*	Lab collection
BTH101	F- *cya-99, araD139 galE15 galK16 rpsL1 (Str^R) hsdR2 mcrA1 mcrB1*	(Karimova et al., 1998)
W3110	*F$^-$ λ$^-$ rph-1 INV(rrnD, rrnE)*	Lab collection
WM1033	*MG1655, parC281::Tn10*	Margonlin, w (unpublished)
PS106	*W3110 leu::Tn10 ftsZ84*	Lab collection
PS1603	*W3110 slmA::cat*	Lab collection
S3	*W3110 leu::Tn10*	(Shen and Lutkenhaus, 2009)
S4	*W3110 leu::Tn10 min::kan*	(Shen and Lutkenhaus, 2009)
S7/pKD3C	*W3110 ftsZ^0 slmA<frt> recA::Tn10*	(Shen and Lutkenhaus, 2009)
DU5	*W3110 leu::Tn10 min::kan slmA::cat*	This study
DU11/pKD3C	*W3110 ftsZ^0 slmA<frt> recA::Tn10*	This study
SD110	*W3110 leu::Tn10 slmA::cat*	This study
SD139	*W3110 parC281::Tn10*	This study
SD140	*W3110 parC281::Tn10 slmA::cat*	This study
SD160	*W3110 leu::Tn10 ftsZ-K190V*	This study
SD161	*W3110 leu::Tn10 ftsZ-K190V slmA::cat*	This study
SD162	*W3110 leu::Tn10 ftsZ-K190V min::kan*	This study
SD163	*W3110 leu::Tn10 ftsZ-D86N*	This study
SD164	*W3110 leu::Tn10 ftsZ-K190V&D86N*	This study
SD165	*W3110 leu::Tn10 ftsZ-D86N slmA::cat*	This study
SD167	*W3110 leu::Tn10 ftsZ-D86N min::kan*	This study
SD170	*W3110 parC281::Tn10 ftsZ-K190V*	This study
SD171	*W3110 parC281::Tn10 ftsZ-D86N*	This study

Table 2. Plasmids used in this study

Plasmid	Description	Source/reference
pKD3C	*pGB2 (repA^{TS}), ftsZ^{+}, Cam^{r}*	(Dai and Lutkenhaus, 1991)
pSD128	*pEXT22, Ptac::slmA Spc^{r} (with AGGAGG binding site)*	This study
pSD133	*pEXT22, Ptac::slmA, Spc^{r}*	This study
pUC18K	*pUC18, Kan^{r}*	This study
p2SBSK	*pUC18, with SBS12-SBS17 Kan^{r}*	This study
pQE80-slmA	*pQE80, Plac::6×his-slmA, Amp^{r}*	This study
pKNT25	*Plac::T25, Kan^{r}*	This study
pUT18	*Plac::T18, Amp^{r}*	This study
pZT25	*pKNT25, Plac::ftsZ-T25, Kan^{r}*	This study
pZT18	*pUT18, Plac::ftsZ-T18, Amp^{r}*	This study
pSlmA-T25	*pKNT25, Plac::slmA-T25, Kan^{r}*	This study
pSlmA-T18	*pUT18, Plac:;slmA-T18, Amp^{r}*	This study
pBANG112	*pACYC, ftsZ^{+}, AmP^{r}*	(Shen and Lutkenhaus, 2009)
pBANG59	*pEXT22, Ptac::minC/minD, Spc^{r}*	(Shen and Lutkenhaus, 2009)
pBS31	*pDSW208, Ptrc::sulA, Amp^{r}*	(Shen and Lutkenhaus, 2010)
pSD119	*pBAD18, Plac::6×his-ftsZ, Amp^{r}*	This study
pSD198	*pQE80, Plac::zipA$_{185-328,}$ Amp^{r}*	This study
pSEB160	*pBAD18, Plac::ftsZ, Amp^{r}*	*Pichoff, S*
pSUMO-SlmA	*pE-SUMO,P$_{T7}$::his-SUMO-SlmA, Amp*	This study

Table 3. FtsZ mutants used in this study

FtsZ alleles	Complementation	Resistance to SBS-SlmA	Resistance to MinCD	Interaction with SBS-SlmA *in vitro*	Source
WT	YES	NO	NO	YES	Collection
K190I	YES	YES	NO		This study
K190V	YES	YES	NO	YES	This study
K190L	YES	YES			This study
K190A	YES	YES			This study
K190N	YES	YES			This study
K190E	YES	YES			This study
K190W	YES	YES			This study
K190R	YES	NO			This study
D86N	YES	YES	NO	YES	This study
D86V	YES	NO			This study
D86K	YES	YES			This study
D86N& K190V	YES (≥37 °C)	YES			This study
L270V	YES	NO	YES ($MinC^{N}D$)		(Shen and Lutkenhaus, 2009, 2010)
R271G	YES	NO	YES ($MinC^{N}D$)		
E276D	YES	NO	YES ($MinC^{N}D$)		
N280D	YES	NO	YES ($MinC^{N}D$)		
D373E	YES	NO	YES ($MinC^{c}D$)		
I374V	YES	NO	YES ($MinC^{c}D$)		
I374M	NO				This study
I374F	YES *(Δmin or Δslm A*)	NO			This study
I374L	NO				This study
I374Y	NO				This study
I374W	NO				This study
I374K	NO			NO	This study
A376P	YES	NO	YES ($MinC^{c}D$)		(Shen and Lutkenhaus, 2009)
L378E	NO			NO	This study
L378V	YES *(Δmin or Δslm A*)		YES ($MinC^{c}D$)		(Shen and Lutkenhaus, 2009)
K380M	YES	YES	YES ($MinC^{c}D$)	YES (Weaker)	
320	NO			NO	This study
360	NO			NO	This study

Blank indicates not determined.

Table 4. SlmA mutants used in this study

SlmA alleles	DNA Binding	FtsZ binding	complementation	Source
WT	YES	YES	YES	Collection
T33A	NO	YES	NO	(Cho et al., 2011)
F65A	YES	NO	NO	(Cho and Bernhardt, 2013)
R73D	YES	NO	NO	
N102A	YES (disassociate faster)	ND	NO	This study
V174F	YES (nonspecifically)	ND	NO	This study

ND: Not determined

N102A binds SBS but it disassociates much faster than WT SlmA

V174F cannot distinguish SBS from nonspecific DNA.

The resultant transductants were checked for UV sensitivity to confirm the inactivation of *recA* and the transductant was named DU11 (*W3110 leu+ ftsZ0 slmA<frt> recA::Tn10*)/pKD3C.

Strain SD139 and SD140 were constructed by transducing the $parC^{TS}$ allele from WM1033 (MG1655, *parC*281::Tn10) into strains W3110 and PS1603 respectively. The $parC^{TS}$ allele was linked to a Tn10 and tetracycline resistant transductants obtained at 30°C were checked for the TS phenotype at 42°C.

Strains SD160, SD163 and SD164 were constructed similarly by replacing the *ftsZ84* allele on the chromosome of the parental strain PS106 with the *ftsZ-K190V*, *ftsZ-D86N* or *ftsZ-K190V&D86N* alleles using the lambda RED system (Datsenko and Wanner, 2000). The PCR products of *ftsZ* fragments containing K190V, D86N or K190V&D86N mutations were electroporated into PS106/pKD46 induced with 0.04% arabinose for 3 hours at 30°C. The recombinants were selected on LB plates without salt at 42°C. 8 recombinants from the plates were randomly selected and then transformed with plasmid pSD133 and p2SBSK to check resistance to delocalized SBS bound SlmA. Recombinants resistant to SBS-SlmA were then checked for the presence of *ftsZ-K190V*, *D86N* or *ftsZ-K190V&D86N* by PCR and sequencing.

SD161 and SD165 were constructed simply by introduction of the *slmA::cat* allele from PS1603 into strain SD160 and SD163 through P1 transduction. Similarly, strain SD162 and SD167 were created by P1 transduction to introduce the *min::kan* allele from S4 into strain SD160 and SD163.

Strains SD170 and SD171 were created in two steps. The first step was to remove the *leu::Tn10* marker from SD160 and SD163 by transduction with P1 grown on PB143 (*leu+* $ftsZ^0$ *recA::Tn10*) and then selecting for Leu+ transductants at 37°C on M9 minimum medium. The colonies grown up were tested for tetracycline sensitivity and resistance to SlmA in the presence of the multicopy plasmid p2SBSK (carryies two SBS sites). The positive colonies were named SD168 and SD169 and then used as template for PCR to amplify the *ftsZ* gene and sequencing to make sure the colonies retained the K190V

or D86N mutation. The second step was to introduce the *parC*^{TS} allele into SD168 and SD169 obtained from the first step. We transduced SD168 and SD169 with P1 grown on WM1033 (*parC*^{TS}*-Tn10*) and selected for tetracycline resistance transductants at 30°. The colonies obtained were purified and tested for temperature sensitivity at 42°C and were named SD170 and SD171.

pUC18K was constructed by replacing the *bla* gene in pUC18 with *kan*. To do this, an *Xho*I site was first introduced into pUC18 (pUC18blaX) at the end of *bla*, using primers XhoI-5': 5'-GTAACTGTCAGACCAAGT*CTCGAG*ATATATACTTTAGATTG-3' and XhoI-3': 5'-CAATCTAAAGTATATAT*CTCGAG*ACTTGGTCTGACAGTTAC-3'. The *aph* coding sequence from pKNT25 was amplified by using primers Kan-5'-SspI: 5'-CAGT*AATATT*CTGATCAAGAGACAGGATGAG-3' and Kan-3'-XhoI: 5'-CAGT*CTCGAG*CATTTCGAACCCCAGAG-3'. The PCR product was digested with SspI and XhoI and cloned into the same sites in puC18blaX (XhoI) to generate pUC18K. A derivative of pUC18K was made by introducing a fragment containing SBS12 and SBS17 to create p2SBSK. This fragment was obtained by PCR using primers SBS12-F-HindIII: 5'-GCAT*AAGCTT*GCGAAGTGAACGCTAACTCACATCTAACAATGCGCTCATCG-3' and SBS17-R-EcoRI: 5'-GCAT*GAATTC*CGTTAGTGACCATTTACTTACTCAGGACGGGTGTGGTCGCCATG-3'. The resulting PCR fragment contains a segment of pBR322 sandwiched between the SBS12 and SBS17 sites, and was digested with EcoRI and HindIII and ligated into pUC18K cut with same enzymes.

Plasmid pSEB160 was created by S. Pichoff by inserting an SstI/HindIII digested fragment containing *ftsZ* into pBAD18 cut with the same enzymes (unpublished data). pSEB160 derivatives containing *ftsZ-360*, *ftsZ-K190V*, *ftsZ-D86N*, *ftsZ-I374K* and *ftsZ-L378M* were generated by site-directed mutagenesis.

Plasmid pSD119 was created by replacing the *ftsZ* coding sequence of pSEB160 with sequence encoding 6× His tagged *ftsZ* ampflied from pSEB160 using primers His-FtsZ-SstI: 5'-

TTC*GAGCTC*AGGCGACAGGCACAAATCGGAGAGAAATATG**CATCACCATCACCATCAC**TTT GAACCAATGGAACTTACC-3' and His-FtsZ-HindIII: 5'-GCCAAAACAG*AAGCTT*CCTCGAAACCCAAATTCCAGTCAATTC-3'. The amplified fragment was digested with SstI and HindIII and ligated to pSEB160 digested with the same enzymes. pSD119 derivatives for 6× His-*ftsZ*-320 and 6× His-*ftsZ*-360 expression were created by site directed mutagenesis by addition of two stop codons after codons FtsZ320 and FtsZ360. Primers used are FtsZ320: 5'-GGCATGGACAAACGT**TGATAA**ATCACTCTGGTGACC-3' and FtsZ360: 5'-GCTAAAGTCGTGAATGAC**TGATAA**CCGCAAACTGCGAAAG-3'.

The plasmid pSD128 was constructed by inserting an *Eco*RI and *Hin*dIII fragment containing the *slmA* coding sequence into the *Eco*RI and *Hin*dIII double digested pBANG59. The *slmA* containing fragment was amplified from chromosomal DNA using primers slmA-5'-EcoRI: 5'-AGT*GAATTC*TTTC**AGGAGG**ATAATGTAACATGGCAGAAAAACAAACTG-3' and slmA-3'-HindIII: 5'-GCG*AAGCTT*TTGGCGTTTAAAGAAACTC-3'. The ribosome binding site for *slmA* translation was changed to the consensus sequence –**AGGAGG-** through this approach. The pSD128 derivatives containing different mutations were constructed by site-directed mutagenesis.

Plasmid pSD133 containing *slmA* with its own ribosome binding site is otherwise similar to pSD128 and was constructed in a similar manner, but the *slmA* containing fragment was amplified from chromosomal DNA using different primer pairs: slmA-For: 5'-CGT*GAATTC*CGCCTGGCAAGTGCTTA-3' and slmA-3'-HindIII.

The plasmid pQE80-*slmA* was created by ligation of a *Bam*HI-*Pst*I fragment containing the *slmA* coding sequence and pQE80 (Qiagen) cut with the same enzymes. The fragment was amplified from chromosomal DNA using primers 5'-6×his-slmA: 5'-GT*GGATCC*GCAGAAAAACAAACTGCG-3' and ttk-PstI-3': 5'-GAAA*CTGCAG*CGGCGTCATATTACTGC-3'. Site-directed mutagenesis was used to introduce different *slmA* mutations into pQE80-*slmA* to obtain various derivatives.

The plasmid pSD198 was created by ligation of a *Bam*HI-*HindIII* fragment containing the *zipA*$_{185-328}$ coding sequence and pQE80 (Qiagen) cut with the same enzymes. The fragment was amplified from chromosomal DNA using primers zipA185-5'-BamHI: 5'-GACT*GGATCC*GATAAACCGAAGCGCAAAG -3' and zipA-3'-HindIII: 5'-GACT*AAGCTT*GGTTCGAAGAGGAGTTAAT-3'.

Plasmids pSlmA-T25 and pSlmA-T18 were constructed by inserting a *Bam*HI/*Hin*dIII cut fragment containing the *slmA* coding sequence into the vectors pKNT25 and pUT18, respectively, cut with the same enzymes. The fragment was amplified from chromosomal DNA using the primer pair slmA-BTHN-BamHI: 5'- GTC*GGATCC*TGCAACTGTGCCGCAAT-3' and slmA-BTHN-HindIII: 5'-TGT*AAGCTT*GGCAGAAAAACAAACTG-3'. Derivatives of pSlmA-T25 and pSlmA-T18 containing *slmA* mutations were created by site-directed mutagenesis. Plasmids pZT25 and pZT18 were made by inserting a *Bam*H1/*Hin*dIII fragment containing the *ftsZ* coding sequence into pKNT25 and pUT18, respectively. Derivatives of these plasmids containing various *slmA* mutations or *ftsZ* mutations were created by site-directed mutagenesis.

Plasmid pSUMO-SlmA was constructed by ligation of a BsaI-XbaI fragment containg the *slmA* coding sequence and pE-SUMO-amp (LiferSensors) cut with the same enzyme. The fragment was amplified from plasmid pSD133 using primers slmA-SUMO-F: 5'-ACGT*GGTCTC*GAGGTGCAGAAAAACAAACTGCGAAAAG-3' and SlmA-SUMO-R: 5'-CAGT*TCTAGA*GTCATCCGGCGTCATATTAC-3'.

Creation of the functional FtsZ mutant libraries and selection for SBS-SlmA resistant *ftsZ* mutations

The procedure was carried out as previously described for selection of MinCD resistant FtsZ mutants (Shen and Lutkenhaus, 2009). PCR random mutagengesis was used to introduce random mutations into the coding region of *ftsZ* gene using pBANG112 as the template and primers: 5'-

GCCTCAGGCGACAGGCACAAATCGGAGAG and 5'-GCTGCAGATATTCGATATCACGCATGAAAC. The purified PCR fragments were then digested with EcoRI and EagI and ligated into pBANG112 digested with the same enzymes. The ligation product was then electroporated into DU11/pKD3C and transformants selected at 42°C on LB plates with ampicillin. All colonies that grew up were pooled together and part of the pooled culture was subjected to plasmid extraction to make a stock of the FtsZ mutant library. To select for the SBS-SlmA resistant FtsZ mutants, the rest of the pooled cells was transformed with plasmid pSD133 and p2SBSK and colonies resistant to delocalized SBS-SlmA were selected with 20 μM IPTG at 30°C on plates containing ampicillin, spectinomycin and kanamycin. Plasmids were isolated from the colonies that grew up and the *ftsZ* gene in the plasmids was sequenced to identify the mutations.

Bacterial two hybrid assay

To detect SlmA-FtsZ and SlmA-SlmA interactions, appropriate plasmid pairs encoding FtsZ-T18 and SlmA-T25 or FtsZ-T18 and SlmA-T25 or their variants were co-transformed into BTH101. Single colonies were resuspended in 1 ml LB medium and 3 μl of each aliquot was spotted on LB plates containing 100 μg/ml ampicillin, 25 μg/ml kanamycin, 40 μg/ml X-gal and 250 μM IPTG. Plates were incubated at 30°C for 36 hours before analysis.

Protein purification

His-SlmA and its variants containing different mutations were expressed and purified from JS238/pQE80-*slmA* and its derivatives following the protocol used to purify 6×his-ZapA (Dajkovic et al., 2008b). An overnight culture of each strain grown in LB with ampicillin (100 μg/ml) and glucose (0.2%) was diluted 1:100 into 1 L fresh LB medium supplemented with ampicillin (100 μg/ml) and incubated at 37°C until OD_{540} reached about 0.4. IPTG was then added to the culture to a final concentration of 1 mM and incubated at 37°C for another 3 hours. Cells were collected by centrifugation, washed with 10 mM Tris-HCl (pH 7.9), and frozen at -80°C until used. On the day of purification, the cells were thawed and

resuspended in 20 ml lysis buffer (20 mM Tris-HCl [pH7.9], 70 mM NaCl and 20 mM imidazole) and passed through the French press twice (10,000 psi). The lysates were then centrifuged at 12,000 rpm for 15 min at 4°C to remove cell debris. The supernatants were removed and loaded onto pre-equilibrated Ni-NTA resin (Qiagen). The column was washed once with high salt wash buffer (20 mM Tris-HCl [pH 7.9], 500 mM NaCl and 20 mM imidazole). It was washed again with the same buffer except the imidazole concentration was increased to 50 mM. The bound protein was eluted with elution buffer (20 mM Tris-HCl [pH 7.9], 500 mM NaCl and 250 mM imidazole). The peak fractions were dialyzed against the storage buffer (25 mM Tris-HCl [pH 7.9], 200 mM KCl, 1 mM EDTA and 10% glycerol) overnight and stored at -80°C until use.

The untagged version of SlmA was expressed and purified from BL21 (λDE3)/pLysS cells containing pSUMO-SlmA. Purification of the H-SUMO-SlmA fusion protein was similar to purification of the 6×his-SlmA. After dialysis, the H-SUMO tag was cleaved with purified 6×His-tagged SUMO protease (Ulp1) for 1 hour at 30°C in the protein storage buffer (25 mM Tris-HCl [pH 7.9], 200 mM KCl, 1 mM EDTA and 10% glycerol) with 1 mM DTT. The released tag and protease were removed by passing it through the pre-equilibrated Ni-NTA resin. Untagged SlmA was collected in the flow through, concentrated and stored at -80°C.

N-terminal 6×His-tagged FtsZ-FL, FtsZ320 and FtsZ360 were purified from JS238 cells containing plasmids pSD119, pSD119-Z320 or pSD119-Z360 respectively. An overnight culture of each strain grown in LB with ampicillin (100 μg/ml) and glucose (0.2%) was diluted 1:100 into 1 L fresh LB medium supplemented with ampicillin (100 μg/ml) and incubated at 37°C until OD_{540} reached about 0.4. Arabinose was then added to the culture to a final concentration of 0.2% and incubated at 37°C for another 3 hours. Cells were collected by centrifugation, washed with 10 mM Tris-HCl (pH 7.9), and frozen at -80°C until used. The subsequent procedures were similar to purification of 6×his-SlmA.

Induction of wild type FtsZ, FtsZ-K190V and FtsZ-D86N was similar to induction of 6×His-tagged FtsZ-FL in JS328 cells containing pSEB160, pSEB160-360, pSEB160-K190V, pSEB160-D86N, pSEB160-I374K and pSEB160-L378E respectively. After collecting the cells, FtsZ-WT, FtsZ-K190V and FtsZ-D86N as well as the other mutant proteins were purified according to the procedure described previously (Mukherjee and Lutkenhaus, 1998b; Shen and Lutkenhaus, 2009).

FtsZ polymerization and Electron Microscopy

FtsZ polymerization reactions were in FtsZ Pol buffer (50 mM HEPES-NaOH [pH 8.0], 200 mM KCl and 10 mM $MgCl_2$). The SBS17 fragment (30 bp) and SlmA or SlmA mutants were mixed together in a separate tube and incubated at room temperature for 10 minutes before addition to the polymerization reactions. Unless specified, the SlmA used was His tagged SlmA. The SBS17 probe used here was prepared by annealing two un-labeled complementary 30 base oligonucleotides SBS17-F and SBS17-R. FtsZ was added to a final concentration of 2 μM in a 50 μl reaction containing pre-formed SBS17-SlmA, or SBS17 alone, or SlmA or just DNA binding buffer. After 5 min incubation, GTP or GMPCPP was added to a final concentration of 1 mM and incubation at room temperature continued for another 5 min before the samples were loaded onto grids. 15 μl of 1% uranyl acetate was spotted on the grid for 1 min and blotted away. The grids were air-dried and imaged on a JEOL-JEM-1400 transmission electron microscope.

The co-sedimentation assay was performed similarly as above except that the protein concentrations were 5 μM. After the addition of GMPCPP, the reactions were subjected to ultracentrifugation at 80,000 rpm for 15 min at 25°C in TLA100.2 rotor and a Beckman TL-100 centrifgue. Supernatants and pellets were then analyzed by SDS-PAGE.

Biolayer interferometry assays

The assays were performed in 250 μl of 1× FtsZ polymerization buffer (50 mM HEPES-NaOH [pH 8.0], 200 mM KCl, 10 mM $MgCl_2$) with the BLItz^{TM} system (FortéBio) at room temperature. The

biotinylated SBS17 probe was prepared by annealing two complementary 30 base oligonucleotides, the biotinylated-SBS17-F and SBS17-R. FtsZ and SlmA proteins were diluted in 1× FtsZ polymerization buffer before the test. To measure the binding affinity of SlmA variants for the biotinylated SBS17 probe, streptavidin-coated biosensors tips were equilibrated with 1× FtsZ polymerization buffer to establish a baseline prior to bionylated SBS17 immobilization. 250 µL of 1× FtsZ polymerization buffer containing 50 nM biotinylated SBS17 was incubated with the biosensor tips with shaking at 2,200 rpm for 5 minutes. After the immobilization, the biosensor tips were washed with 1× FtsZ polymerization buffer for 10 seconds. Association of SlmA-WT or SlmA mutants to the biosensors was monitored for 2 minutes in 250 µl 1× FtsZ polymerization buffer containing 4 µM SlmA with agitation at 2,200 r.p.m. Dissociation was initiated by dipping the biotinylated SBS17-SlmA coated biosensor tips into 250 µl of 1× FtsZ polymerization buffer, and the process was monitored continuously for 2 minutes while agitating at 2,200 rpm. Data were obtained automatically by the BLItz^{TM} User Software version and were subsequently analyzed by global fitting using the GraphPad Prism 5 software.

Binding of FtsZ to the biotinylated-SBS17-SlmA complex was performed similarly as above. After association of SlmA-WT or SlmA mutant to the biotinylated SBS17 coated biosensor tips, the tips were washed with 250 µl of 1× FtsZ polymerization buffer for 10 seconds. FtsZ was preincubated with 1 mM GDP for 5 minutes before the SBS17-SlmA complex coated biosensor tips were dipped into the solution. ZipA*185-328* was added at different concentrations with GDP in the test to see whether it blocked FtsZ binding to SBS-bound SlmA. Association was monitored for 1 minute in 250 µl of 1× FtsZ polymerization buffer containing 4 µM FtsZ with agitation at 2,200 rpm followed by dissociation in the same buffer without FtsZ for 2 minutes. Data were collected and analyzed with Graphpad Prism 5.

Binding of FtsZ tail peptide Ztail-WT, Ztail-I374K or Ztail-L378E to the biotinylated-SBS17-SlmA complex was performed similarly as above. After association of SlmA-WT or SlmA mutant to the biotinylated SBS17 coated biosensor tips, the tips were washed with 250 µl of 1× FtsZ polymerization

buffer for 10 seconds and then dipped into the solution containing different concentrations of FtsZ tail peptides. Association was monitored for 1 minute with agitation at 2,200 rpm followed by dissociation in the same buffer without peptide for 2 minutes. Data were collected and analyzed by Graphpad Prism 5.

In a reciprocal approach, 6×His-tagged FtsZ-FL, FtsZ320 or FtsZ360 was immobilized at the surface of Ni-NTA biosensors and untagged SlmA preincubated with or without SBS DNA was tested for binding to 6×His-tagged FtsZ variants. In these assays, 250 µL of 1× FtsZ polymerization buffer containing 1 µM 6×His-tagged FtsZ varients was incubated with the biosensor tips with shaking at 2,200 r.p.m for 5 minutes. After the immobilization, the biosensor tips were washed with 1× FtsZ polymerization buffer for 10 seconds. Association of untagged SlmA preincubated with or without SBS DNA to the biosensors was monitored for 2 minutes in 250 µl 1× FtsZ polymerization buffer with agitation at 2,200 r.p.m. To test if Ztail peptides competed with FtsZ for binding, different concentrations of Ztail-WT or its mutant versions were preincubated with untagged SlmA in the presence of SBS DNA for 5 minutes. Dissociation was initiated by dipping the FtsZ-SBS-SlmA coated biosensor tips into 250 µl of 1× FtsZ polymerization buffer, and the process was monitored continuously for 2 minutes while agitating at 2,200 r.p.m. Data were generated automatically by the BLItz^{TM} User Software version and were subsequently analyzed by global fitting using the GraphPad Prism 5 software.

Western blot

Overnight cultures of PS1603 (W3110 *slmA::cat*) containing pSD133 expressing various *slmA* mutants were diluted 100 fold in LB medium supplemented with appropriate antibiotics without or with 5 µM IPTG, 10 µM or 100 µM IPTG. W3110 and PS1603 were run in the second and third lanes as controls. The cultures were grown at 30°C until the OD_{600} reached about 0.4. At this time 1 ml from each culture was spun down and the pellet resuspended in 100 µl sample buffer, heated for 5 min, and 10 µl from each sample was then loaded onto the gel for analysis.

Continuous GTPase assay

GTPase activities of wild type FtsZ, FtsZ-K190V and FtsZ-D86N were calculated using the NADH coupled enzymatic assay (Ingerman and Nunnari, 2005). The reactions were carried out at room temperature in 200 µl volume using the FtsZ polymerization buffer (50mM HEPES-NaOH [pH 8.0], 200 mM KCl, 10 mM MgCl2), plus 1 mM PEP-K, 0.5 mM NADH, 5 µL PK/LDH and 0.5 mM GTP. FtsZ or various mutants were added to a final concentration of 2.5 µM. NADH depletion is directly proportional to GTP hydrolysis, thus the reactions were continuously monitored for NADH absorbance at 340 nm for 30 minutes. The data was collected and then plotted using the Prism 5.0 software, and the reaction rates were calculated using the Beer-Lambert law ($A= \varepsilon \times c \times l$).

Chapter III: Study of FtsZ mutants resistant to the NO function of SlmA suggests that SlmA antagonizes FtsZ polymerization by interfering with the communication between the N and C terminal sub-domains of FtsZ

Abstract

Spatiotemporal regulation of Z ring formation is necessary to prevent aberrant cell division in bacteria. In *E. coli*, the nuceloid occlusion (NO) protein SlmA contributes to the coordination of cell division with chromosome segregation by blocking Z ring formation over the nucleoid. Recent studies have shown that SlmA oligomerizes on specific DNA sequences (SBSs) in the chromosome and the SBS bound SlmA affects FtsZ assembly. However, how SBS bound SlmA affects FtsZ assembly is controversial; one model suggests that SBS-SlmA severs FtsZ proto-filaments and another suggests that SlmA sequesters FtsZ filaments to the SBS-SlmA complexes. Here, we report the isolation and characterization of two FtsZ mutants, FtsZ-K190V and FtsZ-D86N, which are resistant to the NO function of SlmA. By analyzing these two mutants, we found that SBS-SlmA indeed antagonizes FtsZ polymerization and our mutants are resistant to the action of SlmA. One of the mutants, FtsZ-D86N, likely confers resistance to SlmA by increasing the lateral interaction of FtsZ proto-filaments. The second mutation FtsZ-K190V locates in the H7 Helix of FtsZ, which has been showed to undergo dramatic conformational changes upon nucleotide exchange and to be important for the communication between the two sub-domains of FtsZ. The positive charge of K190 appears to be critical for sensitivity of SlmA but not for FtsZ-SlmA binding. Our data suggest that SlmA takes advantage of the positive charge of K190 to antagonize FtsZ polymerization by affecting the conformational change occurred upon FtsZ assembly.

Introduction

As mentioned in chapter I, the nucleoid occlusion protein SlmA of *E.coli* coordinates cell division and chromosome segregation by directly blocking Z ring formation over the nucleoid (Bernhardt and de Boer, 2005). Accumulated evidences show that this inhibition of Z ring formation relies on two interactions, SlmA-DNA interaction and SlmA-FtsZ interaction, which are mediated by the N terminal and C terminal domains of SlmA respectively (Cho and Bernhardt, 2013; Cho et al., 2011). Disruption of either one of the two interactions renders the cells deficient in NO (Cho and Bernhardt, 2013; Cho et al., 2011).

The N terminal domain of SlmA forms a canonical HTH motif found in every TetR family protein (Tonthat et al., 2011). When dimerized, the two HTH motifs function as two arms of a SlmA dimer that insert into the grooves of DNA and lock the SlmA dimer on DNA (Tonthat et al., 2013). Residues important for SlmA DNA binding have been revealed by the structures of SlmA in complex with its specific DNA binding sequence (SBS) (Tonthat et al., 2013). Notably, SlmA-T33A abolishes the DNA binding activity of SlmA and renders it defective in NO (Cho et al., 2011). Comparison of the DNA-free and DNA-bound SlmA structures showed that dramatic conformational changes occur upon SlmA binding to DNA (Tonthat et al., 2013). The region between the DNA binding and dimerization domains (residues 103-125) displays various degree of flexibility in the DNA-free forms, but this region adopts a rigid conformation in the DNA bound SlmA dimer (Tonthat et al., 2013). Another region that shows significant change is the the predicted FtsZ binding region. This region is partially occluded by the DNA binding domain of SlmA in the DNA-free structure, but it is fully exposed in the DNA-bound form (Cho and Bernhardt, 2013; Tonthat et al., 2013). Interestingly, SlmA forms an oriented dimer-of-dimers on DNA molecules containing the SBS consensus sequence (GTgAGtaCTcAC), similar to another TetR family protein QacR which also binds DNA as an oriented dimer-of-dimers (Schumacher et al., 2002; Tonthat et al., 2013). However, different than QacR, these SlmA dimer-of-dimers can spread on the

DNA. Formation of SlmA dimer-of-dimers and spreading on the DNA are believed to be critical for SlmA to prevent Z ring formation *in vivo*, but direct evidence is missing so far. The *E. coli* chromosome contains about 24 to 52 SlmA binding sites which are mainly distributed in the origin proximal region of the chromosome (Cho et al., 2011; Tonthat et al., 2011). Thus, the activity of SlmA is spatially and temporally restricted to the locations occupied by the origin-proximal region of the chromosome, allowing Z ring to form once the origin proximal regions are segregated away from the midcell.

The C-terminal domain of SlmA mediates dimerization and interaction with FtsZ (Bernhardt and de Boer, 2005; Cho et al., 2011; Tonthat et al., 2011). Even though studies of the DNA binding mutant SlmA-T33A suggest that SlmA may exist as monomers in the absence of SBS DNA, accumulated evidences indicate that it forms dimers without binding to SBS DNA and SBS DNA binding serves to promote its oligomerization and binding to FtsZ (Cho et al., 2011; Tonthat et al., 2011; Tonthat et al., 2013). Residues important for FtsZ binding have been revealed by an elegant genetic screen by the Bernhardt lab, and include F65, R73, L94, G97, R101 and N102 (Cho and Bernhardt, 2013; Cho et al., 2011). All these residues, when mutated, reduce or eliminate the SlmA-FtsZ interaction and thus abolish the NO function of SlmA. Intriguingly, although SlmA forms a dimer-of-dimers on the SBS DNA, only one FtsZ-interaction interface per dimer is required for SlmA to mediate NO (Cho and Bernhardt, 2013).

In vivo, SlmA associated with DNA blocks FtsZ assembly into the Z ring over the nucleoid until chromosome segregation occurs. This spatiotemporal regulation of Z ring formation depends on the proper localization of SlmA onto its SBSs. When additional SBSs are provided in a multi-copy plasmid that can diffuse randomly inside the cells, SlmA is de-localized to the plasmid and blocks FtsZ assembly throughout the cell (Cho et al., 2011). However, at the molecular level, how SBS bound SlmA prevents FtsZ to assemble into the Z ring is not clear. Results from the Bernhardt lab suggest that when bound with SBS DNA, SlmA stimulates the GTP hydrolysis of FtsZ and disassembles FtsZ proto-filaments (Cho et al., 2011). As SBS-SlmA induced disassembly of FtsZ proto-filaments requires the GTPase activity of

FtsZ, it has been proposed that SBS-SlmA breaks the FtsZ filaments at position where GTP has been hydrolyzed to GDP (Cho et al., 2011). This mechanism is similar to the N terminal domain of MinC, which also prevents Z ring formation (FtsZ polymerization) (Shen and Lutkenhaus, 2010). However, SlmA was observed to have no impact on FtsZ GTPase activity and proto-filament formation by the Schumacher group, which proposed that SlmA prevents Z ring formation by sequestration of FtsZ proto-filaments onto the SlmA-DNA complexes that are unable to support Z ring formation (Tonthat et al., 2013). Here, we tried to understand the SlmA-FtsZ interaction by studying FtsZ mutants resistant to the NO function of SlmA *in vivo*. Our data showed that SBS bound SlmA indeed disassembles FtsZ proto-filaments, consistent with the Bernhardt group. In addition, analysis of the FtsZ mutants suggests that SlmA antagonizes FtsZ polymerization by affecting the conformational change during FtsZ assembly.

Results

Overexpression of SlmA blocks cell divison and condenses the chromosome

Opposing models have been proposed for how SlmA acts on FtsZ to prevent its assembly into the Z ring. However, the SlmA-interaction interface on FtsZ has not been identified, hindering our understanding of SlmA-FtsZ interaction. As SlmA overexpression blocks cell division and causes cell death by recruiting FtsZ to the nucleoids (Bernhardt and de Boer, 2005), we tried to screen for FtsZ mutants that were resistant to SlmA overexpression mediated killing, reasoning that *ftsZ* mutations disrupting the FtsZ-SlmA interaction should rescue the cells from SlmA overexpression. However, we were unable to isolate any SlmA resistant FtsZ mutant. Using SlmA-R73 as a control, we found that overexpression of this mutant also blocked colony formation on plates due to severe chromosome condensation (Fig. 11), which had been indicated by previous studies (Cho et al., 2011). This chromosome condensation is due to the DNA binding activity of SlmA as combining the T33A mutation and R73D mutations eliminated the DNA condensation effect (data not shown). Overexpression of the DNA binding mutant SlmA-T33A only led to cell division block (Fig 11). This result explained the

difficulty of obtaining FtsZ mutants resistant to SlmA overexpression because FtsZ mutants resistant to the division inhibitory activity of SlmA would die of chromosome condensation. Interestingly, we did not observe chromosome condensation by SlmA-WT overexpression unless the protein was expressed at extremely high level, suggesting that either the cell division block caused by SlmA dominates over the chromosome condensation effect or FtsZ counteracts the effect SlmA has on condensation.

Isolation of FtsZ mutants resistant to de-localized SBS-SlmA

De-localization of SBS-SlmA by providing the cells with extra copies of SBSs in a randomly distributed plasmid also leads to severe cell division block and cell death by blocking Z ring formation throughout the cells (Fig. 13A) (Cho et al., 2011). In contrast to overexpression, this killing does not require dramatic overexpression of SlmA, as shown in Fig. 12A. 10 μM IPTG was enough to block colony formation of a strain expressing SlmA from plasmid pSD133 (P*tac::slmA*, note that the pSD128 used above expressed a much higher level of SlmA because the original ribosome binding site for SlmA was changed to the consensus AGGAGG) and containing extra copies of SBS in a multi-copy plasmid (p2SBSK, pUC18K with SBS12 and SBS17). Western blot showed that at this IPTG concentration, SlmA was overexpressed about 4 fold (Fig. 12D). This killing by SlmA depended upon the SlmA-DNA interaction and SlmA-FtsZ interaction as disruption of either one of these two interactions by known *slmA* mutations rescued growth, as shown here (Fig 12A) and by previous studies (Cho and Bernhardt, 2013). In theory, mutations in *ftsZ* that disrupt the FtsZ-SlmA interaction should also rescue the cells. Therefore, we decided to screen for FtsZ mutants under these conditions. We first created a functional FtsZ mutant library by PCR random mutagenesis over the coding region of FtsZ using the plasmid pBANG112 in the strain DU11/pKD3C [*W3110 ftsZ^{0} recA::Tn10 slmA<frt>/pKD3C ftsZ^{+}*](Fig. 13B). pBANG112 has been reported to produce about the chromosomal amount of FtsZ (Shen and Lutkenhaus, 2009). The resultant strain DU11/pBANG112^{M} (M stands for mutant library) was transformed with plasmid p2SBSK and

Fig. 11. Overexpression of SlmA blocks cell division and condenses the chromosome. A) A spot test to test the toxicity of overexpression of SlmA and various mutants. pSD128 (P*tac::slmA*) or its derivatives containing the T33A or R73D mutations was transformed into the Δ*slmA* strain PS1603 (W3110 *slmA::cat*). Single colonies were picked in LB, serially diluted ten fold and 3 µl of each dilution was spotted on plates containing spetinomycin and chloramphenicol with or without IPTG and incubated at 37°C overnight. B) DAPI staining of PS1603 cells expressing *slmA* alleles from pSD128. Overnight cultures of the strains containing the plasmids were diluted 100 times in LB supplemented with antibiotics and incubated at 37°C. At OD_{540} 0.3, the cultures were diluted 10 fold in fresh LB medium with 40 µM IPTG. Cultures were incubated for an additional 2 hours at 37°C and DAPI (final concentration 200 ng/ml) added to the culture 20 min before imaging.

A.

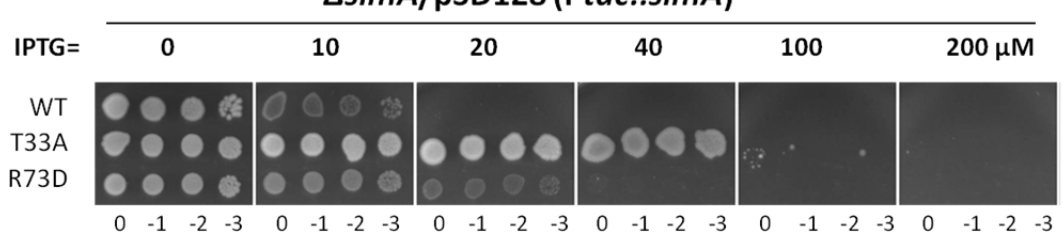
ΔslmA/pSD128 (Ptac::slmA)
IPTG= 0 10 20 40 100 200 μM
WT
T33A
R73D
0 -1 -2 -3 0 -1 -2 -3 0 -1 -2 -3 0 -1 -2 -3 0 -1 -2 -3 0 -1 -2 -3

B.

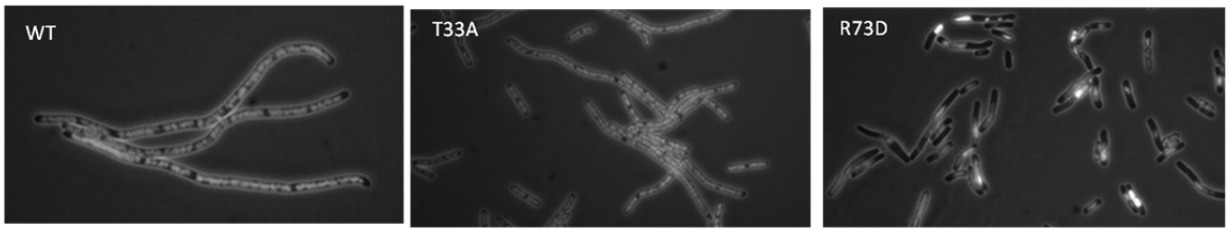
ΔslmA/pSD128 (40 μM IPTG) DAPI staining
WT
T33A
R73D

Fig. 12. De-localized SlmA blocks cell division without dramatic overexpression of SlmA. A) Spot test to check the response of SlmA variants to mislocalized SBSs (contained on a multicopy plasmid). The method was similar to Figure 11A. The plasmid pSD133 (P*tac::slmA*) and its derivatives in combination with pUC18K (Vector) or p2SBSK (2xSBS) were transformed into PS1603 (W3110 *slmA::cat)*. The plates were incubated at 30°C for 20 hours with or without IPTG as indicated. B) Morphology of cells expressing SlmA or SlmA mutants in the presence of pUC18K or p2SBSK from Figure 12A. Cells from the spots at the indicated IPTG concentrations from Figure 12A were resuspended in 200 μL LB medium and examined by phase microscopy. C and D) Western blot to compare the protein level of SlmA mutants and to determine the SlmA level at different concentration of IPTG. Overnight cultures of PS1603 (W3110 *slmA::cat*) containing pSD133 expressing various *slmA* mutants were diluted 100 fold in LB medium supplemented with appropriate antibiotics without or with 5 μM IPTG, 10 μM IPTG or 40 μM IPTG. W3110 and PS1603 were run in the second and third lanes as controls. The cultures were grown at 30°C until the OD_{540} reached about 0.4. At this time 1 ml from each culture was spun down and resuspended in 100 μl sample buffer, heated for 5 min, and 10 μl from each sample or its dilutions was then loaded onto the gel for analysis.

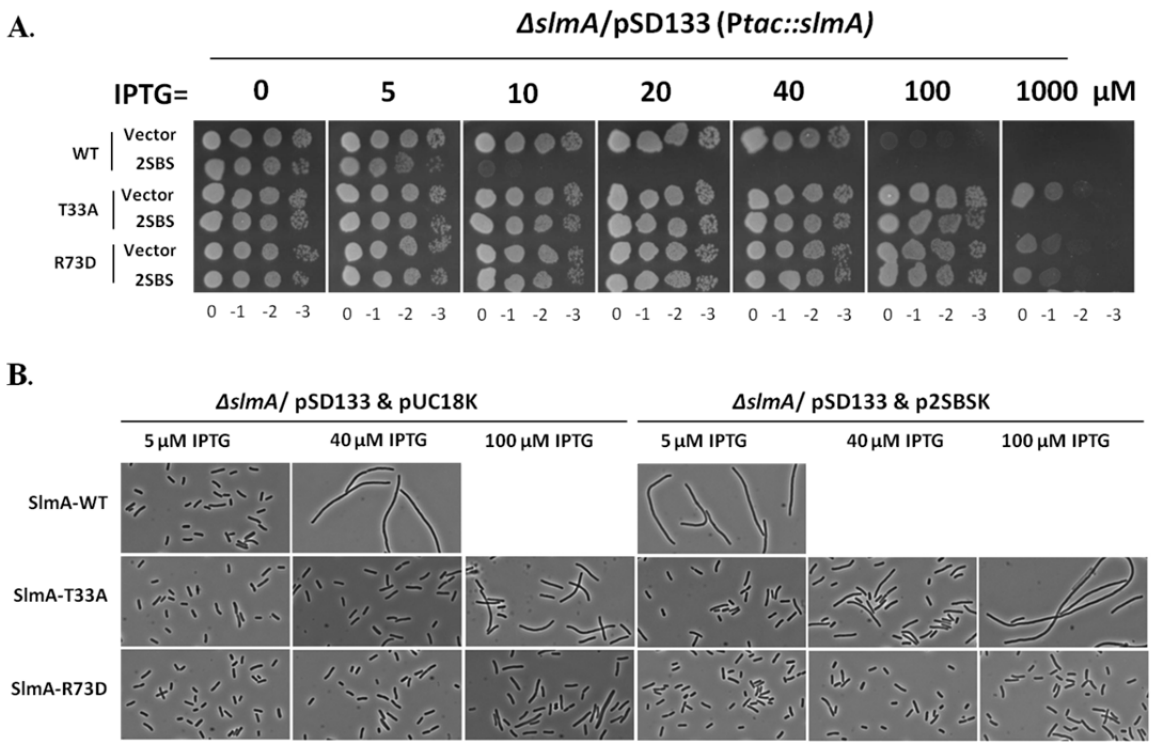
A.
ΔslmA/pSD133 (Ptac::slmA)
IPTG= 0 5 10 20 40 100 1000 μM
WT Vector
2SBS
T33A Vector
2SBS
R73D Vector
2SBS
0 -1 -2 -3
B.
ΔslmA/ pSD133 & pUC18K
ΔslmA/ pSD133 & p2SBSK
5 μM IPTG
40 μM IPTG
100 μM IPTG
SlmA-WT
SlmA-T33A
SlmA-R73D

C.

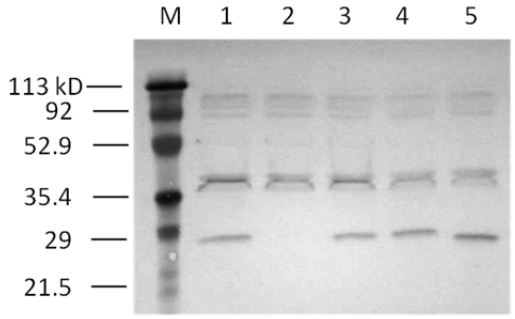

1: W3110
2: W3110 slmA::cat
3: W3110 slmA::cat/pSD133 (5 μM IPTG)
4: W3110 slmA::cat/pSD133-T33A (5 μM IPTG)
5: W3110 slmA::cat/pSD133-R73D (5 μM IPTG)

D.

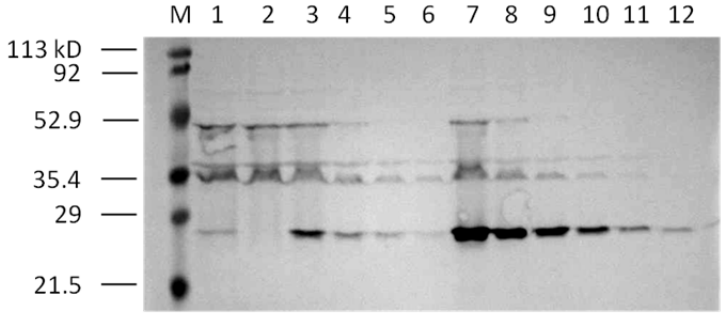

1: W3110
2: W3110 slmA::cat
3: W3110 slmA::cat/pSD133 (10 μM IPTG)
4: 1/2 dilution of 3
5: 1/4 dilution of 3
6: 1/8 dilution of 3
7: W3110 slmA::cat/pSD133 (100 μM IPTG)
8: 1/2 dilution of 7
9: 1/4 dilution of 7
10: 1/8 dilution of 7
11: 1/16 dilution of 7
12: 1/32 dilution of 7

pSD133 and survivors selected in the presence of 20 μM IPTG (cells with wild type FtsZ would be unable to form colonies at 10 μM IPTG). Plasmids were isolated from the survivors and subjected to sequencing to identify *ftsZ* mutations.

Sequence analysis revealed that most of these SlmA resistant FtsZ mutants contained one amino acid substitution at the H7 helix that connects the two sub-domains of FtsZ (*ftsZ-K190I,* Fig 13C&D). Some of the *ftsZ- K190I* containing mutants had additional amino acid substitutions, but when these mutations were introduced into pBANG112, no resistance to SlmA was observed (data not shown). Therefore, these mutations were discarded. Another mutation *ftsZ-D86N* locating at the H3 helix also appeared twice as a double mutant *ftsZ-D86N&G95D* and a triple mutant *ftsZ-D86N&S246Y&M344I* (Fig 13D). Later analysis showed that the resistance was mainly due to D86N. Both *ftsZ-K190I* and *ftsZ-D86N* mutations, when introduced into pBANG112, complemented the *ftsZ* depletion strain DU11/pKD3C at 42°C, 37°C or 30°C, although both seemed to cause a twisted-septum phenotype at or below 37°C (data not shown).

Since *ftsZ-K190I* and *ftsZ-D86N* affected division morpholgy, we substituted *ftsZ-K190* and *ftsZ-D86* with other amino acids to see whether we could obtain mutants that retain resistance to SlmA but with normal division function. For *ftsZ-K190*, changing it to Ala, Leu, Glu, Asp, Trp and Val all conferred some resistance to SlmA in the presence of extra copies of SBS, but only K190V showed similar resistance as *ftsZ-K190I* and displayed better morphology (Fig 13C). Interestingly, *ftsZ-K190R* did not show any resistance to SlmA in the presence of the extra copies of SBS, suggesting that the positive charge at this position is important for the sensitivity to SBS-SlmA. Changing D86 to Lys also reduced the sensitivity to SBS-SlmA, but the FtsZ-D86K mutant displayed a more severely twisted septum (Fig 13C and data not shown). Substitution of D86 to Val did not provide any resistance to SlmA. Since FtsZ-K190V and FtsZ-D86N showed the most resistance to SlmA in the presence of extra copies of SBS with the least affect on septal morphology, they were chosen for further study.

Fig. 13. Mutations in two different regions of FtsZ confer resistance to de-localized SlmA. A) Principles of screening for FtsZ mutants that are resisant to the de-localized SBS-SlmA. SlmA dimer-of-dimers (orange ovals) localized to specific loci on the nucleoid do not affect Z ring formation at the midcell such that cell division and growth are not inhibited. However, in the presence of a multicopy plasmid that carries SBS, SlmA dimer-of-dimers are delocalized to the plasmids. These delocalized SBS-SlmA blocks Z ring formation throughout the cell, resulting in cell filamentation and inhibition of growth on LB plates. This cell death depends on the interaction of SlmA with DNA and FtsZ as elimination of DNA binding by T33A mutation or elimination of interaction with FtsZ by R73D mutation allow cells survive in the presence of extra copies of SBS in the plasmid. Mutations on FtsZ that disrupt FtsZ-SlmA interaction should also allow cells survive regardless of the delocalized SBS-SlmA. B) Steps to screen for the SlmA resistant FtsZ mutants. C) A spot test of the resistance of FtsZ mutants to the de-localized SBS-SlmA. Plasmids pSD133 (P*tac::slmA*) and p2SBSK (pUC18 with 2SBS sites) were introduced into the *ftsZ*- strain DU11 (*ftsZ*^{0} *slmA<frt> recA::Tn10*) complemented with pBANG112 or its derivatives containing different *ftsZ* alleles. One colony of each resultant strain was resuspended in 1ml LB medium, serially diluted by 10 and 3 µl from each dilution was spotted on LB plates containing various concentrations of IPTG and supplemented with ampicillin, spectinomycin and kanamycin. The plates were incubated at 30°C for 30 hours before being photographed. pUC18K was used as control for resistance to the overproduction of SlmA. D.) Locations of the *ftsZ* mutations that showed resistance to delocalized SBS-SlmA. The structure of the FtsZ monomer from *Pseudomonas* (PDB# 1OFU) is shown and the residues corresponding to those mutated in *E. coli* are indicated. FtsZ-K190 (*A190 in Pseudomonas*) is in blue and FtsZ-D86 in red.

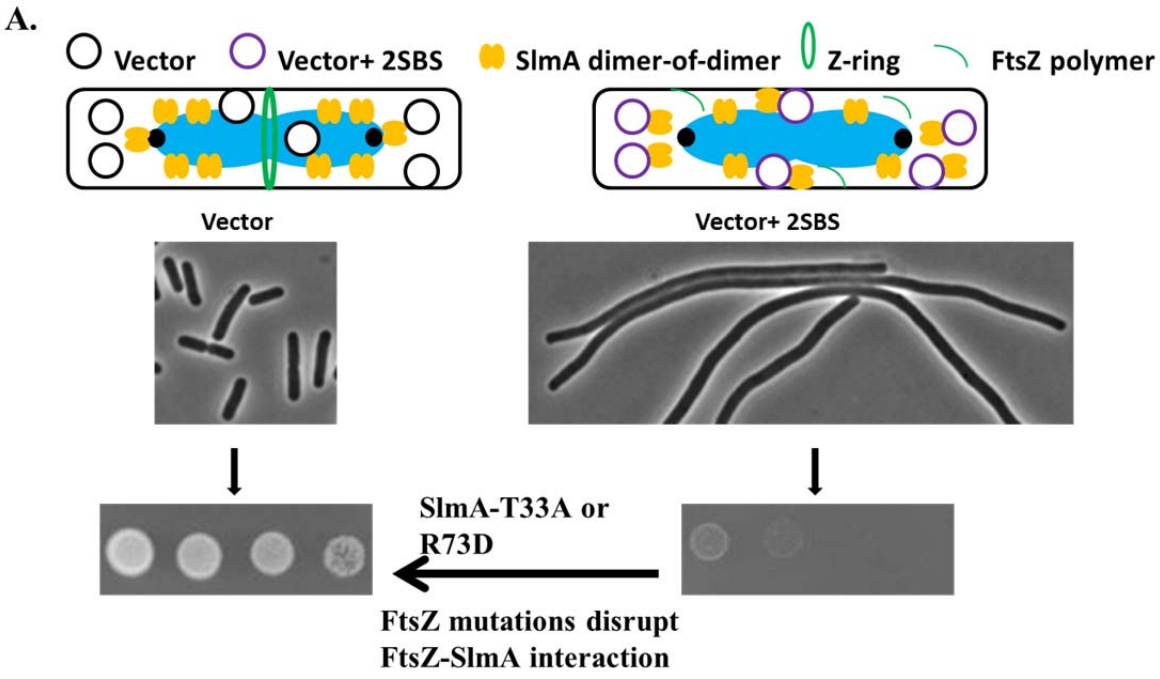
A.
Vector
Vector+ 2SBS
SlmA dimer-of-dimer
Z-ring
FtsZ polymer
Vector
Vector+ 2SBS
SlmA-T33A or
R73D
FtsZ mutations disrupt
FtsZ-SlmA interaction

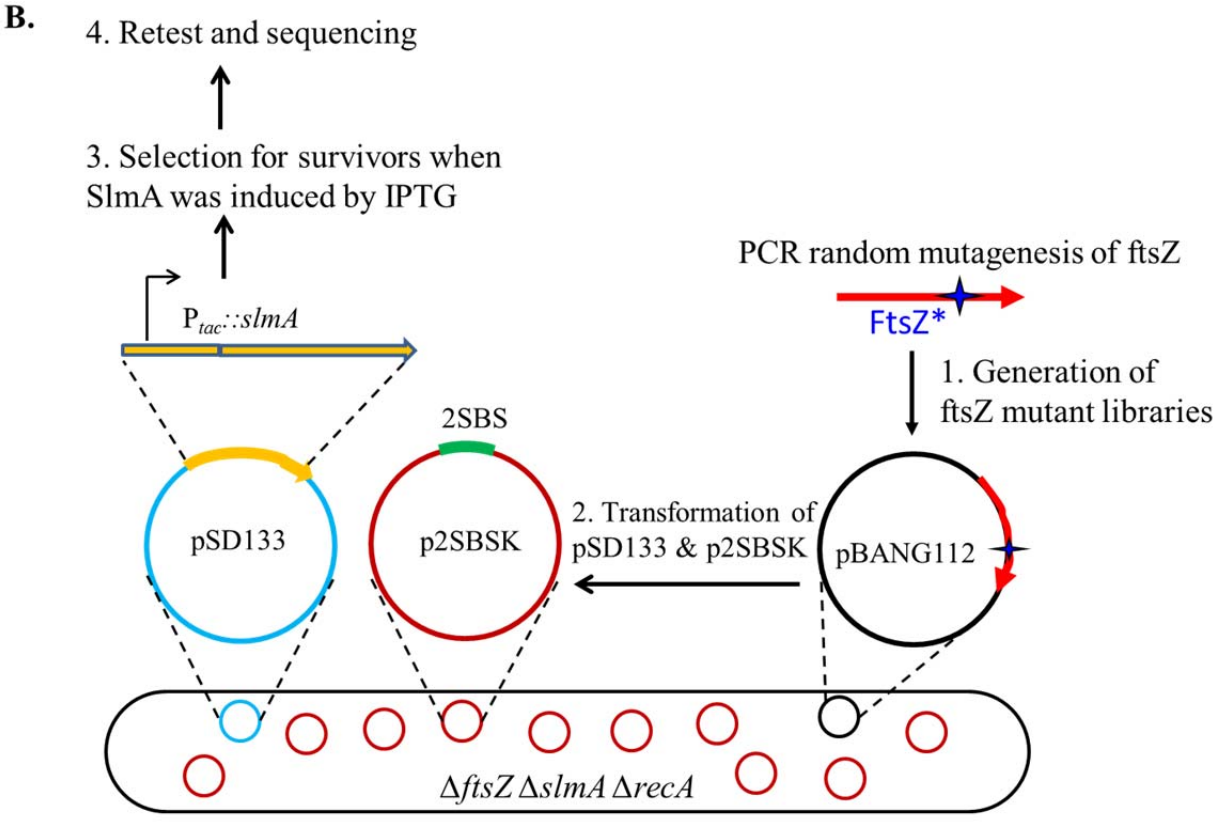
B.
4. Retest and sequencing
3. Selection for survivors when
SlmA was induced by IPTG
P$_{tac}$::*slmA*
2SBS
pSD133
p2SBSK
2. Transformation of
pSD133 & p2SBSK
pBANG112
PCR random mutagenesis of ftsZ
FtsZ*
1. Generation of
ftsZ mutant libraries
Δ*ftsZ* Δ*slmA* Δ*recA*

C.

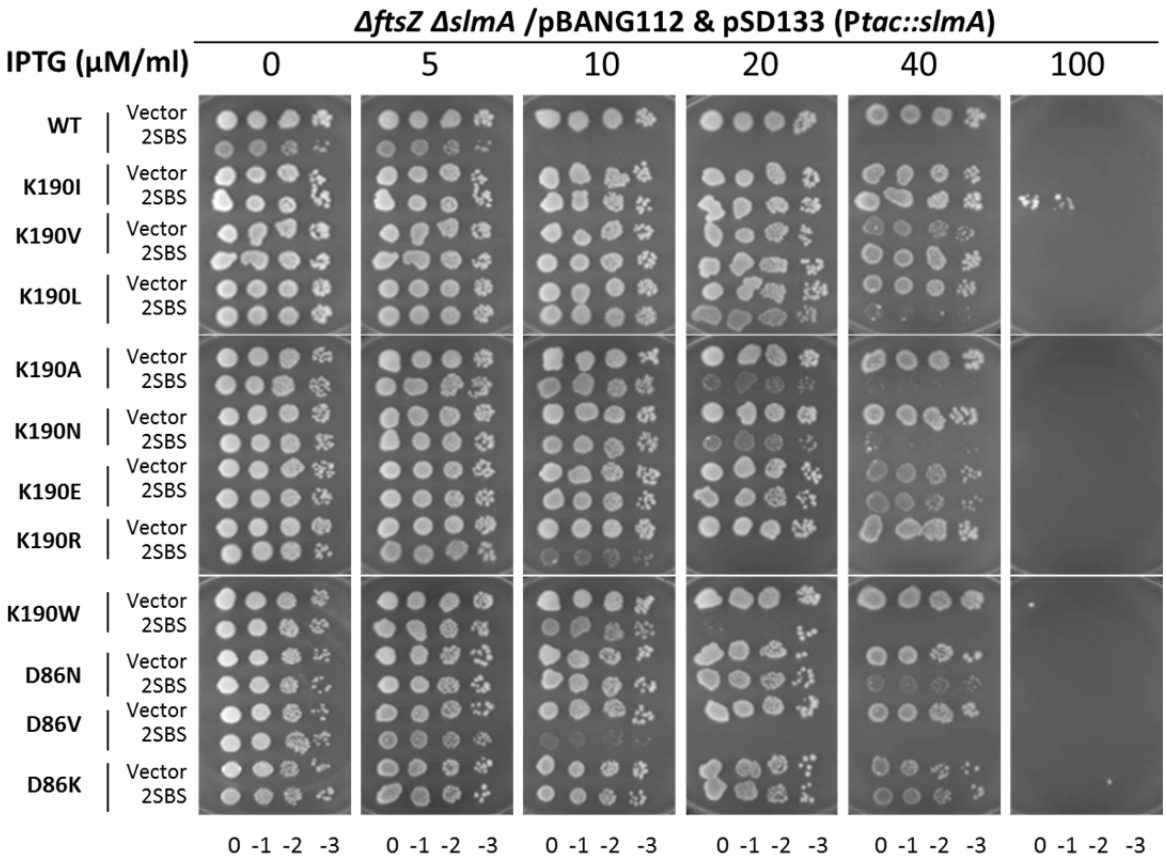
ΔftsZ ΔslmA /pBANG112 & pSD133 (Ptac::slmA)
IPTG (μM/ml)
0
5
10
20
40
100
WT
K190I
K190V
K190L
K190A
K190N
K190E
K190R
K190W
D86N
D86V
D86K
Vector
2SBS
0 -1 -2 -3

D.

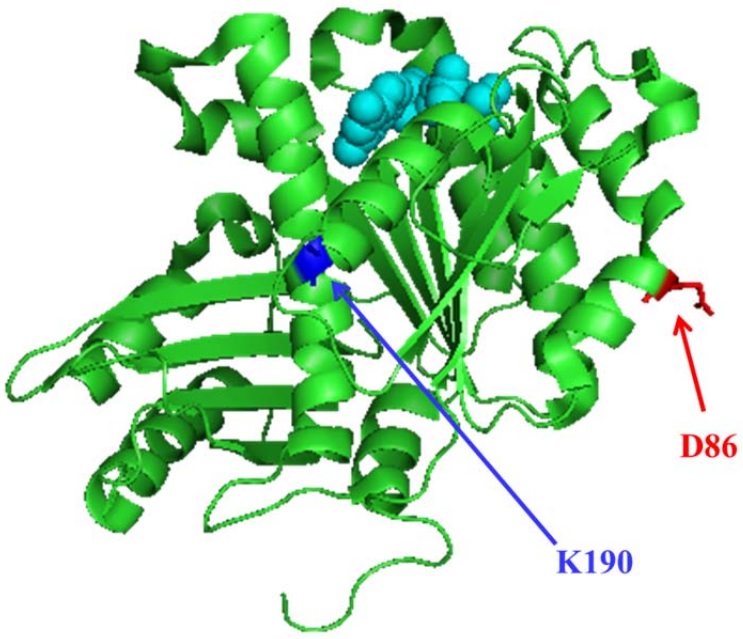
D86
K190

Fig. 14. Characterization of FtsZ-K190V, FtsZ-D86N and FtsZ-K190V&D86N mutant strains. A) Morphology of the FtsZ mutant strains growing at different temperatures. Overnight cultures of the indicated strains grown at 42°C were diluted 100 times in LB supplemented with antibiotics and incubated at 42°C. At OD_{540} = 0.3, the cultures were diluted 10 fold in fresh LB medium, split into three parts, and grown at 42°C, 37°C and 30°C for an additional 2 hours before imaging. B) FtsZ-K190V&D86N double mutant does not confer more resistance to de-localized SBS-SlmA than the single mutants. Plasmids pSD133 (P*tac::slmA*) and p2SBSK (pUC18 with 2SBS sites) were introduced into the FtsZ mutant strains containing different *ftsZ* alleles. One colony of each strain was resuspended in 1 ml LB medium, serially diluted by 10 and 3 µl from each dilution was spotted on LB plates containing various concentration of IPTG and supplemented with spectinomycin and kanamycin. The plates were incubated at 37°C for 30 hours before being photographed.

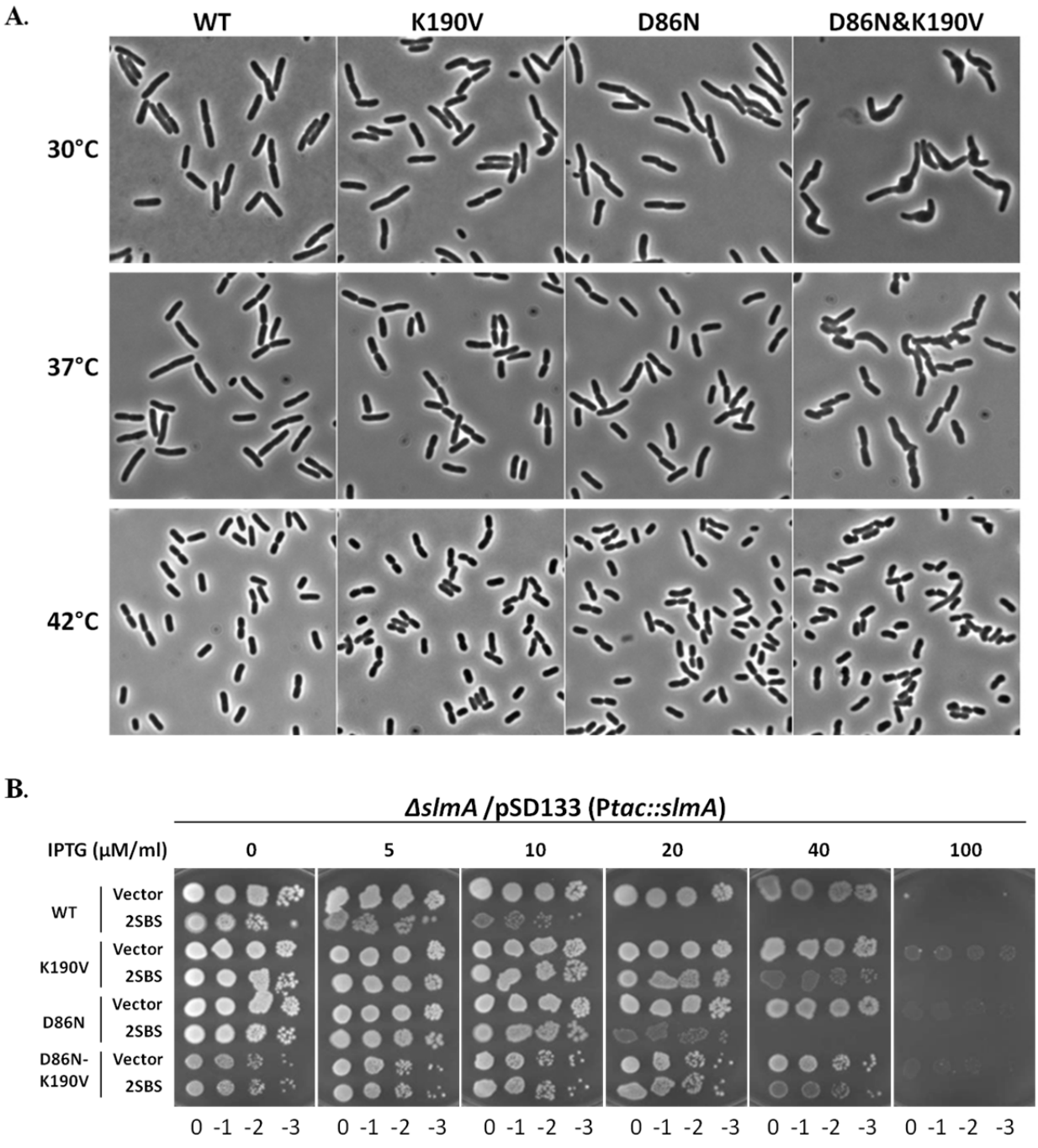
A.
WT
K190V
D86N
D86N&K190V
30°C
37°C
42°C
B.
ΔslmA /pSD133 (Ptac::slmA)
IPTG (μM/ml)
0
5
10
20
40
100
WT
K190V
D86N
D86N-K190V
Vector
2SBS
0 -1 -2 -3

Characterization of FtsZ-K190V and FtsZ-D86N

To further characterize the ftsZ-K190V and ftsZ-D86N mutations, we first introduced them into the chromosome at their native locus by the lambda RED recombineering system (Datsenko and Wanner, 2000). The resultant strains SD160 (*leu::Tn10 ftsZ-K190V*) and SD163 (*leu::Tn10 ftsZ-D86N*) did not show any significant difference to the wild type strain in growth rate (data not shown). However, the morphology of the mutant cells varied with temperature. At 42°C and 37°C, both SD160 and SD163 cells looked similar to wild type cells. However, as the temperature decreased to 30°C, some of the SD160 cells seemed to have a twisted septum while a large population of SD163 showed the twisted septum morphology (Fig. 14A). Further inactivation of *slmA* to create SD161 (*leu::Tn10 ftsZ-K190V slmA::cat*) or SD165 (*leu::Tn10 ftsZ-D86N slmA::cat*) did not result in any new phenotype. Combining K190V and D86N in the plasmid pBANG112 severely affected its ability to complement the FtsZ null strain (data not shown), but SD164 carrying these two mutations in the chromosome (*leu::Tn10 ftsZ-K190V&D86N*) grew at 42°C and 37°C but not 30°C due to formation of twisted septa and swollen middle zone (Fig. 14A). Sicne the strain did not show an increased resistance to SlmA in the presence of extra copies of SBS (Fig. 14B), it was not studied further.

A reduction in GTPase activity of FtsZ appears to be a common mechanism for resistance to FtsZ inhibitors, such as SulA and MinC (Bi and Lutkenhaus, 1990a; Dai et al., 1994; Dajkovic et al., 2008a; Dajkovic et al., 2008b). Therefore, we tested whether the resistance conferred by *ftsZ-K190V* and *ftsZ-D86N* are specific for SlmA. As shown in Fig. 15A, *ftsZ-K190V* and *ftsZ-D86N* did not show any resistance to SulA. However, SD160 (*leu::Tn10 ftsZ-K190V*) and SD163 (*leu::Tn10 ftsZ-D86N*) expressing MinCD were able to form colonies with higher IPTG concentration compared to the wild type strain (Fig. 15B). This better survival seemed to indicate resistance to MinCD, however, SD160 and SD163 expressing MinCD were as filamentous as wild type expressing MinCD (Fig. 15C). Thus, the

better survival was due to an unknown mechanism rather than specific resistance to the division inhibitory activity of MinCD.

FtsZ-K190V and FtsZ-D86N are resistant to delocalized SBS-SlmA and overpexpression of SlmA or SlmA-T33A

Creation of strains SD161 (*leu::Tn10 ftsZ-K190V slmA::cat*) and SD165 (*leu::Tn10 ftsZ-D86N slmA::cat*) allowed us to confirm the resistance of K190V and D86N to de-localized SBS-SlmA without any contribution from the slightly higher level provided by pBANG112. As shown in Fig. 16A, an *ftsZ-WT* strain SD120 (*leu::Tn10 slmA::cat*) containing the *slmA* expression plasmid pSD133 and plasmid p2SBSK failed to form colonies at or above 10 μM IPTG. However, the mutant strains harboring the same pair of plasmids survived at higher concentrations of IPTG. Similar to the result in Fig. 13C, SD161/pSD133&p2SBSK, containing the *ftsZ-K190V* mutation, formed colonies on plates until the IPTG concentration reached 100 μM (40× SlmA), at which SlmA with the control plasmid pUC18K blocked cell division completely. SD165/pSD133&p2SBSK showed a lower resistance, failing to form colonies at 20 μM IPTG. Consistent with the spot test, cells of SD120/pSD133&p2SBSK expressing SlmA in the presence of extra SBS were highly filamentous even without IPTG induction, while cells of SD161/pSD133&p2SBSK and SD165/pSD133&p2SBSK were not filamentous until the IPTG was added at 40 μM and 10 μM respectively (30× and 4× SlmA). Thus, these results confirmed that *ftsZ-K190V* and *ftsZ-D86N* show resistance to the delocalized SBS-SlmA with *ftsZ-K190V*being more resistant than *ftsZ-D86N*.

In the presence of the control plasmid pUC18K, cells carrying *ftsZ-WT* were killed by SlmA overexpression at IPTG concentration of 100 μM (40× chromosomal level). However, cells of SD161/pSD133&pUC18K and SD165/pSD133&pUC18K survived, suggesting that *ftsZ-K190V* and *ftsZ-D86N* provide resistance to SlmA overproduction. To ensure this was the case, we examined the morphology of cells expressing SlmA with the control plasmid pUC18K. As expected, cells of the *ftsZ-*

Fig. 15. FtsZ-K190V and FtsZ-D86N do not confer resistance to SulA or MinCD. A & B) Spot test of the resistance of FtsZ-K190V and FtsZ-D86N to SulA and MinCD. Strains containing the indicated *ftsZ* mutations were transformed with the SulA expression plasmid pBS31 or MinCD expression plasmid pBANG59. A single colony of each resultant strain was then resuspended in 1 ml LB medium, diluted serially by 10 and 3 µl of each dilution was spotted on LB plates supplemented with spectinomycin (pBANG59) or ampicillin (pBS31) and various IPTG concentrations. The plates were then incubated at 37°C overnight before taking pictures. C) Effect of MinCD expression of the morphology of strains carrying the indicated *ftsZ* mutations. Overnight cultures of each of the indicated strains was diluted 100 fold in LB medium with or without IPTG and then grown at 37°C for 2 hours before photography.

A.

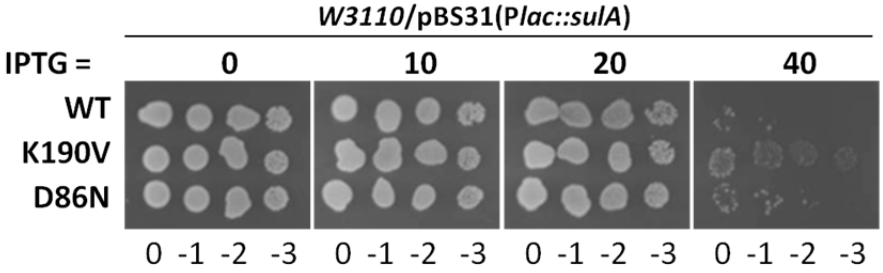
W3110/pBS31(Plac::sulA)
IPTG =
0
10
20
40
WT
K190V
D86N
0 -1 -2 -3 0 -1 -2 -3 0 -1 -2 -3 0 -1 -2 -3

B.

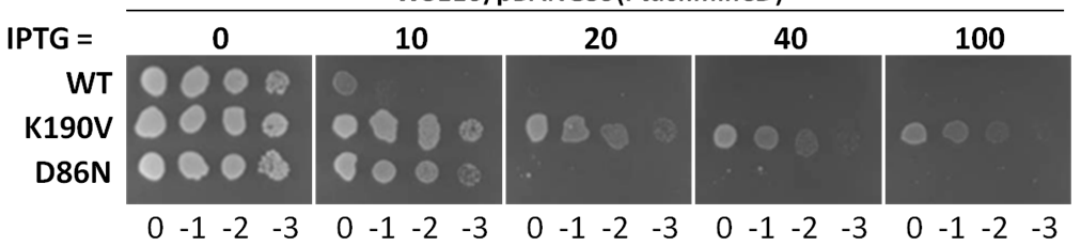
W3110/pBANG59(Ptac::minCD)
IPTG =
0
10
20
40
100
WT
K190V
D86N
0 -1 -2 -3 0 -1 -2 -3 0 -1 -2 -3 0 -1 -2 -3 0 -1 -2 -3

C.

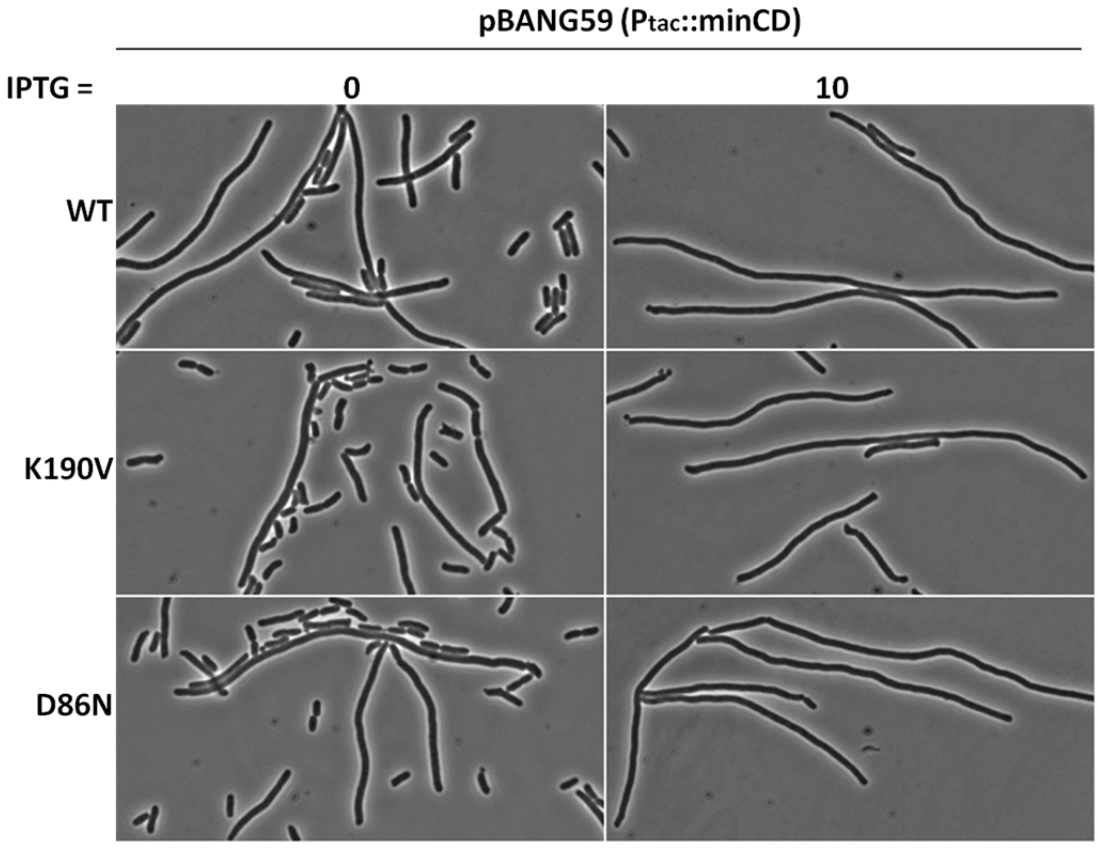
pBANG59 (Ptac::minCD)
IPTG =
0
10
WT
K190V
D86N

Fig. 16. FtsZ-K190V and FtsZ-D86N show resistance to de-localized SBS-SlmA and overproduction of SlmA. A) K190V and D86N display significant resistance to SBS-SlmA and SlmA overproduction when introduced into the chromosome. A spot test was carried out using the strains SD110 (*leu::Tn10 slmA::cat*), SD161 (*leu::Tn10 ftsZ-K190V slmA::cat*) and SD165 (*leu::Tn10 ftsZ-D86N slmA::cat*) and plasmid pairs pSD133&p2SBSK or pSD133&pUC18K, following the procedure described in Fig. 12A. B) Morphology of cells in A) grown in liquid culture with appropriate IPTG concentrations. Overnight cultures of the indicated strains were diluted 100× in LB medium supplemented with appropriate antibiotics, grown at 30°C for 2 hours and then diluted 10 times and grown for 2 1/2 half hours in the presence of IPTG added at the indicated concentrations to induce the expression of SlmA.

A.

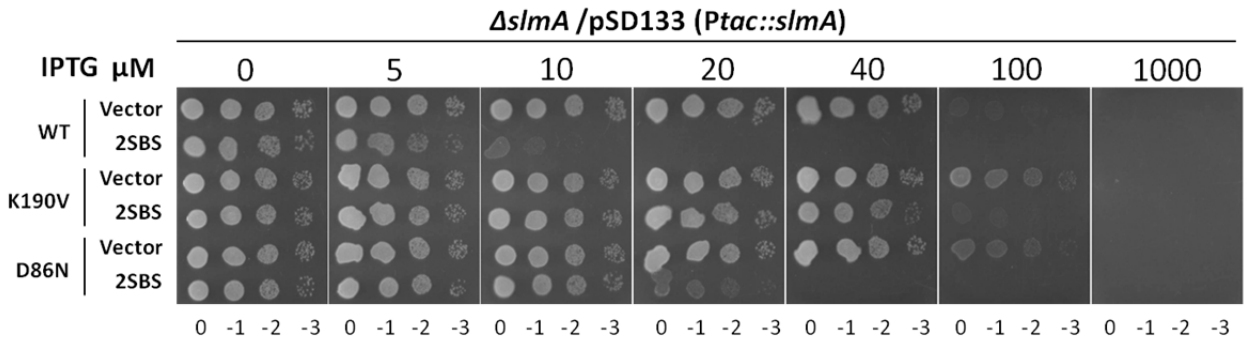
ΔslmA /pSD133 (Ptac::slmA)
IPTG µM
0
5
10
20
40
100
1000
WT
Vector
2SBS
K190V
Vector
2SBS
D86N
Vector
2SBS
0 -1 -2 -3 0 -1 -2 -3 0 -1 -2 -3 0 -1 -2 -3 0 -1 -2 -3 0 -1 -2 -3 0 -1 -2 -3

B.

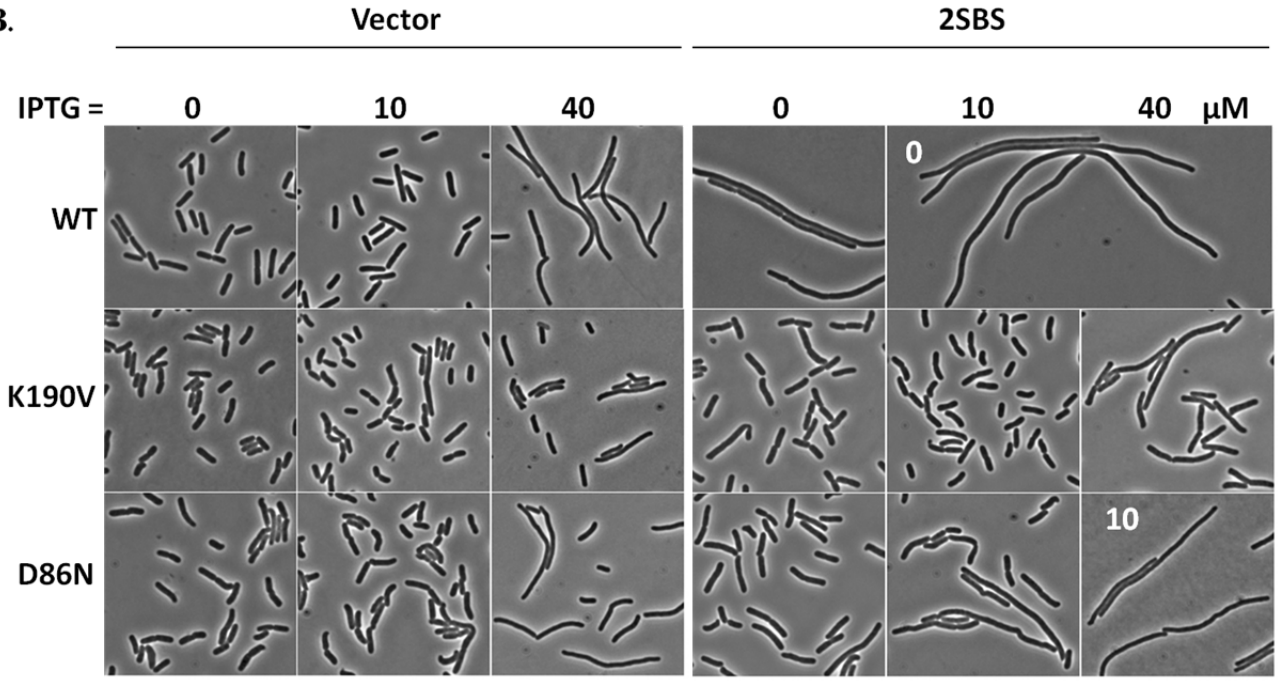
Vector
2SBS
IPTG =
0
10
40
0
10
40 µM
WT
K190V
D86N
0
10

Fig. 17. FtsZ-K190V and FtsZ-D86N display resistance to overproduction of SlmA-T33A. A) A spot test to determine the resistance of FtsZ-K190V and FtsZ-D86N to overproduction of SlmA-T33A. Strains SD120, SD161 and SD165 were transformed with plasmid pSD128-T33A and the test was carried out as described iin the legend to Fig 12A. B) Morphology of cells in A) growing in liquid LB medium with the indicated IPTG concentration. Experiments were performed as in Fig 16B.

A.

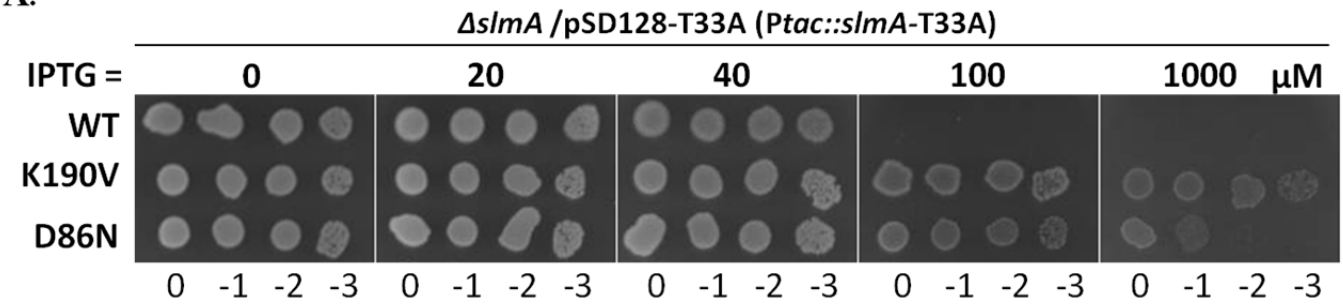
ΔslmA /pSD128-T33A (Ptac::slmA-T33A)
IPTG =
0
20
40
100
1000
μM
WT
K190V
D86N
0 -1 -2 -3 0 -1 -2 -3 0 -1 -2 -3 0 -1 -2 -3 0 -1 -2 -3

B.

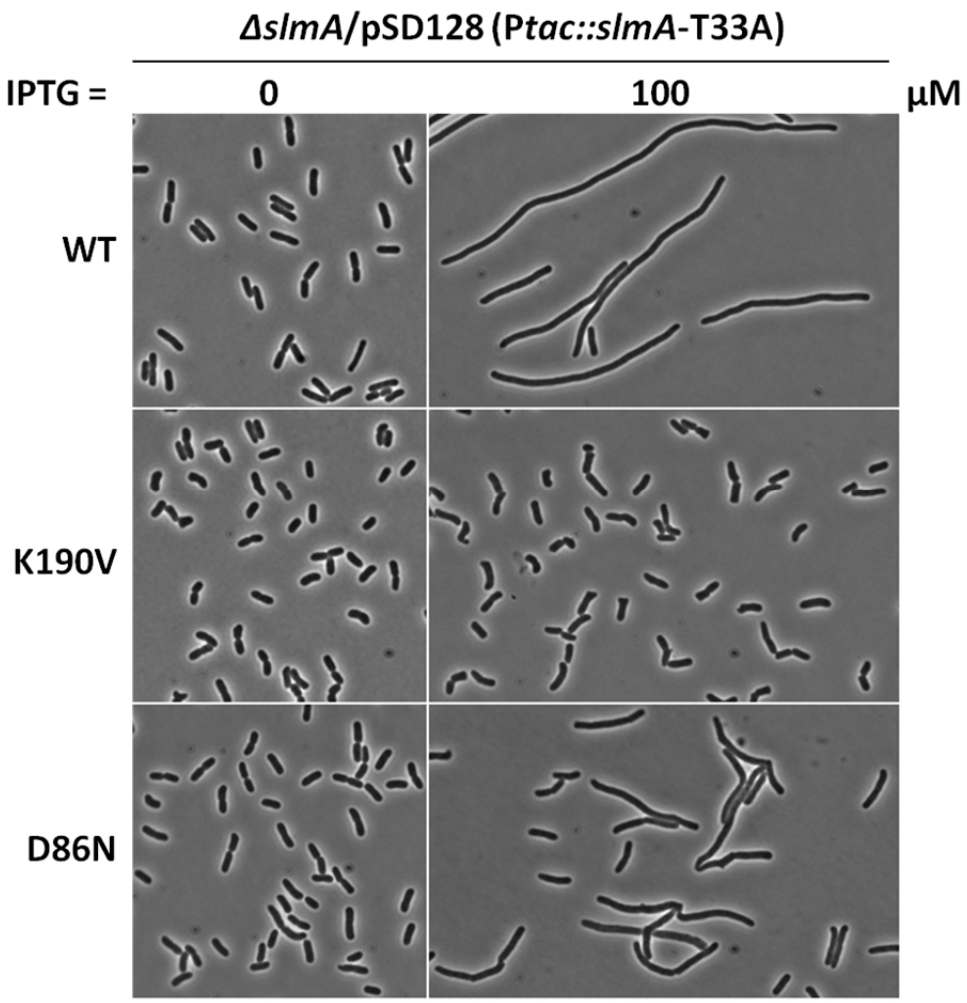
ΔslmA/pSD128 (Ptac::slmA-T33A)
IPTG =
0
100
μM
WT
K190V
D86N

WT strain SD120 containing the control plasmid pUC18K along with pSD133 became filamentous at 40 μM IPTG. However, cells of strain SD161/pSD133&pUC18K only became mildly elongated at this IPTG concentration, indicating FtsZ-K190V provides resistance to SlmA overxpression. Similar to the results with p2SBSK, cells carrying the *ftsZ-D86N* mutation were more filamentous than cells carrying the *ftsZ-K190V* mutation with pUC18K, but were less filamentous than *ftsZ-WT* containing cells under the same conditions. Therefore, these results indicated that both *ftsZ-K190V* and *ftsZ-D86N* reduce the sensitivity to overproduction of SlmA even when SlmA is not delocalized by SBSs on a multicopy plasmid.

SlmA-T33A is a nucleoid occlusion defective mutant because it does not bind DNA (Cho et al., 2011). However, SlmA-T33A is able to interact with FtsZ *in vitro* and disrupt Z rings when overproduced (Cho et al., 2011). Therefore, we tested whether *ftsZ-K190V* and *ftsZ-D86N* provide resistance to overproduction of SlmA-T33A. As shown in Fig. 17, *ftsZ-WT* strain SD120 expressing SlmA-T33A from plasmid pSD128-T33A failed to form colonies on plates with 40 μM IPTG or above. However, SD161 and SD165 expressing SlmA-T33A survived even at 1000 μM IPTG and 100 μM IPTG respectively, suggesting that they are resistant to SlmA-T33A overexpression. Microscopy analysis of the cells showed that at 100 μM IPTG, cells with wild type FtsZ were homogeneously filamentous, while cells containing FtsZ-D86N were less filamentous, consistent with the spot test. Cells from the strains with FtsZ-K190V were not elongated, but they tended to have blunt poles and twisted septa (Fig. 17B). Since SlmA-T33A cannot bind to DNA, its inhibitory activity on cell division is likely due to effects on FtsZ for polymerization, suggesting that ftsZ-K190 and FtsZ-D86 may be directly involved in binding SlmA.

FtsZ-K190V but not FtsZ-D86N impairs cell division of the *min* mutant

SlmA was first identified as a gene synthetic lethal with *min* deletion because the cells could not divide or assemble functional Z-rings (Bernhardt and de Boer, 2005). To further examine *ftsZ*-K190V and *ftsZ*-D86N, we tested whether either of them was synthetic lethal with the *min* deletion. We reported recently that the Δ*min*Δ*slmA* double mutant could not grow at temperatures below 37°C, but at 42°C the

cells grow well (Shen and Lutkenhaus, 2010). Thus we created strains SD162 (*leu::Tn10 ftsZ-K190V min::kan*) and SD167 (*leu::Tn10 ftsZ-D86N min::kan*) at 42°C and then monitored their growth upon shift to 30°C. As expected, the Δ*min*Δ*slmA* double mutant DU5 (*min::kan slmA::cat*) could not form single colonies at 30°C on an LB plate, but surprisingly, both SD162 and SD167 were able to grow at 30°C indicating they were not synthetic lethal with Δ*min* (Fig 18A). Microscopic analysis of cell morphology indicated that cells of SD162 were much longer than the cells of the *min* deletion strain S4 (*leu::Tn10 min::kan*), while cells of SD167 were similar to S4 (Fig. 18B). To quantify the difference between them, we measured the average cell lengths of all four strains grown at 42°C and after they were shifted to 30°C for two and a half hours. As shown in Fig. 18C, the average cell lengths of all four strains were very similar at 42°C. After growth at 30°C for two and a half hours, the Δ*min* strain only increased slightly in cell length, whereas the Δ*min*Δ*slmA* double mutant DU5 stop dividing and the average cell length increased to 26.8 μm. The average cell length of strain SD162 increased from 6.8 μm to 16.7 μm indicating decreased division at 30°C. The cell length of SD167 also increased, but it was similar to that of the *min* deletion strain S4. Taken together, these results indicate that the more resistant *ftsZ-K190V* is synthetic sick with Δ*min* while the less resistant *ftsZ-D86N* is not.

FtsZ-K190V and FtsZ-D86N are resistant to SlmA mediated NO

SlmA is required to prevent division over unreplicated nucleoids in DnaA depleted cells (Bernhardt and de Boer, 2005). Presumably, SlmA is also required for the protection of unsegregated chromosomes because Z-rings rarely form over the unsegregated nucleoid in a $parC^{TS}$ mutant at the nonpermissive termperature (Yu and Margolin, 1999). To test this, *slmA* was deleted in the $parC^{TS}$ strain SD139 ($parC^{TS}$*-Tn10*) to create SD140 ($parT^{TS}$*-Tn10 slmA::cat*). Cells of SD139 and SD140 were grown in LB medium at 30°C to an OD_{540} of 0.4, diluted 10-fold and then shifted to 42°C for an hour. DAPI was added to the culture before imaging so that septation over the DNA could be visualized. As reported previously, most of the SD139 cells were mildly elongated and contained a single nucleoid mass (Fig.

Fig. 18. FtsZ-K190V but not FtsZ-D86N is synthetic sick with a min deletion. A) Spot test to examine the synthetic lethality of strains S4 (*W3110 min::kan*), DU5 (*W3110 min::kan slmA::cat*), SD162 (*W3110 ftsZ-K190V min::kan*) and DU167 (*W3110 ftsZ-D8N min::kan*). A single colony of each strain grown on LB plates at 42°C was resuspended in 1 ml LB medium and serially diluted by 10. 3 ul of each dilution was then spotted on two LB plates supplemented with kanamycin, one of which was incubated at 42°C overnight and the other was incubated at 30°C for 20 hours. B) Morphology of the above strains after being shifted to 30°C for 2 and half hours. An overnight culture of each strain grown at 42°C was diluted 100×in fresh LB medium supplemented with kanamycin. The diluted cultures were then grew at 42°C for 2 hours, diluted by 10× and split to two parts, one grown at 42°C while the other one was incubated at 30°C for 2 and half hours. Images of the cells grown at 42°C are not shown.

A.

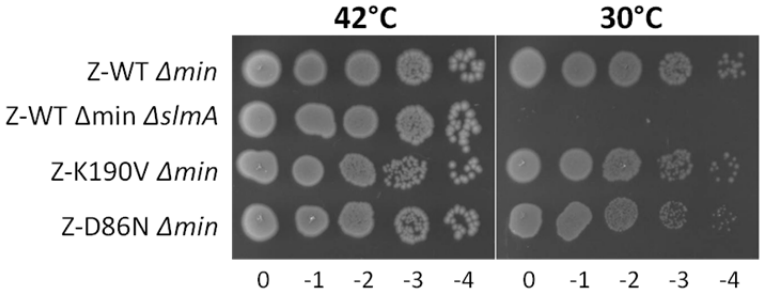

B.

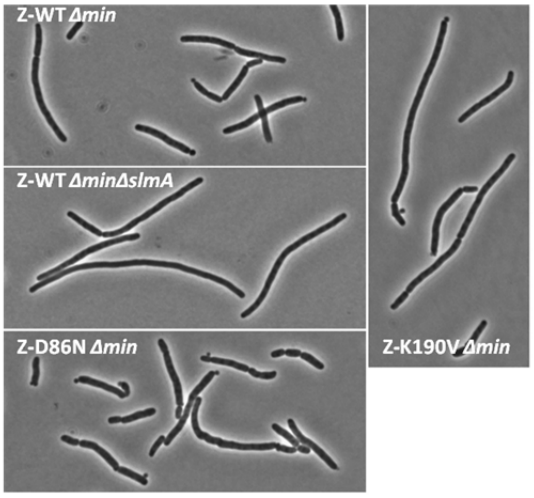

	Strain	Total cells	Average cell length (μm)
42 °C	Z-WT *Δmin*	216	7.2±5.6
	Z-WT *ΔminΔslmA*	301	6.0±3.6
	Z-K190V *Δmin*	229	6.8±4.1
	Z-D86N *Δmin*	235	7.8±4.3
30 °C	Z-WT *Δmin*	292	10.9±7.2
	Z-WT *ΔminΔslmA*	208	26.8±12.5
	Z-K190V *Δmin*	209	16.7±10.0
	Z-D86N *Δmin*	227	10.0±5.3

Fig. 19. FtsZ-K190V and FtsZ-D86N redcue SlmA mediated NO protection of unsegregated chromosomes. A) DAPI staining of cells of indicated genotypes after being shifted to 42°C for an hour. Overnight cell cultures of each strain was diluted 100× in LB medium supplemented with tetracycline and grwon at 30°C for ~3 hours until the OD_{540} reached about 0.4. The culture was then diluted 5× and split into two parts, one of which was grown at 30°C and the other was shifted to 42°C for an hour. DAPI was added to the culture at a final concentration of 400 ng/ml 20 minutes before imaging. B) Cells in A were quantified to calculate the percentage of cells with septa and the percentage of septa over unsegregated nucleoids. Data shown are the average of three experiments with more than 200 cells for each.

A.

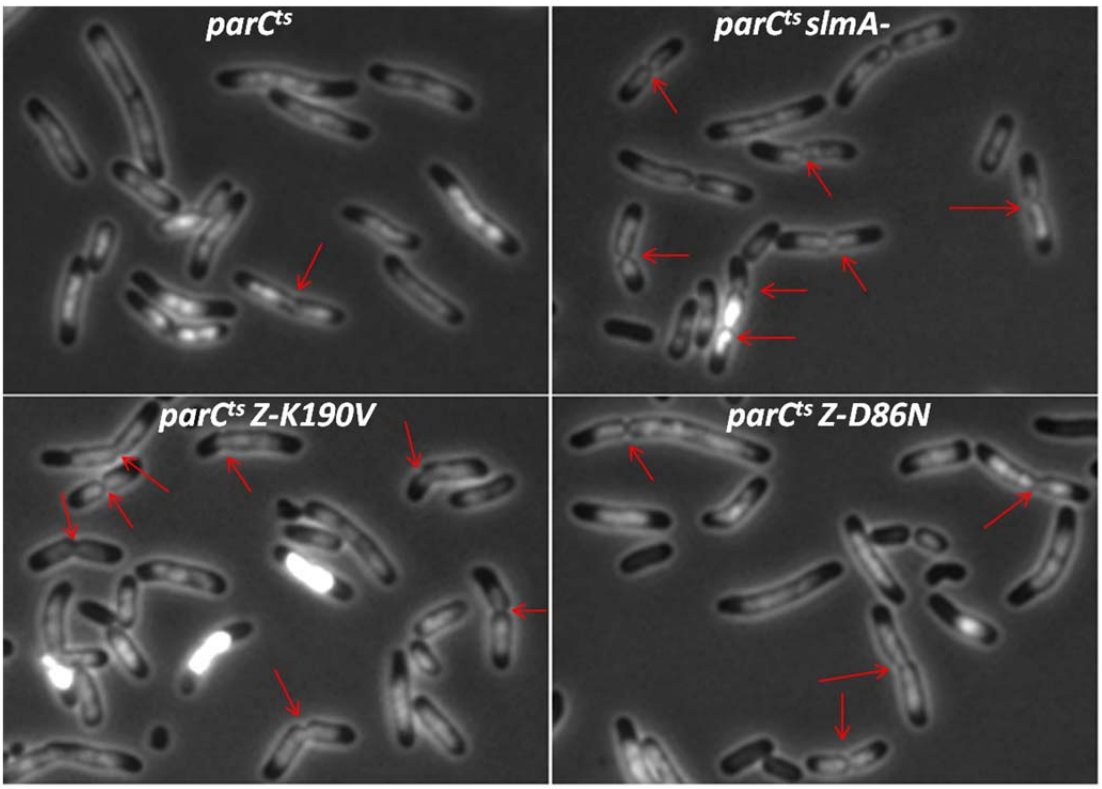
parC^ts
parC^ts slmA-
parC^ts Z-K190V
parC^ts Z-D86N

B.

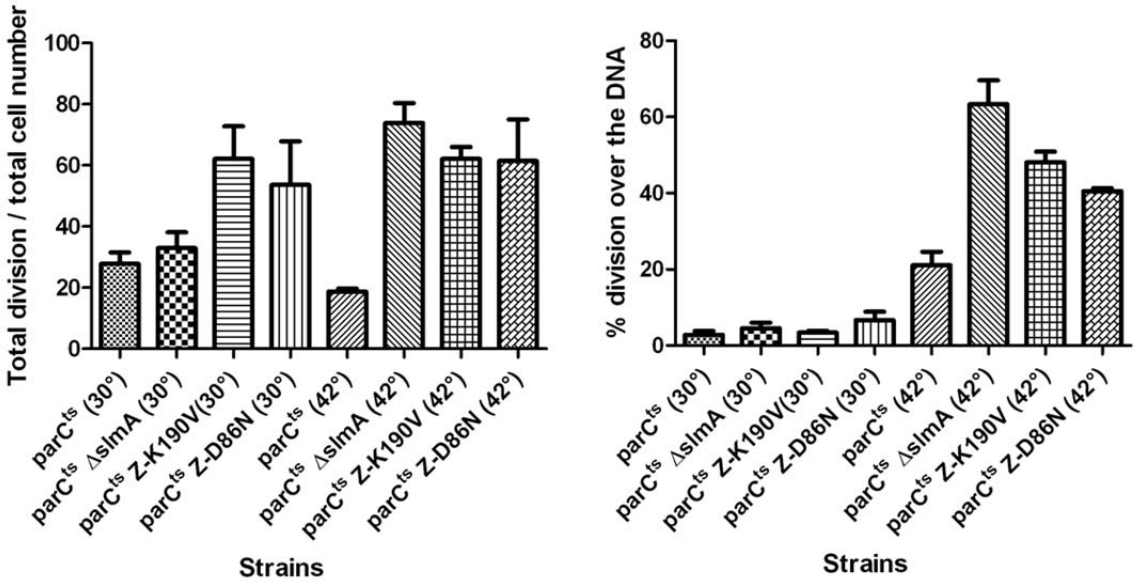
Total division / total cell number
100
80
60
40
20
0
parC^ts (30°)
parC^ts ΔslmA (30°)
parC^ts Z-K190V(30°)
parC^ts Z-D86N (30°)
parC^ts (42°)
parC^ts ΔslmA (42°)
parC^ts Z-K190V (42°)
parC^ts Z-D86N (42°)
Strains
% division over the DNA
80
60
40
20
0
parC^ts (30°)
parC^ts ΔslmA (30°)
parC^ts Z-K190V(30°)
parC^ts Z-D86N (30°)
parC^ts (42°)
parC^ts ΔslmA (42°)
parC^ts Z-K190V (42°)
parC^ts Z-D86N (42°)
Strains

19A). The percentage of cells with septa decreased about 50% compared to those grown at 30°C, however, among those cells with septa, 21.7% of them were observed over the DNA. The percentage of divisions over the DNA seemed to be high compared to results observed after DnaA depletion. However, *parC*^{TS} mutant is only defective in the last step of segregation so it is likely that the chromosomes are at least partially segregated leading to some division. As expected, the percentage of cells with septa was much higher in the *slmA* deleted strain SD140 at non-permissive temperature (67.3%) and more than half of the divisions were over the nucleoids (56.8%). Therefore, SlmA mediated nucleoid occlusion was required for the prevention of division over the unsegregated chromosomes.

To further confirm FtsZ-K190V and FtsZ-D86N are resistant to the SlmA mediated nucleoid occlusion, we created strain SD170 (*parC*^{TS}*-Tn10 ftsZ-K190V*) and SD171 (*parC*^{TS}*-Tn10 ftsZ-D86N*) by introducing the *parC*^{TS} alleles into the strains SD168 (*ftsZ-K190V*) and SD169 (*ftsZ-D86N*) by P1 mediated transduction. SD170 and SD171 were subjected to the same treatment as described above and divisions over the DNA were counted. Similar to SD140, almost 60% of the SD170 cells were observed with septa, and about half of these divisions (50.5%) occurred over the nucleoids at the non-permissive temperature. Cells of SD171 also displayed a similar phenotype to SD140 and SD170 when shifted to 42°C, but the percentage of cells with division (45.8%) and percentage of the division over the nucleoids (40.1%) were lower. The percentage of cells with septa for strains SD170 and SD171 seemed to be high at 30°C, but that was likely due to the fact they had twisted septa at 30°C. Nonetheless, compared to SD139 (*parC*^{TS}), these results clearly showed that SlmA mediated nuceloid occlusion was less effective when *ftsZ-K190V* or *ftsZ-D86N* were present.

FtsZ-K190V and FtsZ-D86N are partially resistant to SBS-SlmA *in vitro*

The results above show that FtsZ-K190V and FtsZ-D86N are resistant to SlmA *in vivo*, so it is likely they would be also resistant to the SBS bound SlmA *in vitro*. However, the impact of SBS bound SlmA on FtsZ polymerization is controversial. To test whether our mutants provide resistance to SlmA *in*

vitro, we first had to address the disparity of previous reports. We employed electron microscopy to monitor the effect of SBS-SlmA complexes on FtsZ polymerization using the same SBS17-30mer (CAAAAGTAA**GTAAATGGTCAC**TAACGTTGA) and buffer as the Bernhardt group (Cho's buffer:50 mM PIPES, pH 6.7, 10 mM $MgCl_2$ and 200 mM KCl) and follwed their procedure (Cho et al., 2011). Consistent with their observations, SlmA (2 μM) in the presence of SBS17 DNA (2 μM) dramatically reduced the amount of FtsZ (2 μM) polymers on the grid, while SlmA alone or the SBS17-30mer alone appeared to have no effect on FtsZ polymerization (Fig. 20A). SlmA-R73D, which is defective in SlmA-FtsZ interaction, had no effect (Fig. 20C). To make sure this antagonizing effect by SBS-SlmA on FtsZ assembly was not buffer specific, we performed the reactions two additional buffers: one that we use routinely in the lab (DU's buffer, 50 mM HEPES pH 8.0, 10 mM $MgCl_2$ and 200 mM KCl) and the buffer Schumacher group used (50 mM HEPES pH7.7, 100 mM KAcetate and 5 mM MgAcetate). Consistent with results with the Bernhardt group buffer, FtsZ polymerization was significantly reduced by SlmA in the presence of SBS17-30mer DNA in both buffers (Fig. 20B and data not shown). Again, SlmA or SBS17-30Mmer DNA did not affect FtsZ polymerization. Thus, the different observations of the effect of SBS bound SlmA on FtsZ polymerization is not due to the difference in buffer components.

The above results suggest that the different effects on FtsZ assembly by SBS bound SlmA in the two studies might be due to the different SBS DNA used for the assays (the Schumacher group used a SBS-18mer DNA [CCCAAT**GTGAGTGCTCAC**] containing the consensus sequences at one end of the molecule) (Tonthat et al., 2013). The structure of the SlmA-SBS-20mer structure (the consensus sequence was centered) showed that SlmA makes two additional base interactions and one additional phosphate interaction on each side of the DNA molecule compared to the SlmA-SBS-12mer structure. In agreement with this, SlmA displays a higher affinity for SBS-20mer compared to SBS-12mer (Tonthat et al., 2013). SlmA was likely not fully activated when bound with the SBS-18mer used in the Schumacher study, due to the absence of three contacts on one side of the molecule. To test this idea, we used three shorter SBS DNA molecules for the assays. In the presence of a shorter version of SBS17 (SBS17-20mer,

GTAA**GTAAATGGTCAC**TAAC) SlmA dramatically reduced the FtsZ filaments in the grid, but it worked less efficiently than bound with SBS17-30mer (Fig 20B). When the SBS-18mer and an SBS-14mer (A**GTGAGTACTCAC**T) were used for the reactions, similar results were observed. This reduction in activity with shorter SBS DNA molecules was more obvious in the buffer Schumacher group used (data not shown), indicating that SlmA works less well in this buffer. All the three SBS DNA probes were able to activate SlmA (His-tag free) to bind to FtsZ (Fig 24D). Taken together, the results suggest that when bound with SBS DNA, SlmA appears to antagonize FtsZ protofilament formation and the conflicting observations from previous studies are likely due to the use of different SBS DNA molecules and buffers.

We next tested whether our mutants FtsZ-K190V and FtsZ-D86N provide resistance to the inhibitory activity of SBS bound SlmA using SBS17-30mer in Du's buffer. As showed in Fig. 21, polymerization of wild type FtsZ was again significantly affected by the addition of SlmA with SBS17-30mer DNA, only short polymers were occasionally observed. However, the proto-filaments formed by FtsZ-K190V were largely unaffected by the addition of SlmA with SBS17-30mer DNA to the reaction, although the proto-filaments seemed to be shorter and not as smooth (Fig. 21). Consistent with the low resistance to SlmA *in vivo*, some proto-filaments of FtsZ-D86N were observed in the presence of SlmA and SBS17-30mer DNA, but less than FtsZ-K190V (Fig. 21). Polymers formed by wild type FtsZ or the FtsZ mutants FtsZ-K190V and FtsZ-D86N were largely not affected by the addition of SlmA or addition of the SBS17 DNA (2 μM). Interestingly, although wild type FtsZ and FtsZ-K190V (2 μM) assembled into smooth single-stranded filaments, FtsZ-D86N tended to form twin-filaments. At a higher concentration of FtsZ-D86N (5 μM), the bundling phenomenon was more dramatic and most of the filaments were engaged in multi-stranded polymers consisting of more than four or five proto-filaments (data not shown). This concentration dependent bundling was much less dramatic with WT FtsZ or FtsZ-K190V. These results indicated that although FtsZ-D86N showed some resistance to the action of SBS-SlmA and this resistance may be due to the tendency of this mutant to bundle.

Fig. 20. SlmA is activated by an SBS DNA to antagonize FtsZ polymerization. A) FtsZ polymerization with or without the addition of SlmA and SBS17-30mer in Cho's buffer. Reactions were performed in 50 µl volume containing FtsZ (2 µM) and GTP (1 mM) with or without the addition of SlmA and SBS17-30mer DNA (2 µM). Reactions were incubated at room temperature for 5 minutes and then samples were spotted onto carbon-coated grids for 1 minute and negatively stained with 1% uranyl acetate and visualized by electron microscopy. B) FtsZ polymerization with or without the addition of SlmA and SBS DNA of different lengths in Du's buffer. Reactions were performed as in A). C) Control showing that a SlmA mutant (R73D) defective in SlmA-FtsZ interaction did not affect FtsZ polymerization. Reactions were formed as in A) but in Du's buffer. Scale bar is 100 nm.

A.

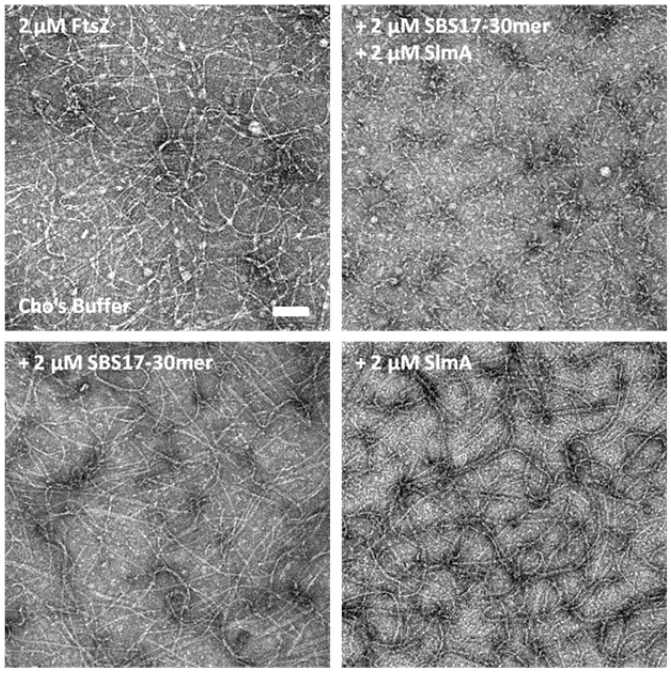
2 μM FtsZ
Cho's Buffer
+ 2 μM SBS17-30mer
+ 2 μM SlmA
+ 2 μM SBS17-30mer
+ 2 μM SlmA

B.

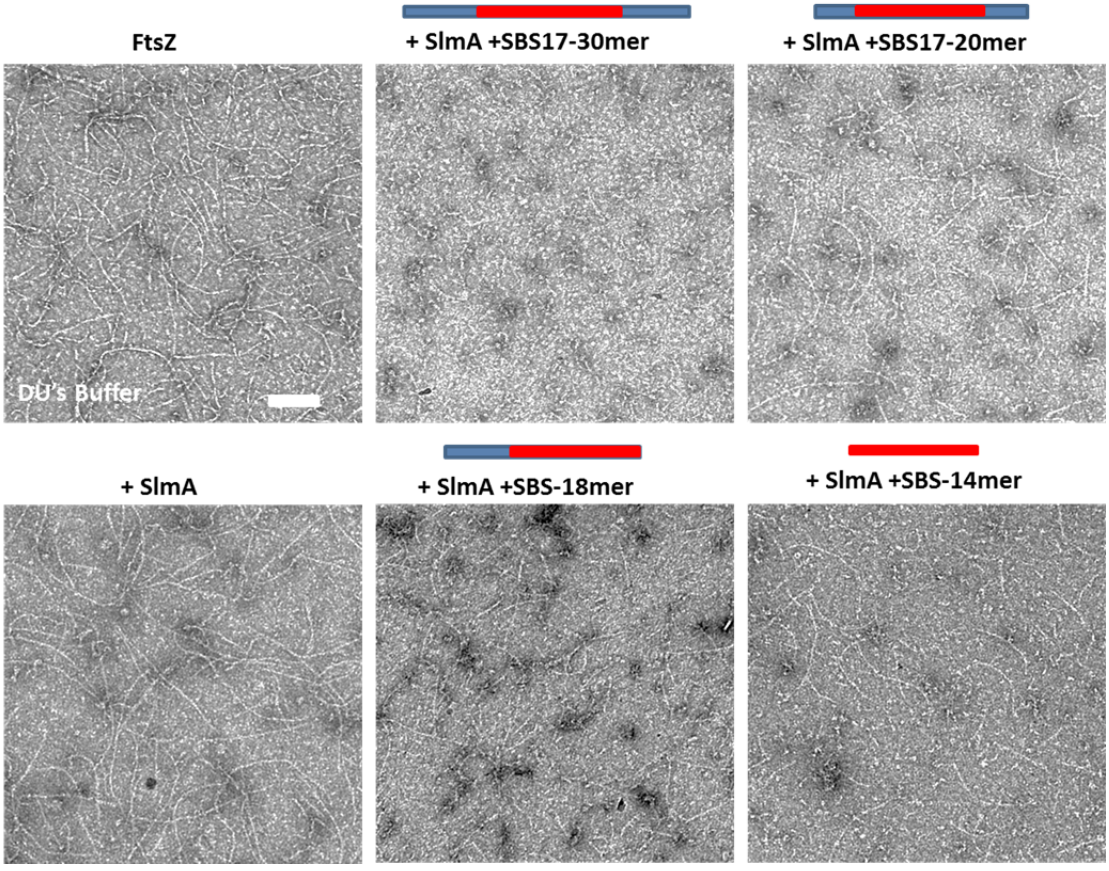
FtsZ
DU's Buffer
+ SlmA +SBS17-30mer
+ SlmA +SBS17-20mer
+ SlmA
+ SlmA +SBS-18mer
+ SlmA +SBS-14mer

C.

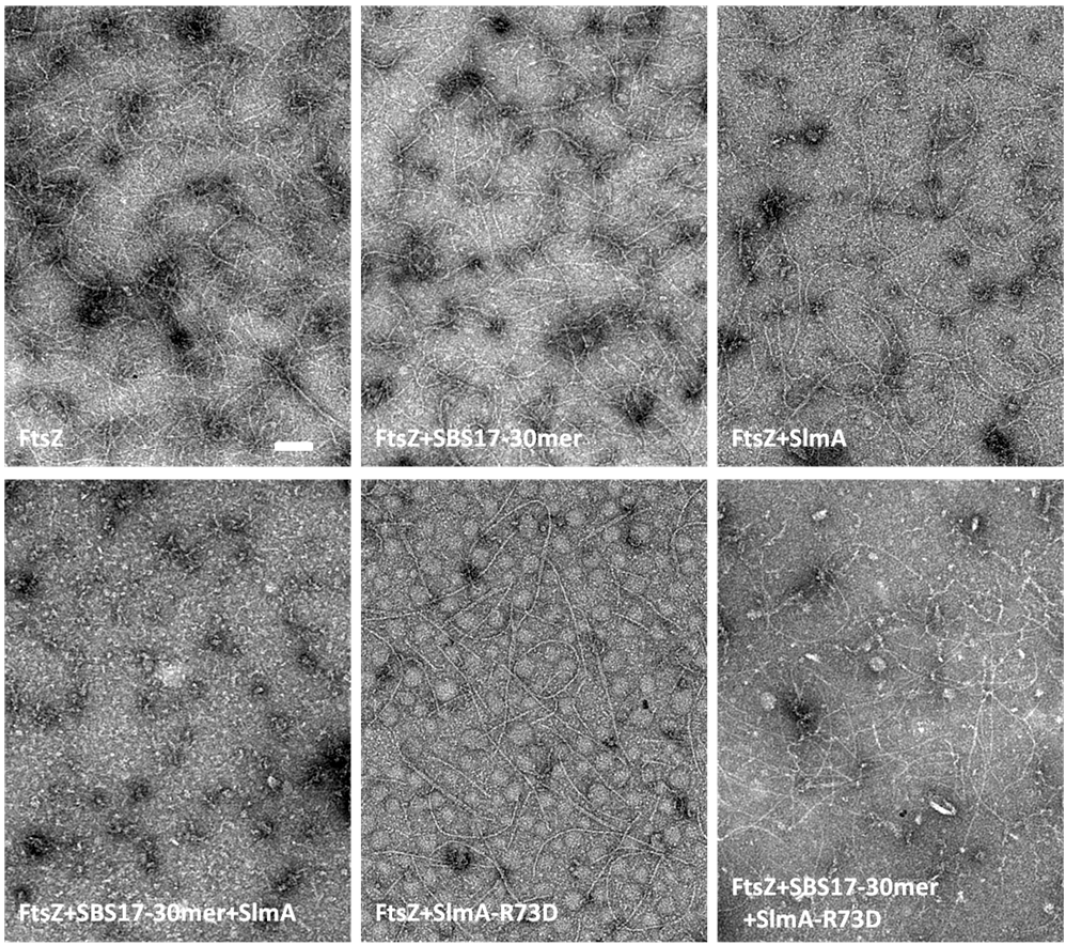
FtsZ
FtsZ+SBS17-30mer
FtsZ+SlmA
FtsZ+SBS17-30mer+SlmA
FtsZ+SlmA-R73D
FtsZ+SBS17-30mer
+SlmA-R73D

Fig. 21. Assembly of FtsZ-K190V and FtsZ-D86N is resistant to SlmA *in vitro*. A. FtsZ polymerization reactions were performed in 50 µl volumes containing FtsZ or its mutants (2 µM) and GTP (1 mM) with or without the addition of SlmA and SBS17-30mer DNA (2 µM). Reactions were incubated at room temperature for 5 minutes and then samples were spotted onto carbon-coated grids for 1 minute, negatively stained with 1% uranyl acetate and visualized by electron microscopy. Scale bar is 100 nm

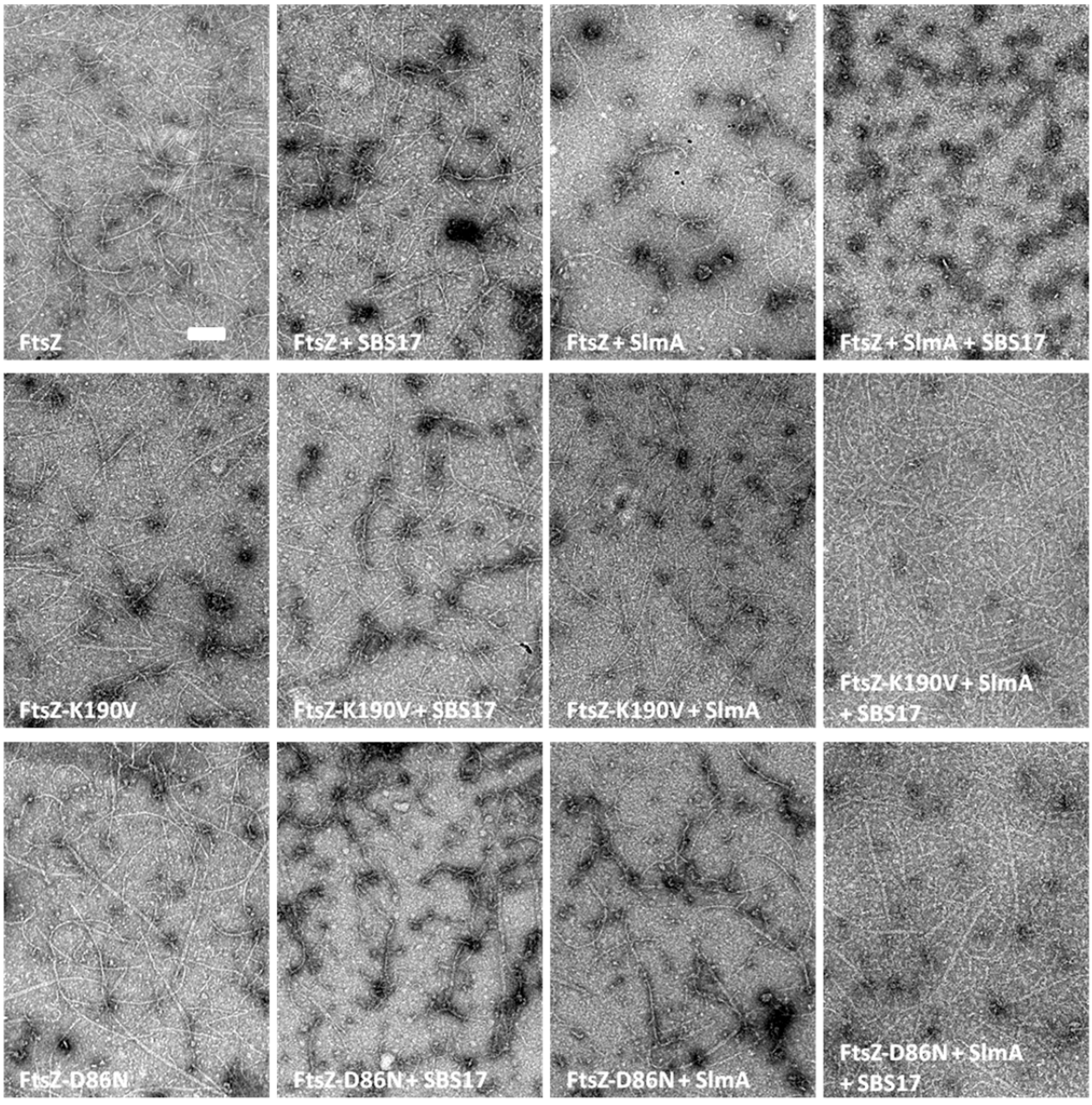
FtsZ
FtsZ + SBS17
FtsZ + SlmA
FtsZ + SlmA + SBS17
FtsZ-K190V
FtsZ-K190V + SBS17
FtsZ-K190V + SlmA
FtsZ-K190V + SlmA + SBS17
FtsZ-D86N
FtsZ-D86N + SBS17
FtsZ-D86N + SlmA
FtsZ-D86N + SlmA + SBS17

K190V and D86N do not affect FtsZ binding to SlmA

According to the current model for SlmA function, there are two ways for *ftsZ* mutations to confer resistance to SlmA: 1) lower the GTPase activity of FtsZ or 2) disrupt the FtsZ-SlmA interaction. The fact that *ftsZ-K190V* and *ftsZ-D86N* are sensitive to the division inhibitory activities to MinCD and SulA suggest that they should not affect the GTPase of FtsZ dramatically. Indeed, the GTPase activities of these two mutants only appeared slightly lower than FtsZ-WT (Table 5, FtsZ-WT 4.6 GTP/FtsZ/Min, FtsZ-K190V 4.0 GTP/FtsZ/Min and FtsZ-D86N 3.5 GTP/FtsZ/Min at 50 mM KCl; at 200 mM KCl, the turnover rates were calculated to be 9.8, 4.4 and 5.3 GTP/Min/FtsZ for wild type FtsZ, FtsZ-K190V and FtsZ-D86N respectively) indicating that they likely provide resistance by other mechanisms.

To test whether these two mutations disrupt FtsZ-SlmA interaction *in vivo*, we used bacterial two-hybrid assay to monitor the interactions between FtsZ and SlmA. We first made sure that the bacterial two hybrid assay reports SlmA-SlmA interaction and FtsZ-SlmA interaction by using SlmA mutants defective in self-interaction or interaction with FtsZ. Surprisingly, we found that the SlmA-T33A mutant which has been reported to be deficient in self-interaction interacted strongly with wild type SlmA as well as other SlmA mutants (Fig. 22A). This difference could be due to the way SlmA was fused to the T18 or T25 domain of adenylate cyclase. In the previous study (before the structure of SlmA was known), T18 and T25 were fused to the N terminus of SlmA, which we now know are far away from each other in the SlmA dimer (Cho et al., 2011). In our test, T18 or T25 was fused to the C terminal of SlmA, which are close to each other when SlmA dimerizes. Thus, the previous test is likely reporting the interaction between SlmA dimers when SlmA forms dimer-of-dimers or oligomerizes around the SBS, while our test reports SlmA dimerization. The assay also successfully reported SlmA-FtsZ interaction, as SlmA-R73D did not show any signal with FtsZ (Fig. 22A). We also tested two other SlmA mutants defective in NO, SlmA-N102A and SlmA-V174F (these two mutants were isolated by selecting for SlmA mutants that bind DNA but not block cell division, not studied in detail), they also failed to interact with FtsZ. As

showed in Fig. 22B, neither K190V nor D86N affected the interaction of FtsZ with SlmA in the bacterial two-hybrid test, indicating that K190 and D86 are not directly involved in binding SlmA.

Using a GTPase defective FtsZ mutant, FtsZ-D212N, *Cho et. al* showed that SlmA co-sedimented with FtsZ-D212 polymers in the presence of SBS17-30mer DNA (Cho et al., 2011). We reasoned that using the non-hydrolyzable GTP analog GMPCPP with wild type FtsZ should be equivalent. Indeed, as shown in Fig. 22C, SlmA (5 μM) co-sedimented with FtsZ-GMPCPP (5 μM) polymers in the presence of SBS17-30mer DNA (2 μM) but not without the SBS, in agreement with the idea that SBS binding stimulates the interaction between SlmA and FtsZ. As expected, the FtsZ binding mutant, SlmA-R73D did not co-sediment with FtsZ-GMPCPP polymers. Note that some SlmA co-sedimented with stable FtsZ polymers even in the absence of SBS DNA, which is the background in our assay. If the two FtsZ mutants still interact with SlmA, filaments formed with GMPCPP should also recruit SlmA to the pellets in the presence of SBS17-30mer DNA. As we expected, SlmA co-sedimented with FtsZ-K190V and FtsZ-D86N polymers in the presence of SBS17-30mer DNA, but not in its absence, consistent with the bacterial two hybrid results. Thus, the resistance of FtsZ-K190V and FtsZ-D86N to SlmA is unlikely due to a defect in the direct binding to SlmA.

Since SlmA associates with the FtsZ polymers formed with GMPCPP in the presence of SBS17-30mer DNA, we wondered whether such interaction would influence the morphology of FtsZ polymers. Therefore, we examined reactions using proteins at 2 μM (at 5 μM, the polymers would be too crowded on the grid) but with or without SlmA and the SBS17-30mer DNA by electron microsopy. As shown in Fig. 23A, wild type FtsZ formed smooth long filaments with GMPCPP that sometimes tended to bundle into 2 stranded filaments. As expected, addition of SlmA alone did not affect the morphology of the polymers formed by FtsZ, however, addition of SlmA and SBS17-30mer DNA together altered the morphology of the FtsZ-GMPCPP polymers. Large FtsZ-GMPCPP polymer bundles were prevalent on the grid, indicating that SBS bound SlmA dimer induces bundling of the FtsZ polymers. This may not be

surprising considering that SlmA makes dimer of dimers on the SBS and, therefore, may be able to crosslink FtsZ polymers.Also obvious was that these bundles were not like the smooth bundles formed by FtsZ alone, but seemed to contain additional structures on top of the filament surfaces. The control, SlmA-R73D, which does not interact with FtsZ, did not affect the morphology of FtsZ-GMPCPP polymers (Fig. 23A bottom). FtsZ-D86N polymers formed with GMPCPP tended to bundle into 4 or 5 stranded filaments, in agreement with its preference to bundle observed above. Similar to FtsZ GMPCPP polymers, FtsZ-D86N-GMPCPP polymers formed big bundles when SlmA with SBS17-30mer DNA was added to the reaction. To our surprise, the effect of SBS bound SlmA on FtsZ-K190V-GMPCPP polymers was quite different from that for wild type FtsZ and FtsZ-D86N. The filaments were smoother and the large bundles were very rare and short. When SlmA was increased two fold, more FtsZ- K190V bundles appeared, but FtsZ-WT formed really large bundles at the same condition (Fig 23B&C). Interestingly, the FtsZ-K190V bundles induced by SBS-SlmA appeared to contain complexes sandwiched by straight filaments. These results suggest that even though the FtsZ-K190V-GMPCPP polymers recruited SBS-SlmA to the pellet in the sedimentation assay, they were not as sensitive as FtsZ-WT polymers to the SBS-SlmA-induced bundling.

To further confirm these two FtsZ mutants still interact with SBS-SlmA, we utilized the *BLItz* system to monitor their binding to SBS bound SlmA. The *BLItz* system is an instrument that allows label-free analysis of biomolecular interactions based on Bio-Layer Interferometry (BLI). In these assays, biotinaylted SBS17-30mer DNA molecules were immobilized on the surface of streptavidin sensors and SlmA and FtsZ were added sequentially. Interaction between SlmA and the immobilized SBS17-30mer DNA increased the optical thickness of the surface of the biosensor, producing the first wavelength shift. Interaction between FtsZ and SBS-bound SlmA further increased the optical thickness, resulting in the second wavelength shift. Using this system, we could successfully measure the binding affinity between SlmA and SBS17-30mer DNA. As shown in Fig 24A, SlmA and its mutants SlmA-F65A and SlmA-R73D bound SBS17-30mer DNA with similar kinetics, and with similar apparent Kds between 60 nM

Table 5. GTPase activity of FtsZ mutants measured by the continuous GTPase assay.

FtsZ alleles	GTPase activity at 50 mM KCl (GTP/Min/FtsZ)	GTPase activity at 200 mM KCl (GTP/Min/FtsZ)
WT	4.6	9.8
K190V	4.0	4.4
D86N	3.5	5.3

Fig. 22. FtsZ-K190V and FtsZ-D86N still associate wtih SlmA. A and B) Bacterial two hybrid assay to analyze the interaction between SlmA and FtsZ or FtsZ mutants. Plasmid pairs, as indicated, were co-transformed into BTH101. Individual colonies were resuspended in 1ml LB medium and spotted on LB plates supplemented with Amp, Kan, 40 μg/ml X-gal and 250 μM IPTG. Plates were incubated at 30°C for 36 hours before taking pictures. C, D and E) SBS17-30mer bound SlmA co-sedimented with stable FtsZ polymers formed with GMPCPP. C) Principles of co-sedimentation assay. In the presence of GMPCPP (Non hydrolysable GTP analog), FtsZ (black dots) polymerizes into filaments (black ribbons) which could be spinned down by centrifugation. SlmA (Red triangle) interacts with FtsZ, some of the SlmA molecules co-sediment with the FtsZ filaments. Polymerization assays were performed as in Fig. 19 except that the protein concentration was 5 μM and GTP was replaced by GMPCPP. After the reactions were incubated at room temperature for 5 minutes, FtsZ polymers were sedimented by ultracentrifugation. Proteins in the supernatant and pellett fractions were separated by SDS-PAGE gel.

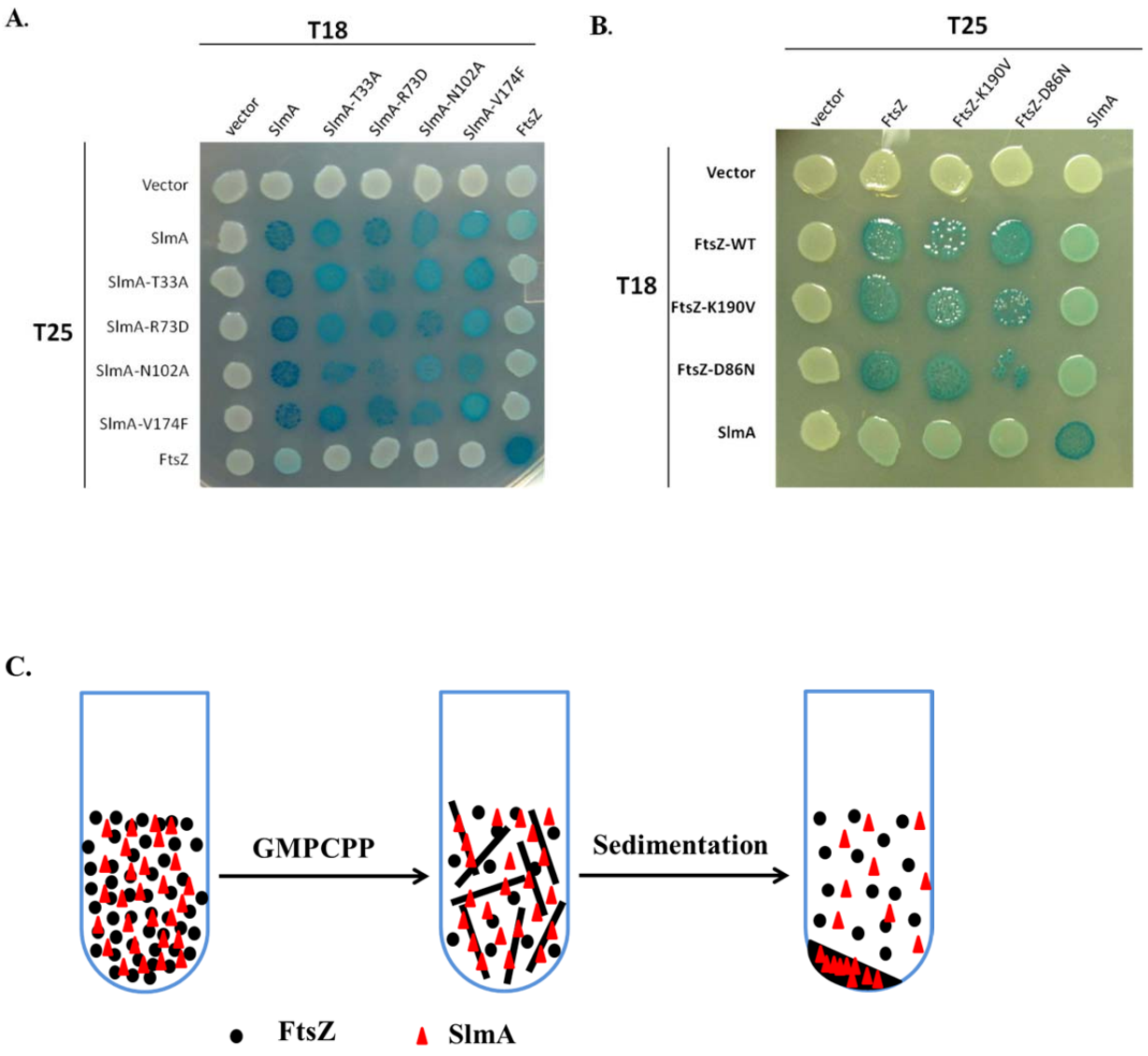
A.
T18
vector
SlmA
SlmA-T33A
SlmA-R73D
SlmA-N102A
SlmA-V174F
FtsZ
T25
Vector
SlmA
SlmA-T33A
SlmA-R73D
SlmA-N102A
SlmA-V174F
FtsZ
B.
T25
vector
FtsZ
FtsZ-K190V
FtsZ-D86N
SlmA
T18
Vector
FtsZ-WT
FtsZ-K190V
FtsZ-D86N
SlmA
C.
GMPCPP
Sedimentation
FtsZ
SlmA

D.

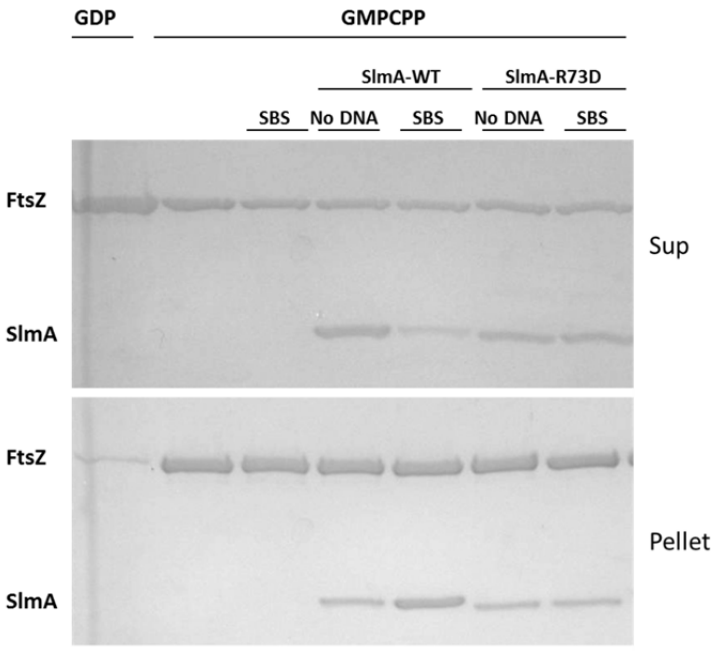
GDP
GMPCPP
SlmA-WT
SlmA-R73D
SBS
No DNA
SBS
No DNA
SBS
FtsZ
SlmA
Sup
FtsZ
SlmA
Pellet

E.

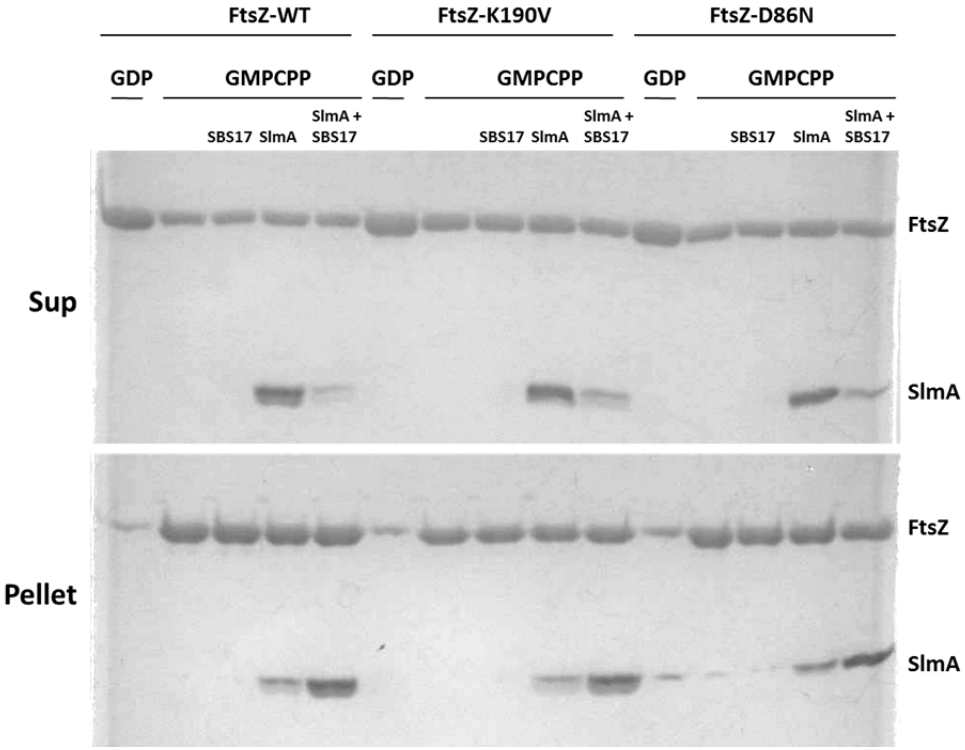
FtsZ-WT
FtsZ-K190V
FtsZ-D86N
GDP
GMPCPP
GDP
GMPCPP
GDP
GMPCPP
SBS17
SlmA
SlmA + SBS17
SBS17
SlmA
SlmA + SBS17
SBS17
SlmA
SlmA + SBS17
Sup
Pellet
FtsZ
SlmA
FtsZ
SlmA

Fig. 23. SBS17-30mer bound SlmA promotes bundling of stable FtsZ polymers. A) Polymerization assays were performed as in Fig. 19 except that the protein conentration was 2 μM and GTP was replaced by GMPCPP. Note that FtsZ-D86N tends to form larger bundles in the absence of SBS17-30mer and SlmA and stable FtsZ-K190V polymers were less prone to forming bundles in the presence of SBS17-30mer and SlmA. B) and C) comparison of stable FtsZ-WT and FtsZ-K190V polymers after addition of SBS17-30mer with SlmA. Note that complexes decorate the FtsZ-K190V bundles. Scale bar is 100 nm.

A.

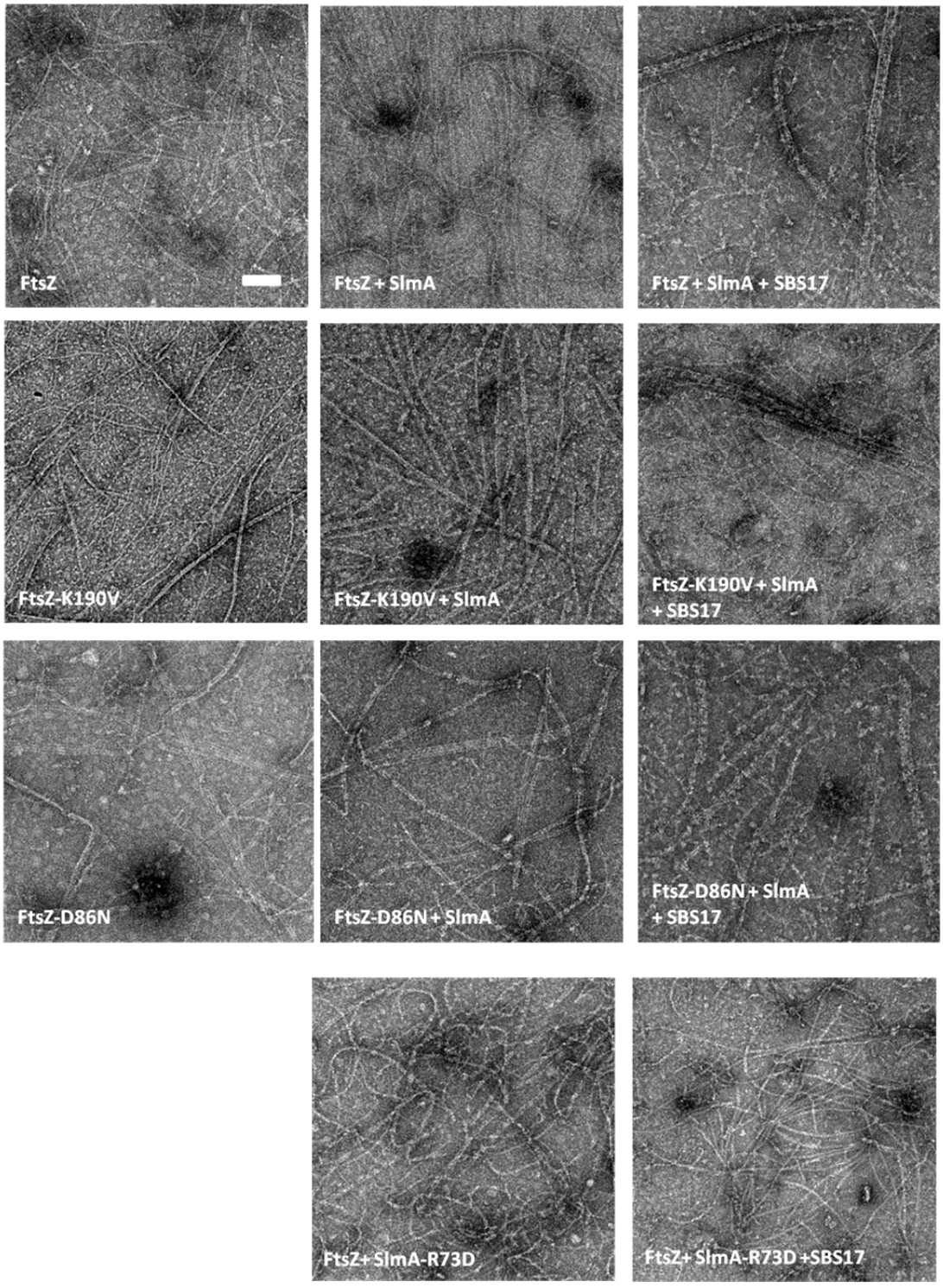
FtsZ
FtsZ + SlmA
FtsZ + SlmA + SBS17
FtsZ-K190V
FtsZ-K190V + SlmA
FtsZ-K190V + SlmA
+ SBS17
FtsZ-D86N
FtsZ-D86N + SlmA
FtsZ-D86N + SlmA
+ SBS17
FtsZ+ SlmA-R73D
FtsZ+ SlmA-R73D +SBS17

B.

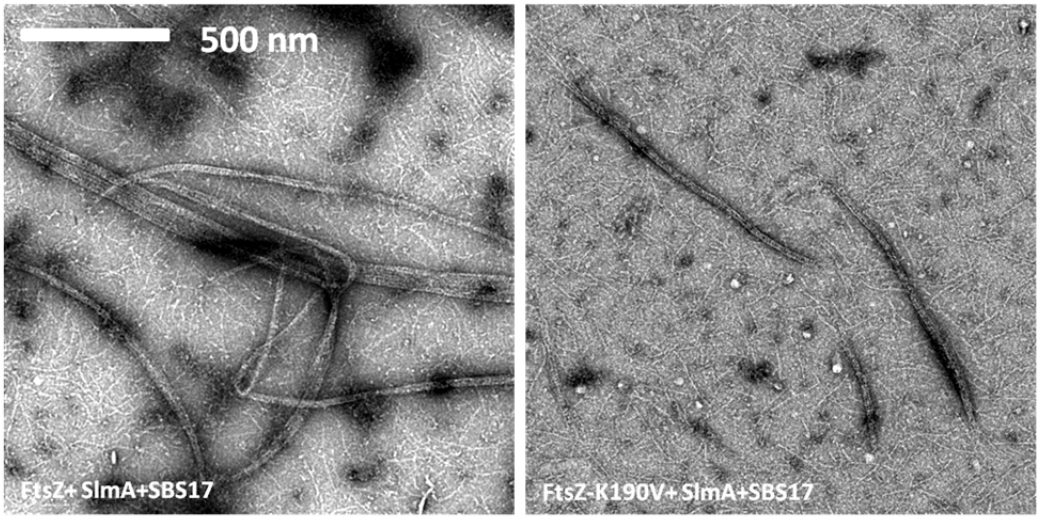
500 nm
FtsZ+ SlmA+SBS17
FtsZ-K190V+ SlmA+SBS17

C.

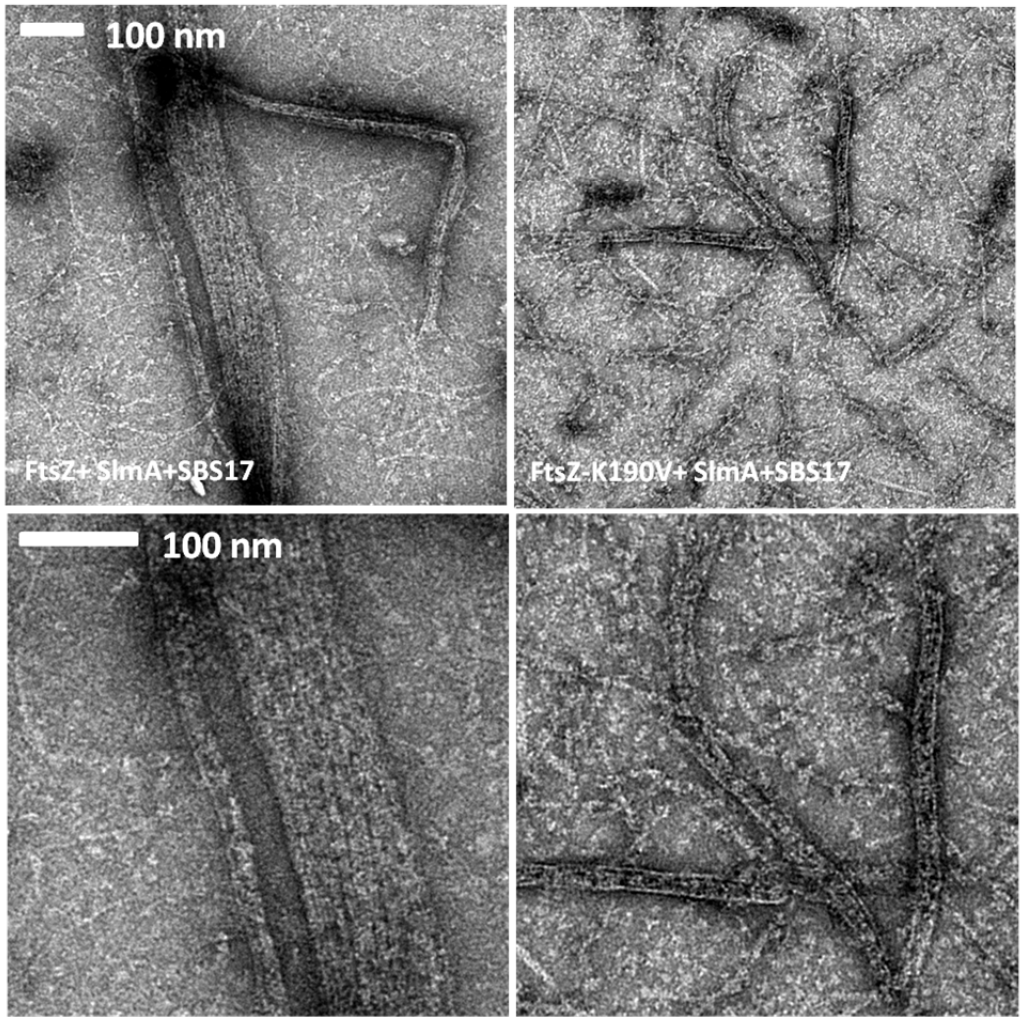
100 nm
FtsZ+ SlmA+SBS17
FtsZ-K190V+ SlmA+SBS17
100 nm

Fig. 24. Biolayer interferometry assay to assess SlmA binding to DNA and FtsZ. A) Streptavidin biosensor tips were loaded with 50 nM biotinylated SBS17-30mer for 5 minutes followed by a 10 second wash. Association was initiated by moving the SBS17-30mer coated tips to tubes containing 4 μM SlmA or SlmA mutants. Two minutes after incubation, the tips with biotinylated SBS17-30mer and SlmA or SlmA mutants bound were moved to tubes containing FtsZ polymerization buffer to measure dissociation for 2 minutes. The DNA binding mutant SlmA-T33A was used as a control. B) SlmA-WT interacts with FtsZ. SBS17-30mer-SlmA complexes were generated as in (A). The tips were then moved to tubes containing 4 μM FtsZ to measure the association for 1 minute and then into buffer lacking FtsZ to follow dissociation for 2 minutes (dissociation step is not shown). FtsZ-R73D and FtsZ-F65A, which do not interact with SlmA, were used as controls. C) FtsZ-K190V and FtsZ-D86N are not significantly affected in FtsZ-SlmA binding. Similar to B), 4 μM FtsZ or FtsZ mutants was included in tubes containing FtsZ polymerization buffer to measure the association for 1 minute and then into buffer lacking FtsZ to follow dissociation for 2 minutes (dissociation step is not shown). D) SBS DNA bound SlmA (His-tag free) binds to 6×His-FtsZ. Ni-NTA biosensor tips were loaded with 1 μM 6×His-FtsZ for 5 minutes followed by a 10 second wash. Association was initiated by moving the 6×His-FtsZ coated tips to tubes containing SlmA (untagged version, 1 μM) with or without SBS DNA of various lengths (1 μM) preincubated for 10 minutes. Two minutes after the incubation, the tips were moved to tubes containing FtsZ polymerization buffer to monitor the dissociation for 2 minutes. Data were generated automatically by the BLItz™ software and then analyzed by GraphPad Prism 5.0.

A.

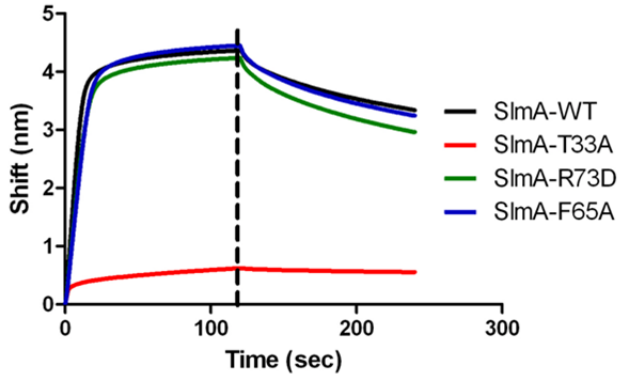
Shift (nm)
Time (sec)
SlmA-WT
SlmA-T33A
SlmA-R73D
SlmA-F65A

B.

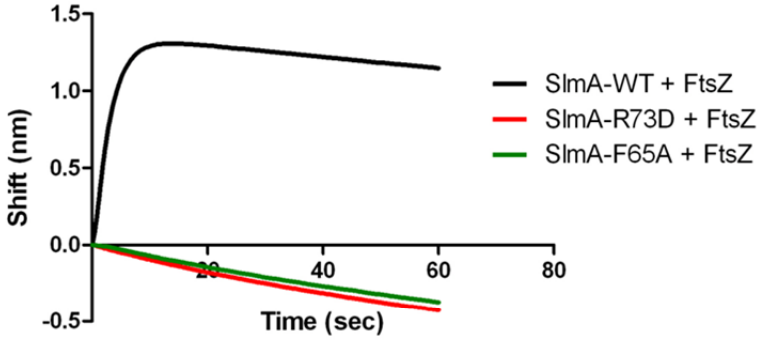
Shift (nm)
Time (sec)
SlmA-WT + FtsZ
SlmA-R73D + FtsZ
SlmA-F65A + FtsZ

C.

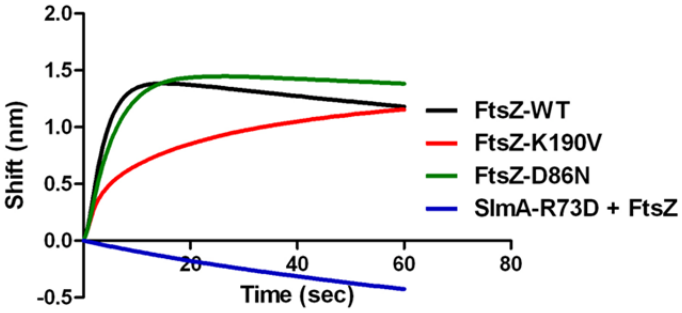
Shift (nm)
Time (sec)
FtsZ-WT
FtsZ-K190V
FtsZ-D86N
SlmA-R73D + FtsZ

D.

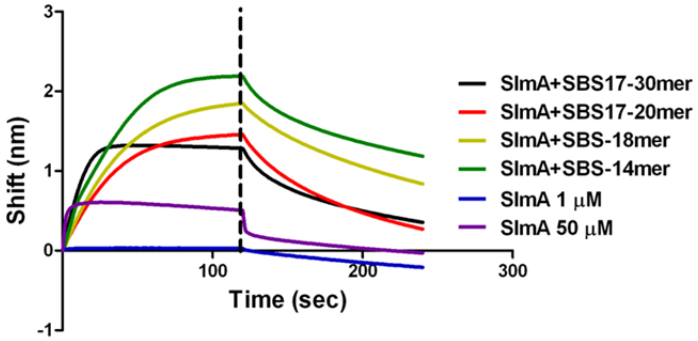
Shift (nm)
Time (sec)
SlmA+SBS17-30mer
SlmA+SBS17-20mer
SlmA+SBS-18mer
SlmA+SBS-14mer
SlmA 1 μM
SlmA 50 μM

Table 6. Binding affinities of SlmA and SlmA mutants for biotinylated SBS17-30mer as well as binding affinities of SBS bound SlmA for immbolized 6×His-FtsZ. See Fig. 24 and the text for details about the reaction conditions to measure the binding affinities. K_D of SlmA and its mutants for biotinylated SBS17-30mer were calculated by equation $K_D=k_{off}/k_{on}$. The binding affinity of SlmA or SBS bound SlmA for 6×His-FtsZ was calculated similarly and the K_D shown is the representative of three independent binding experiments.

Binding affinities of SlmA mutants for the biotinylated SBS17-30mer				
	K_D **(M)**	k_{on} **[1/(M*s)]**	k_{off} **(1/s)**	R^2 *****
SlmA-WT	6.29×10^{-8}	$3.24\times10^{+4}$	2.04×10^{-3}	**0.98**
SlmA-F65A	11.44×10^{-8}	$2.48\times10^{+4}$	2.83×10^{-3}	**0.98**
FtsZ-R73D	10.63×10^{-8}	$2.31\times10^{+4}$	2.46×10^{-3}	**0.98**
SlmA-T33A	**No binding**			
Binding affinities of SlmA and SBS-SlmA for 6×His-FtsZ				
SlmA	210×10^{-7}	$0.71\times10^{+4}$	14.9×10^{-2}	**0.97**
SlmA + SBS17-30mer	2.10×10^{-7}	$7.40\times10^{+4}$	1.55×10^{-2}	**0.98**
SlmA + SBS17-20mer	7.89×10^{-7}	$1.81\times10^{+4}$	1.43×10^{-2}	**1.0**
SlmA + SBS-18mer	3.09×10^{-7}	$2.16\times10^{+4}$	0.67×10^{-2}	**1.0**
SlmA + SBS-14mer	2.06×10^{-7}	$2.75\times10^{+4}$	0.57×10^{-2}	**0.98**

R^2 is the coefficient of determination estimating the goodness of a curve fit reported by the GraphPad Prism 5.0 s software.

to 120 nM. The SlmA DNA binding mutant SlmA-T33A as expected did not bind to the immobilized SBS17-30mer. Addition of FtsZ to SBS17-30mer-SlmA but not to SBS17-30mer-SlmA-R73D/F65A resulted in a rapid and strong binding signal, but this binding signal slowly decreased after the binding signal reached a plateau, presumably because SlmA slowly dissociates from the DNA (Fig. 24B). Therefore, we could not use the binding kinetics to calculate the binding affinity between FtsZ and SBS bound SlmA, but we could still use the system to monitor FtsZ mutants binding to SBS17-SlmA. Addition of FtsZ-D86N resulted in a similar binding curve as FtsZ-WT, however, addition of FtsZ-K190V displayed slower binding kinetics (Fig. 24C). Rather than the rapid binding observed with FtsZ-WT and FtsZ-D86N, which reached a plateau within 15 sec, FtsZ-K190V bound to SBS17-30mer-SlmA slowly but reached the same plateau. We were not sure whether this different binding kinetics was due to a deficiency in direct binding with SlmA or FtsZ-K190V may exist in a slightly different conformation that affects its binding to SlmA indirectly. As FtsZ-K190V interacts with SBS bound SlmA in bacterial two-hybrid test and co-sedimentation assay, we considered FtsZ-K190V did not affect FtsZ-SlmA binding significantly.

In a reciprocal approach, we immobilized 6×His tagged FtsZ on Ni-NTA biosensors and monitored SBS17-30mer bound SlmA binding to FtsZ. As showed in Fig. 24D, addition of SlmA (His-tag free) pre-incubated with SBS17-30mer resulted in rapid and stable binding signal, while addition of SlmA alone did not cause any signal. Pre-incubation of SlmA with shorter SBS DNA prolbes also resulted in rapid and stalbe binding signal. This stable binding kinetics allowed us to calculate the binding affinity between SBS bound SlmA with FtsZ to be between 200 and 800 nM depending on the SBS probes, consistent with previous published measurements obtained by other methods (Tonthat et al., 2011).

Discussion

Ever since its identification, SlmA has been of great interest because it prevents Z ring formation over the nucleoid through direct interaction with FtsZ (Bernhardt and de Boer, 2005). Recent studies have

shown that SlmA binds to specific DNA sequences (SBSs) that are restricted to the origin proximal region of the chromosome, explaining how SBS bound SlmA is removed from the midcell by chromosome segregation (Cho et al., 2011; Tonthat et al., 2011). However, the mechanism by which SBS bound SlmA prevents FtsZ from assembling into the Z ring has been controversial. In this study, we showed that SlmA bound to SBS DNA antagonizes FtsZ proto-filament formation, consistent with the observation of the Bernhardt group (Cho et al., 2011). The efficiency of SlmA to antagonize FtsZ polymerization correlates with the length of the bound SBS DNA: the longer the more potent. Furthermore, removing the positive charge from K190, a residue located in the H7 helix of FtsZ, and substitution of D86 to Asn, a residue in the H3 helix, render FtsZ resistant to the NO function of SlmA. Extensive genetic and biochemical characterization of these mutants showed that they confer resistance to SlmA by indirect mechanisms rather than directly affecting the binding to SlmA.

SlmA is a DNA activated FtsZ polymerization antagonist

SlmA was initially observed to recruit FtsZ to the nucleoid *in vivo* and promote bundling of FtsZ filaments *in vitro* (Bernhardt and de Boer, 2005), but two recent investigations found that SlmA is an antagonist of FtsZ assembly (Cho et al., 2011; Tonthat et al., 2011). In one study, SlmA in the presence of a SlmA binding sequence was found to disassemble FtsZ proto-filaments, while in the other study, SBS bound SlmA was observed to force FtsZ proto-filaments to grow into some antiparallel structures, which may not be suitable for Z ring formation (Cho et al., 2011; Tonthat et al., 2011). Even though these two studies disagreed on the mechanism by which activated SlmA prevents the Z ring formation, they both reached the same conclusion that SlmA is activated (about 40-fold) by the SlmA binding sequences (Cho et al., 2011; Tonthat et al., 2011). However, the controversy was furthered by a subsequent report in which SlmA was observed to have no impact on FtsZ proto-filament formation. This latest observation conbined with the unexpected finding that SlmA forms an oriented dimer-of-dimers on SBS DNA, which may spread on the DNA, led to the hypothesis that SlmA prevents Z ring formation by sequestration of

FtsZ filaments onto the SlmA-DNA complexes (Tonthat et al., 2013). The FtsZ proto-filaments on the SlmA-DNA run in different directions that would prevent FtsZ filaments from coalescing into a Z ring.

Here, using SBS-DNA molecules of different lengths and performing the reactions in buffers used in previous studies, we show that SlmA is indeed a DNA activated FtsZ antagonist. The reason that the latest study (Tonthat et al., 2013) observed no impact of SBS-SlmA on FtsZ polymerization is likely due to the SBS DNA and the buffer used for the assays. While we rarely observed FtsZ proto-filaments in the presence of SlmA and the SBS17-30mer DNA (CAAAAGTAA**GTAAATGGTCAC**TAACGTTGA), we observed lots short proto-filaments when shorter SBS DNA, SBS17-20mer (GTAA**GTAAATGGTCAC**TAAC), SBS-18mer (CCCAAT**GTGAGTGCTCAC**) and SBS-14mer (A**GTGAGTACTCAC**T) were used in the FtsZ polymerization reaction. These results indicate that the efficacy of SlmA to antagonize FtsZ polymerization reduces as the bound SBS DNA gets shorter. Previous study has showed that SlmA makes three additional contacts on each side of the consensus sequence when it is in the middle (TTAC**GTGAGTACTCAC**GTAA) of a long seqence compared to a 12mer SBS DNA with just the consensus sequence (**GTGAGTACTCAC)** (Tonthat et al., 2013)**.** This reduction in contacts results in a 2-3 fold lower binding affinity of SlmA for the 12mer SBS DNA compared to that of the longer SBS DNA (TTAC**GTGAGTACTCAC**GTAA) (Tonthat et al., 2013), explaining the reduced effect on FtsZ polymerization of SlmA in presence of the short SBS DNA. In Tonthat's buffer, although SlmA antagonizes FtsZ polymerization efficiently in the presence of SBS17-30mer, SlmA had only minor effect on FtsZ polymerization when shorter SBS DNA were used. These results suggest that the buffer also contributes to the observation that SlmA has no impact on FtsZ polymerization (Tonthat et al., 2013). As previously reported, SlmA in the absence of SBS DNA molecules does not influence FtsZ proto-filament formation. Thus, our data is consistent with the observation of the Bernhardt group: SBS binding activates SlmA to antagonize FtsZ polymerization (Cho et al., 2011).

Previous biochemical and genetic tests indicated that SBS DNA binding stimulates SlmA dimerization and induces a conformational change in the SlmA dimer to fully expose an occluded FtsZ binding site such that it can bind to FtsZ with high affinity (Cho and Bernhardt, 2013). Although it has been shown SlmA forms dimers in the absence of SBS DNA, it is not clear why SlmA-T33A fails to self interact in the bacterial two hybrid assay used in a previous study (Cho et al., 2011). We show here that SlmA-T33A is able to interact with itself as well as other SlmA mutants. The failure to detect the self-interaction of SlmA in the previous study is due to the fact that the T18 and T25 domains of adenylate cyclase were fused to the N terminal domain of SlmA (Cho et al., 2011), which are far away when SlmA forms dimers. Our data thus confirm that SlmA exists as dimers and SBS binding activates SlmA by inducing a conformational change to the dimer. Structural analysis of SlmA with and without DNA also supports such a model. However, the observation from SAXS studies (done at very high protein concentrations and without SBS DNA) that SlmA dimer was sandwiched by two FtsZ molecules in the absence of SBS DNA and that SlmA forms oriented dimer-of-dimer with SBS DNA led to the assumption that the conformational change induced by SBS DNA binding made a minor contribution to FtsZ binding (Tonthat et al., 2011; Tonthat et al., 2013). Using a non-hydrolyzeable GTP analog, GMPCPP, we observed co-sedimentation of SlmA with FtsZ-GMPCPP polymers in the presence but not in the absence of the SBS17-30mer DNA, indicating that SBS binding is critical for SlmA to bind FtsZ. This result is consistent with previous observation that SlmA co-sedimented with polymers formed by the FtsZ catalytic mutant FtsZ-D212N in the presence of the SBS17-30mer DNA (Cho et al., 2011). Visualization of FtsZ-GMPCPP polymers under electron microscopy showed that addition of SlmA with SBS17-30mer DNA induced the formation of large bundles of FtsZ-GMPCPP polymers, but addition of SlmA or SBS17-30mer alone had no impact on the FtsZ-GMPCPP polymers. It seems reasonable that these large bundles are SlmA bound to the SBS sandwiched between FtsZ polymers. Similar results were also observed with shorter SBS DNA. Thus, taken together, our data agrees with the model that SBS DNA

binding activates SlmA to bind FtsZ by inducing a conformational change in the dimer to expose the FtsZ binding site.

SlmA forms an oriented dimer-of-dimers on the SBS DNA, allowing four FtsZ molecules to bind to the SBS at the same time. Thus, it has been proposed that the SlmA dimer-of-dimers force the four bound FtsZ proto-filaments to grow in different directions, clash and unable to make lateral interactions necessary for Z ring formation (Tonthat et al., 2013). Our finding that SBS bound SlmA promotes the bundling of FtsZ stable polymers suggests that this "SlmA induced FtsZ proto-filaments clash" is unlikely to happen. Addition of SlmA with SBS17-30mer DNA induces FtsZ-GMPCPP filaments to bundle into large structures that are up to several μm long. Small complexes were found on the surfaces, or sandwiched between proto-filaments in the bundles, which stand out clearly in the small bundles formed by FtsZ-K190V-GMPCPP. Although we do not have direct evidence, these complexes likely represent the SBS-SlmA complexes sandwiched between FtsZ filaments. Therefore, in the absence of GTP hydrolysis, SBS bound SlmA promotes the bundling of FtsZ proto-filaments rather than inhibit their growth by promoting clashing.

Previous SAXS analysis of FtsZ (lacking the C-terminal tail) at the concentration of 1 to 2 mg/ml indicated that FtsZ in the presence of GDP self associates in a proto-filament like structure (Tonthat et al., 2011). However, addition of SlmA without an SBS resulted in a SAXS profile indicative of aggregation-free SlmA-FtsZ complexes suggesting that SlmA-FtsZ interaction reduced the FtsZ-FtsZ interaction. Superimposing the SlmA dimer structure into the SAXS envelope suggested that the SlmA dimer is sandwiched by two FtsZ molecules and it was suggested that SlmA interacts with helix 10 of FtsZ (Tonthat et al., 2011). These complexes were observed without an SBS present (and without the FtsZ C-terminal tail which we show in the next section is necessary for high affinity binding) indicating this may

Fig 25. Examinaiton of FtsZ mutants resistant to the N terminal domain of MinC for resistance to de-localized SlmA. Plasmids pSD133 (P*tac::slmA*) and p2SBSK (pUC18 with 2SBS sites) were introduced into the *ftsZ*- strain DU11 (*ftsZ*^{0} *slmA<frt> recA::Tn10*) complemented with pBANG112 or its derivatives containing different *ftsZ* alleles. One colony of each resultant strain was resuspended in 1 ml LB medium, serially diluted by 10 and 3 μl from each dilution was spotted on LB plates containing various concentration of IPTG and supplemented with ampicillin, spectinomycin and kanamycin. The plates were incubated at 30°C for 30 hours before photography. Helix 10 was colored as blue and substitutions of residues resistant to the N terminal domain of MinC were colored as green. K190 and D86 were colored as yellow and red respectively.

A.

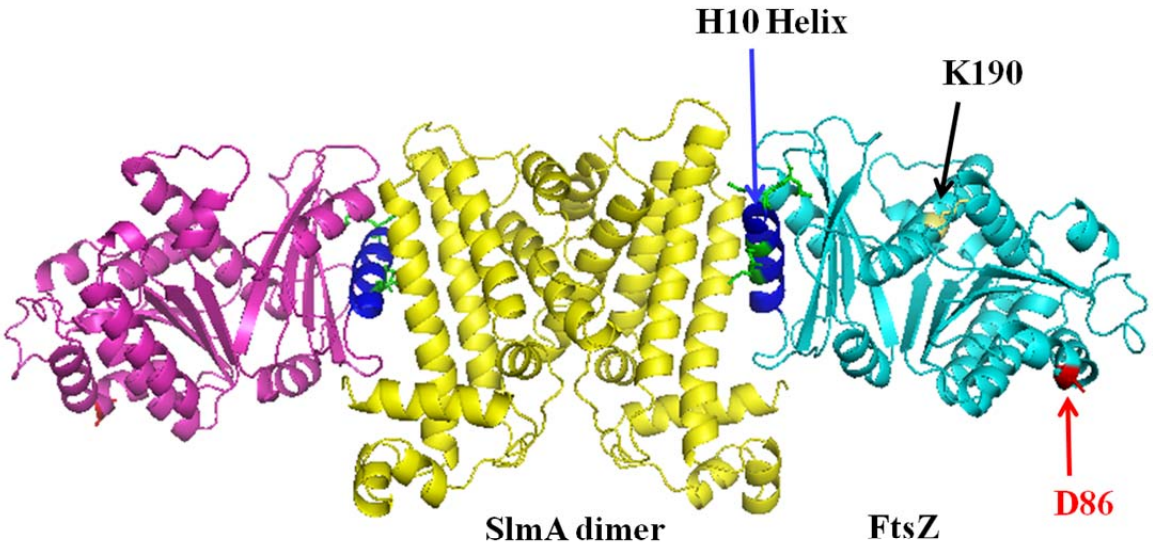
H10 Helix
K190
D86
SlmA dimer
FtsZ

B.

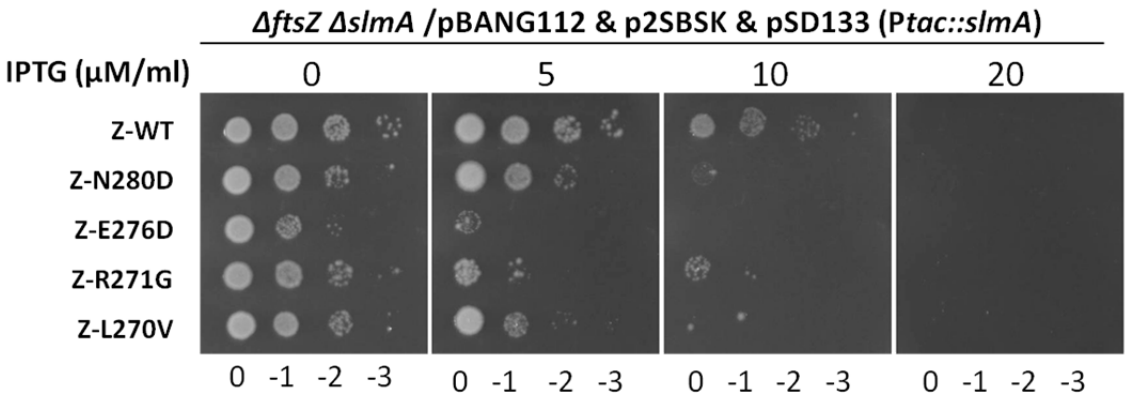
ΔftsZ ΔslmA /pBANG112 & p2SBSK & pSD133 (Ptac::slmA)
IPTG (μM/ml)
0
5
10
20
Z-WT
Z-N280D
Z-E276D
Z-R271G
Z-L270V
0 -1 -2 -3
0 -1 -2 -3
0 -1 -2 -3
0 -1 -2 -3

Fig. 26. Model for how SlmA antagonizes FtsZ polymerization. FtsZ exists in two different conformations, FtsZ-GDP form (assembly incompetent form) and FtsZ-GTP form (assembly competent form). Above its critical concentration, FtsZ in the assembly competent form assembles into polymers in the presence of GTP. FtsZ polymers undergo hydrolysis to produce FtsZ-GDP, which depolymerizes. The two sub-domains of FtsZ as well as H7 helix undergo conformational changes following GTP hydrolysis; some of the residues undergoing dramatic change are indicated: R29, D86, N186S and K190 are colored orange, red, cyan and magenta respectively; GDP is colored brown. Note the different positions of R29 and N186 in the two different conformations. PC190723 stablizes FtsZ in the FtsZ-GTP form such that FtsZ assembles into polymers without a critical concentration. SlmA takes advantage of the positive charge of K190 to stimulate the conformational change that is required for GTP hydrolysis, resulting in faster turnover of the FtsZ and breakdown of FtsZ polymers.

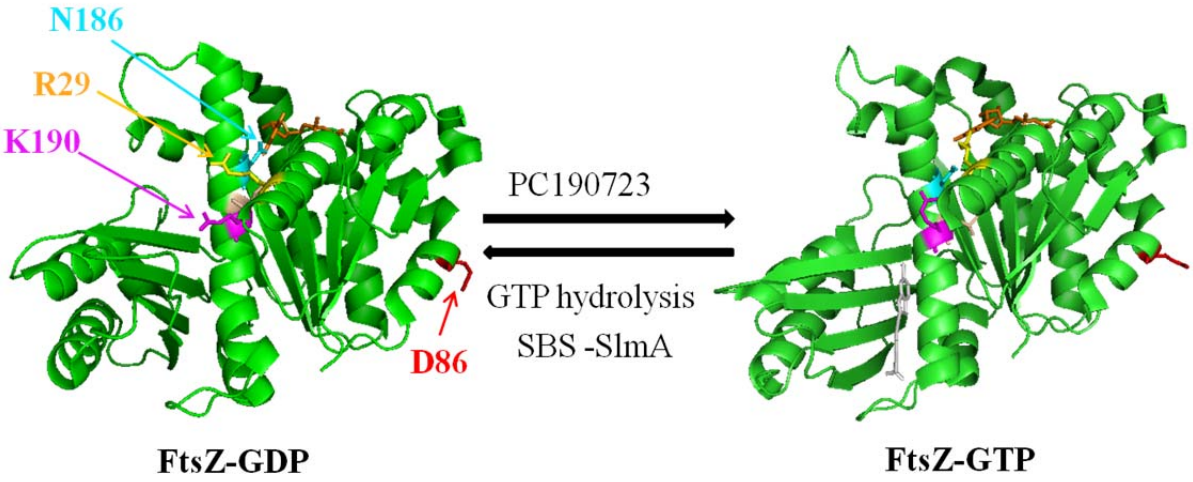
N186
R29
K190
D86
PC190723
GTP hydrolysis
SBS -SlmA
FtsZ-GDP
FtsZ-GTP

be a weak interaction since we have shown that SlmA must be bound to SBS to observed high affinity binding to FtsZ.

SlmA binding site on FtsZ

Our data strongly supports the model that SBS associated SlmA prevents Z ring formation over the nucleoid by antagonizing FtsZ polymerization. However, the mechanism by which activated SlmA antagonizes FtsZ polymerization is not clear. Previous studies showed that activated SlmA stimulates the GTPase activity of FtsZ and requires the GTPase of FtsZ to disassemble the FtsZ filaments (Cho et al., 2011), the latter we confirmed in this study. Thus, it appears that SlmA prevents FtsZ polymerization by two actions: stimulating FtsZ-GDP formation within the filaments and severing the FtsZ filaments at positions where the GTP has been hydrolyzed to GDP. Such a working mechanism is very similar to the proposed mechanism of MinC except that MinC does not stimulate the GTPase activity of FtsZ (Shen and Lutkenhaus, 2010). Genetic studies indicated that MinC binds to the α10 helix of FtsZ, most of which is hidden when FtsZ is within the filaments (Shen and Lutkenhaus, 2010). Thus, it was proposed that MinC can only break FtsZ filaments after the α10 helix is exposed by GTP hydrolysis (Shen and Lutkenhaus, 2010). Interestingly, SAXS analysis of SlmA-FtsZ or SBS-SlmA-FtsZ complexes indicates that SlmA binds to FtsZ around helix 10 (Tonthat et al., 2011; Tonthat et al., 2013). A spot test of FtsZ mutants resistant to the N terminal domain of MinC showed that these mutants were more sensitive to SlmA in the presence of extra SBSs in a plasmid rather than resistant (Fig. 25). Therefore, even if the α10 helix is involved in SlmA binding, the way it interacts with SlmA is likely different than that of MinC. In addition, the fact that SlmA still co-sedimented with the FtsZ-GMPCPP polymers suggests that the α10 helix is unlikely to be the primary binding site for SlmA because it would not be available in the FtsZ-GMPCPP polymers. The association of the SBS-SlmA complexes with the FtsZ-GMPCPP polymers

suggests that SBS activated SlmA either binds to the tail of FtsZ or binds to the lateral surface of FtsZ globular domain exposed in filaments.

The basis of D86N and K190V conferred resistance

FtsZ-D86N shows some resistance to the NO function of SlmA *in vivo* and some resistance to the inhibitory activity of SlmA *in vitro*. However, it does not seem to affect SlmA binding, suggesting that it is not a binding site mutant and it is likely provide resistance to SlmA through by an indirect mechanism. Our data suggests that the D86N mutation likely lowers the sensitivity of FtsZ filaments to the activated SlmA by promoting the bundling of proto-filaments. At concentrations where FtsZ-WT and FtsZ-K190V assemble into single-stranded filaments, FtsZ-D86N tends to form bundles that are 2-3 stranded. The bundling of FtsZ-D86N filaments is even more dramatic when assembled with GMPCPP or at low salt conditions (50 mM KCl, data not showed). Formation of FtsZ bundles by the FtsZ-D86N can lead to SlmA resistance in two ways: masking the SlmA binding site and lowering the GTPase of FtsZ such that fewer FtsZ-GDP would be available for SlmA to attack. Although the first possibility is hard to prove, the D86N mutation indeed reduces the GTPase activity. Substitution of D86 to Lys also confers resistance to SlmA *in vivo*, and this mutant has been characterized *in vivo* and in *vitro* before. *In vivo*, FtsZ-D86K assembles into extensive spirals of three or four turns that extend along the length of the cells rather than forming sharp Z rings (Stricker and Erickson, 2003). *In vitro*, FtsZ-D86K showed a strong tendency to assemble into multistranded tubes, suggesting that D86 may be important for the lateral interaction of FtsZ (Lu et al., 2001). Mutations of E83 and R85, which are also located α3 helix, have also been shown to affect the GTPase activity and assembly of FtsZ, indicating that the α3 helix might be involved in lateral interaction (Shin et al., 2013). In addition, proteins or agents that promote bundling of FtsZ proto-filaments lower the GTPase activity of FtsZ and confer resistance to FtsZ inhibitors. For example, ZapA induces bundling of FtsZ proto-filaments, resulting in insensitivity to the action of MinC (Dajkovic et al.,

2008a). Consistent with this, when we deleted *zapA* from the chromosome, cells become much more sensitive to the killing of SlmA by overproduction or addition of extra SBSs in the plasmid (data not shown). Thus, the resistance of FtsZ-86N to SlmA likely stems from its increased tendency to form bundles.

FtsZ-K190V shows strong and specific resistance to SlmA *in vivo* and *in vitro*, however, it does not show a strong defect in SlmA binding. Bacterial two-hybrid tests showed similar interaction of FtsZ-K190V –SlmA and FtsZ-WT-SlmA. Consistent with this, SBS bound SlmA co-sedimented with the FtsZ-K190V-GMPCPP polymers, suggesting that if there is any binding defect, it is minor. However, we noticed a slight binding defect between FtsZ-K190V and SBS bound SlmA in two situations. First, the FtsZ-K190V-GMPCPP polymers are less prone to bundle by addition of SlmA with SBS DNA compared to the filaments formed by FtsZ-WT. Second, FtsZ-K190V binds immobilized SBS-SlmA with a slower kinetics compared to that of FtsZ-WT or FtsZ-D86N. At present, it is not clear whether this slow binding kinetics is responsible for FtsZ-K190V's resistance to SlmA or just a side effect of the mutation on FtsZ.

Interestingly, K190 is located in the middle of the H7 helix, which mediates the conformational change between the two sub-domains of the globular domain of FtsZ (Elsen et al., 2012). Comparison of SaFtsZ-PC190723-GDP structure (represents the FtsZ-GTP conformation) with that of FtsZ-GDP shows that the side chain of K190 rotates about 90°. It is not clear whether this rotation is important for FtsZ assembly, but it is clear that mutating this residue affects FtsZ function. Mutating K190 to Ala, Leu, Ile, Val, Asn, Glu, Trp and Arg did not affect complementation of an FtsZ null strain. However, all of these substitutions, except for the K190R mutation, conferred resistance to SlmA, suggesting that the positive charge of K190 is critical for SlmA to disassemble the FtsZ polymers. A R191P (R191 corresponds to K190 in *E. coli*) mutation of *Staphylococcus aureus* FtsZ confers resistance to the FtsZ inhibitor PC190723 and renders *S. aureus* dependent on PC190723 for growth (Haydon et al., 2008). However, in

both cases K190/R191 does not appear to be important for binding the inhibitor. The K190V mutation only slightly affects the binding kinetics of FtsZ with SlmA, while R191 does not make any contact with the PC190723 compound in the SaFtsZ-PC190723-GDP structure. Why mutation of this residue provides resistance to two different FtsZ inhibitors? The location of K190/R191 implies that it has to do with the communication between the two sub-domains of FtsZ upon assembly/disassembly. Affecting the communication between the two sub-domains of FtsZ can lead to many outcomes, for example, stabilization of FtsZ in one conformation that promotes cooperative assembly of FtsZ as in the case of PC190723 (Elsen et al., 2012). Disruption of the communication can also lead to disassembly of the FtsZ filaments. As K190 appears to be unimportant for SlmA binding, we propose that SlmA bound to another site on FtsZ takes advantage of the positive charge of K190 to influence the communication of the two sub-domains of FtsZ, which leads to the breakdown of FtsZ polymers.

Chapter IV SlmA targets the conserved C-terminal tail of FtsZ

Abstract

In the previous chapter, we showed that SlmA is a specific DNA activated FtsZ polymerization antagonist and mutations affecting residues at two different locations in FtsZ provide resistance to SlmA. However, as discussed above, these two mutations are not binding site mutations and they confer resistance to SlmA by indirect mechanisms rather than disruption of the FtsZ-SlmA interaction. In this chapter, we found that the conserved C-terminal tail of FtsZ is the primary binding site of SlmA. Deletion of the tail of FtsZ or single substitutions of highly conserved residues in the tail abolished SlmA binding and rendered FtsZ resistant to the action of SlmA. Pre-incubation of FtsZ with ZipA, which also binds the tail of FtsZ, blocks FtsZ binding to the SBS bound SlmA, suggesting that competition for the conserved C-terminal tail of FtsZ between the FtsZ membrane anchors and the negative regulators is important for the regulation of the Z ring formation. Combined with previous data, our finding suggests that activated SlmA, similar to MinC, acts on FtsZ by two steps: binding to the conserved C-terminal tail and breaking the filaments.

Introduction

SlmA is a potent division inhibitor in the presence of extra SBS in a multicopy plasmid that diffuses randomly inside the cell (Cho et al., 2011). Evidence showed that it blocks cell division by preventing Z ring formation through direct interaction with FtsZ (Bernhardt and de Boer, 2005; Cho et al., 2011). However, how the SBS activated SlmA prevents FtsZ from assembling into the Z ring is not clear. There is some evidence suggesting that SlmA oligomerized on the DNA blocks Z ring formation by recruiting t FtsZ polymers to the SlmA-DNA complexes (Tonthat et al., 2013), but data from the Bernhardt group (Cho et al., 2011) and our lab suggest that it is more likely that SlmA blocks Z ring formation by antagonizing FtsZ polymerization. Studies of the SlmA resistant mutant FtsZ-K190V indicate that SBS activated SlmA may disassemble the FtsZ polymers by affecting the communication between the two sub-domains within the globular domain of FtsZ. However, this mutation does not seem to disrupt the FtsZ-SlmA interaction. As the SlmA binding site on FtsZ has not been identified yet, it is not clear how SlmA interacts with FtsZ leads to FtsZ disassembly.

Previous studies from the Schumacher lab suggested that the conserved C-terminal tail of FtsZ is not necessary for SlmA binding as a truncated derivative of FtsZ, FtsZ360, binds to SBS-SlmA as well as wild type FtsZ (Tonthat et al., 2011). The linker region also appears to be unimportant for SlmA binding as SAXS analysis showed that $FtsZ_{316}$-GFP binds to SlmA and forms a sandwich like complex (Tonthat et al., 2011). In an attempt to confirm that the linker region and the conserved C-terminal tail of FtsZ are not necessary for SlmA binding, we found unexpectedly that the conserved C-terminal tail of FtsZ is absolutely required for SlmA binding and susceptibility to the action of SlmA. Single amino acid substitutions or deletion of the conserved C-terminal tail of FtsZ resulted in loss of SlmA binding. Furthermore, a 14 amino acids peptide corresponding to the conserved C-terminal tail of FtsZ was sufficient to bind SlmA and blocked SlmA binding to FtsZ. ZipA, which tethers FtsZ polymers to the

membrane through binding the conserved C-terminal tail of FtsZ, blocks FtsZ binding to SlmA, suggesting underestimated competition for the tail of FtsZ in regulation of Z ring formation. Consistent with this, we isolated one FtsZ tail mutant that only supported growth in the absence of one of the negative regulators, the Min system or SlmA. Although SlmA disassembles FtsZ polymers, its primary binding site has nothing to do with polymerization. This paradox suggests that SlmA acts on FtsZ in two steps: first, binding to the conserved C-terminal tail of FtsZ, which activates its secondary binding; second, breaking the FtsZ polymers through disruption of the communication between the two sub-domains of FtsZ.

Results

The conserved C-terminal tail of FtsZ is required for SlmA binding and susceptibility to SlmA action

Co-sedimentation of stable FtsZ polymers (FtsZ polymer formed with GMPCPP or FtsZ-D212N polymers) with SlmA in the presence of SBS DNA showed that SlmA is recruited to FtsZ polymers, suggesting that SBS activated SlmA must bind to the surface of the FtsZ polymers because the longitudinal interfaces are occluded within the polymers. Consistent with this idea, EM analysis of stable FtsZ polymers with SBS DNA and SlmA showed that the FtsZ polymers were decorated by complexes that likely represent the SBS-SlmA complexes. Thus, SlmA either binds to the surface of the globular domain, or the linker and the conserved C-terminal tail of FtsZ. However, previous studies have shown that the linker and the conserved C-terminal tail of FtsZ are not required for SlmA binding (Tonthat et al., 2011). To confirm these findings, we purified 6×His tagged FtsZ320 which misses the linker and the conserved C-terminal tail, and tested whether it would bind to SlmA in the *BLItz* system. To our surprise, the 6×His-FtsZ320 showed no binding signal with SlmA bound with SBS17-30mer immobilized on the

Fig. 27. The conserved C-terminal tail of FtsZ is necessary for SBS-SlmA binding to FtsZ. A) BLItz assays to monitor the binding of FtsZ C-terminal truncations to SlmA bound to SBS17-30mer immobilized on SA biosensors. Reactions were performed as in Fig. 24B. B) SBS bound SlmA does not co-sediment with stable FtsZ-360 polymers formed with GMPCPP. Reactions were performed as in Fig. 22D. C) SBS-SlmA promotes bundling of stable FtsZ polymers but not stable FtsZ-360 polymers. Reactions were performed as Fig. 23C.

A.

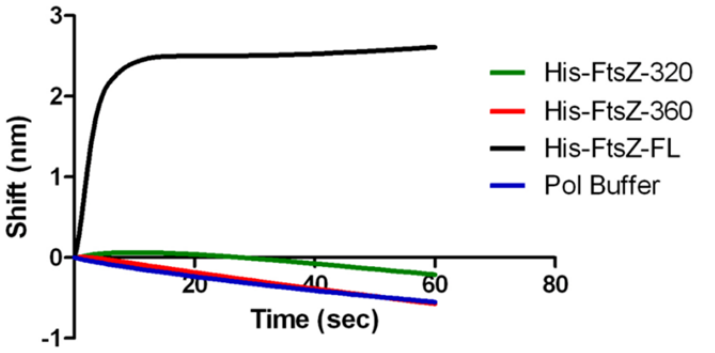
Shift (nm)
Time (sec)
His-FtsZ-320
His-FtsZ-360
His-FtsZ-FL
Pol Buffer

B.

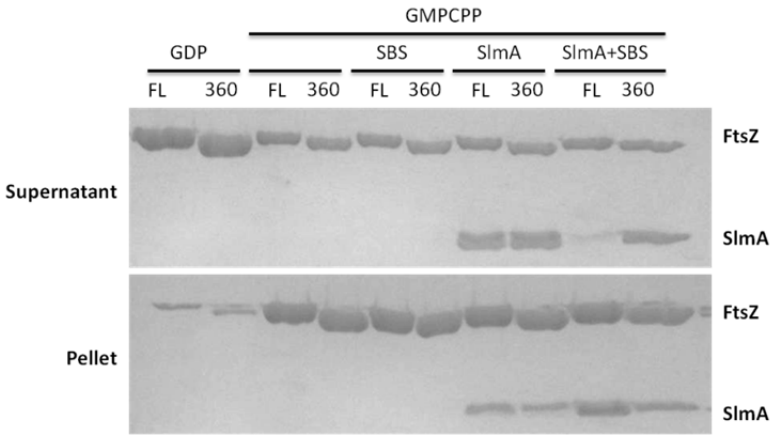
GMPCPP
GDP
SBS
SlmA
SlmA+SBS
FL
360
Supernatant
Pellet
FtsZ
SlmA

C.

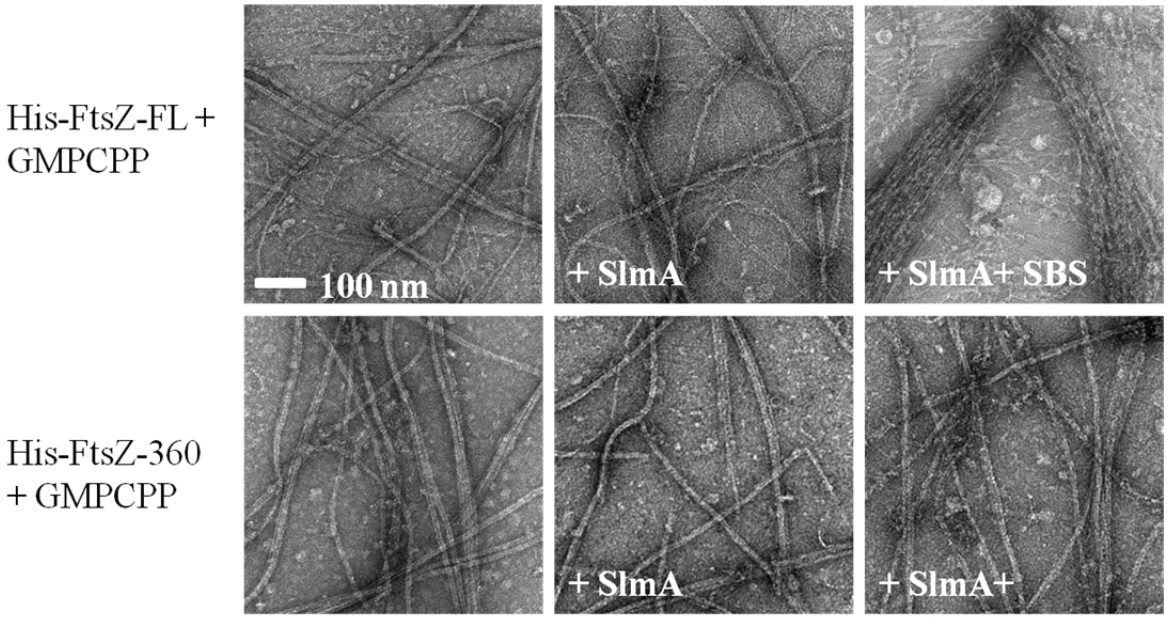
His-FtsZ-FL + GMPCPP
His-FtsZ-360 + GMPCPP
100 nm
+ SlmA
+ SlmA+ SBS
+ SlmA
+ SlmA+

Fig. 28. The conserved C-terminal tail of FtsZ is necessary for SlmA to antagonize FtsZ polymerization. FtsZ polymerization reactions performed with or without the addition of SlmA bound to SBS17-30mer. Reactions were performed in 50 μl volume containing FtsZ (2 μM) and GTP (1 mM) with or without the addition of SlmA and SBS17-30mer DNA (2 μM). Reactions were incubated at room temperature for 5 minutes and then samples were spotted onto carbon-coated grids for 1 minute and negatively stained with 1% uranyl acetate and visualized by electron microscopy.

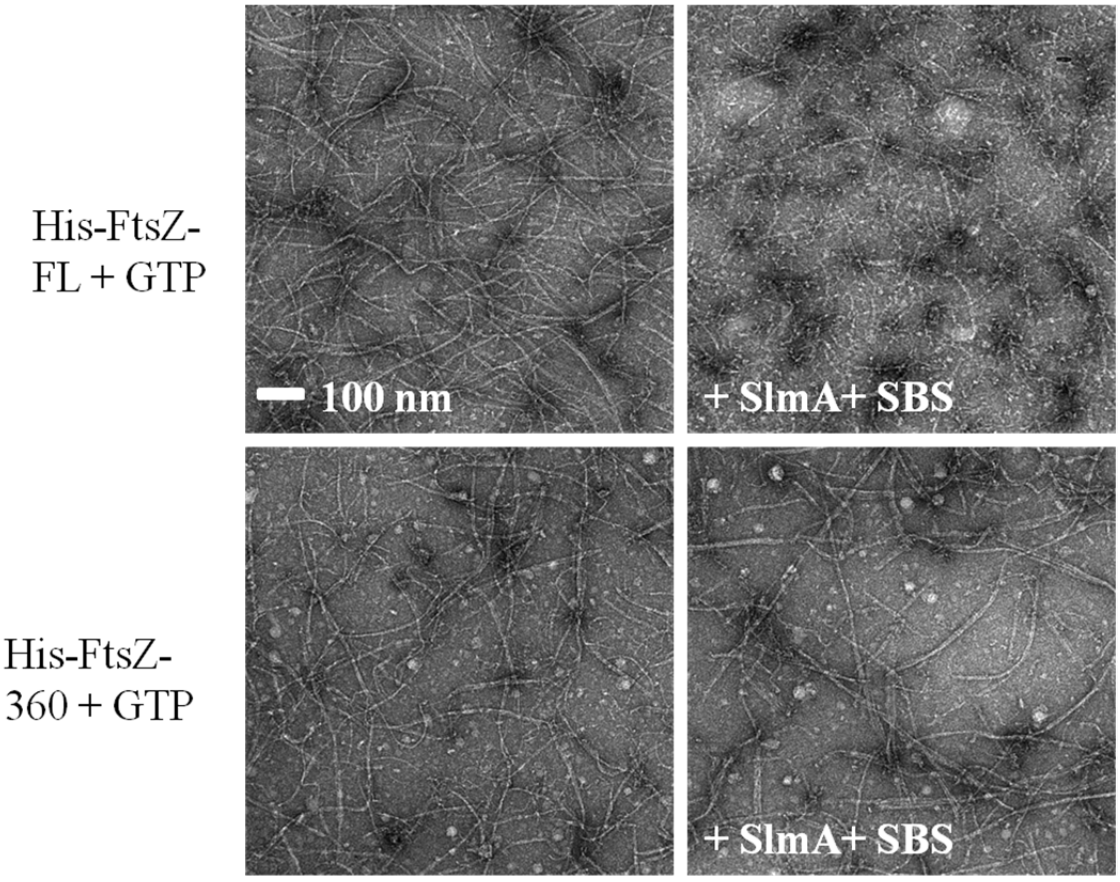
His-FtsZ-
FL + GTP
100 nm
+ SlmA+ SBS
His-FtsZ-
360 + GTP
+ SlmA+ SBS

biosensor (Fig. 27A) suggesting that either the linker region or the conserved C-terminal tail is necessary for SlmA binding.

We therefore purified 6×His-FtsZ360 and tested whether it would bind to SlmA. Similar to 6×His-FtsZ320, 6×His-FtsZ360 did not bind to immobilized SBS17-30mer-SlmA, arguing that the conserved C-terminal tail, and not the linker, is required for SlmA binding. To make sure this lack of binding signal was not due to the 6×His tag, we further purified FtsZ-360 and monitored its binding to SBS17-30mer-SlmA. Consistent with the results with 6×His-FtsZ360, FtsZ-360 showed no binding signal with SBS17-30mer-SlmA, while 6×His-FtsZ and FtsZ both bound to SBS17-30mer-SlmA (Figs. 27 and 29). Thus, the conserved C-terminal tail of FtsZ is likely responsible for FtsZ binding to SlmA.

To further confirm the conserved tail of FtsZ is required for interaction with SlmA, we tested whether SBS17-30mer bound SlmA would co-sediment with stable 6×His-FtsZ360 polymers. As shown in Fig. 27B, most SlmA stayed in the supernatant fraction and did not co-sediment with 6×His-FtsZ360 and SBS17-30mer DNA, while SlmA cosedimented with 6×His-FtsZ-FL stable polymers, in agreement with the above observations. We also visualized the stable polymers under electron microscopy. As shown before, addition of SlmA with SBS17-30mer DNA caused dramatic bundling of the stable polymers formed by 6×His-FtsZ-FL, however, the stable 6×His-FtsZ360 polymers were unaffected by the addition of SBS with SBS17-30mer DNA (Fig. 27C). Furthermore, we did not observe any decoration on the polymers, which was prominent in the samples of 6×His-FtsZ-FL. Therefore, the conserved C-terminal tail of FtsZ is necessary for SlmA co-sedimentation and the bundling induced by SBS DNA bound SlmA.

We further checked whether the conserved C-terminal tail of FtsZ is required for SBS-SlmA induced disassembly of FtsZ proto-filaments. As shown in Fig. 28, both 6×His-FtsZ360 and 6×His-FtsZ-

FL assembled into single and double stranded filaments in the presence or absence of SlmA. However, addition of SlmA with SBS17-30mer DNA dramatically reduced the number and length of the 6×His-FtsZ-FL polymers but had no effect on the 6×His-FtsZ-360 polymers, suggesting that SBS17-30mer bound SlmA could not promote the disassembly of FtsZ polymers in the absence of the conserved C-terminal tail of FtsZ. Taken together, SlmA depends on the conserved C-terminal tail of FtsZ for interaction and disassembly of FtsZ polymers.

Single substitutions at the conserved C-terminal tail of FtsZ abolish FtsZ-SlmA interaction

The C-terminal tail of FtsZ (DYLDIPAFLRKQAD) is widely conserved across bacterial species and many proteins involved in cell division have been reported to bind to the tail of FtsZ. In *E. coli*, the tail of FtsZ has been suggested or shown to be the binding site for five different proteins, including ZipA, FtsA, MinC, ZapD and ClpX (Camberg et al., 2009; Durand-Heredia et al., 2012; Haney et al., 2001; Mosyak et al., 2000; Shen and Lutkenhaus, 2009; Szwedziak et al., 2012). For three of them that have been characterized *in vivo* and *in vitro* (ZipA, FtsA and MinC), FtsZ residues I374 and L378 are critical for the interaction (Haney et al., 2001; Shen and Lutkenhaus, 2009). Various substitutions at these two residues have also been reported to render FtsZ resistant to the action of $MinC^{C}$-MinD and to abolish FtsZ interaction with ZipA and FtsA (Haney et al., 2001; Shen and Lutkenhaus, 2009). As the tail of FtsZ is required for FtsZ-SlmA interaction, it is highly possible that mutations in these two residues would also disrupt the FtsZ-SlmA interaction. Therefore, we mutated these two residues to I374K and L378E respectively and tested the corresponding mutants interaction with SlmA in the *BLItz* system. As shown in Fig. 29, neither of these two FtsZ mutants generated a binding signal with SlmA bound with SBS17-30mer immobilized on the biosensor. Thus, I374 and L378 appear to be important for FtsZ-SlmA interaction.

Fig. 29. Single amino acid substitutions in the FtsZ tail abolish FtsZ-SlmA binding. Experiments were performed as in Fig. 23B. Streptavidin biosensor tips were loaded with 50 nM biotinylated SBS17-30mer for 5 minutes followed by a 10 second wash. SBS17-30mer-SlmA complexes were generated by moving the SBS17-30mer coated tips to tubes containing 4 μM SlmA. Two minutes after incubation, the tips with the biotinylated SBS17-30mer and SlmA bound were washed for 10 seconds and then moved to tubes containing FtsZ or its mutants to measure the association for 1 minute. Dissociation was initiated by moving the tips into buffer lacking FtsZ and following dissociation for 2 minutes (dissociation step is not shown).

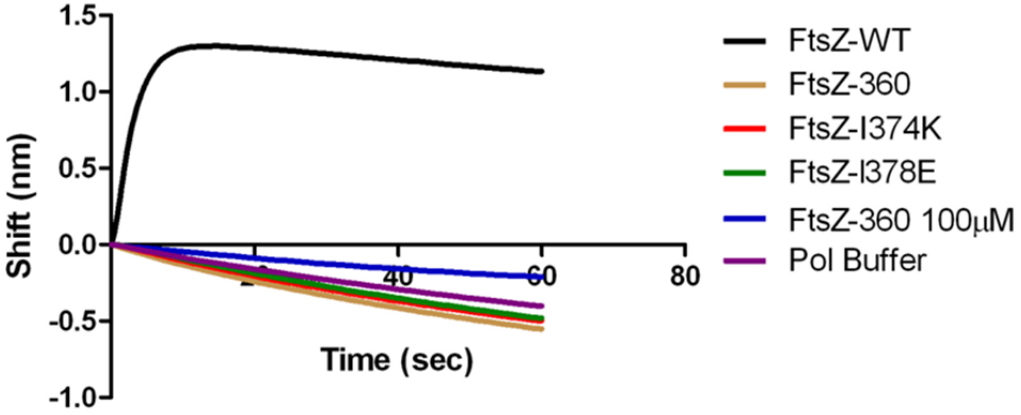
1.5
1.0
0.5
0.0
-0.5
-1.0
Shift (nm)
40
60
80
Time (sec)
FtsZ-WT
FtsZ-360
FtsZ-I374K
FtsZ-I378E
FtsZ-360 100μM
Pol Buffer

SBS activated SlmA disassembles FtsZ polymers, but the conserved C-terminal tail of FtsZ is not involved in polymerization, indicating that SlmA has to bind to a secondary site in the globular domain of FtsZ to prevent FtsZ assembly. Consistent with this idea, previous SAXS analysis of SlmA-FtsZ316-GFP complex showed that a SlmA dimer was sandwiched between two FtsZ316-GFP molecules (Tonthat et al., 2011). Although SAXS studies are normally performed with high concentrations of protein, which may cause some non-physiological association of proteins, the arrangement of molecules in this complex is very similar to that of the SBS-SlmA-FtsZ complex, in which each dimer of SlmA is sandwiched bewteeen two FtsZ molecules (Tonthat et al., 2013). Thus, formation of the SlmA-FtsZ316-GFP complexes is likely due to the secondary binding between the FtsZ globular domain and SlmA. Thus, we tested whether we could detect interaction between FtsZ360 and SBS17-30mer bound SlmA. Unfortunately, we did not detect any binding signal between FtsZ360 and SBS17-30mer-SlmA in the *BLItz* system even when FtsZ360 was added at 100 μM. One possibility is that the binding affinity between FtsZ360 and SlmA is too low to be picked up by the system, but further investigation is required for clear this paradox.

FtsZ tail peptide is sufficient for SlmA binding and blocks SBS-SlmA binding to FtsZ

Peptides corresponding to the C-terminal tail of FtsZ form stable complexes with ZipA and FtsA, even though they bind with low affinity (Mosyak et al., 2000; Szwedziak et al., 2012). Therefore, we tested whether a synthesized 14 amino acid peptide (Ztail-WT, DYLDIPAFLRKQAD) representing the conserved C-terminal tail of *E. coli* FtsZ would bind to SlmA bound with SBS17-30mer. As shown in Fig. 30A, this peptide bound to SBS17-30mer-SlmA in a concentration dependent manner. At 40 μM, there was almost no binding signal, however, as the concentration increased, the binding signal increased gradually and reached plateau at about 320 μM. Analysis of the binding curves shown that the Kd for SBS17-30mer-SlmA was about 81±10 μM, dramatically lower than that of FtsZ (Fig 30B and Table 6).

Fig. 30. The FtsZ tail peptide is sufficient for SBS-SlmA binding. A) Experiments were performed as in Fig. 23B. Streptavidin biosensor tips were loaded with 50 nM biotinylated SBS17-30mer for 5 minutes followed by a 10 second wash. SBS17-30mer-SlmA complexes were generated by moving the SBS17-30mer coated tips to tubes containing 4 μM SlmA. Two minutes after incubation, the tips with biotinylated SBS17-30mer and SlmA bound were washed for 10 seconds and then moved to tubes containing FtsZ tail peptide (Ztail-WT) or its mutants to measure the association for 2 minutes. Dissociation was initiated by moving the tips into buffer lacking FtsZ and following dissociation for 2 minutes (dissociation step is not shown). B) A concentration dependent binding curve of FtsZ peptide Ztail-WT to SBS17-30mer bound SlmA. The end point binding signals were plotted against the peptide concentration. C) FtsZ tail peptide reduces SBS17-30mer bound SlmA binding to 6×His-FtsZ. Ni-NTA biosensor tips were loaded with 1 μM 6×His-FtsZ for 5 minutes followed by a 10 second wash. Association was initiated by moving the 6×His-FtsZ coated tips to tubes containing SlmA (untagged version, 1 μM) with or without the FtsZ tail peptide (Ztail-WT) or its mutants (40 to 160 μM) preincubated for 10 minutes. Two minutes after the incubation, the tips were moved to tubes containing FtsZ polymerization buffer to monitor the dissociation for 2 minutes. Data were generated automatically by the BLItz^{TM} software and then analyzed by GraphPad Prism 5.0.

A.

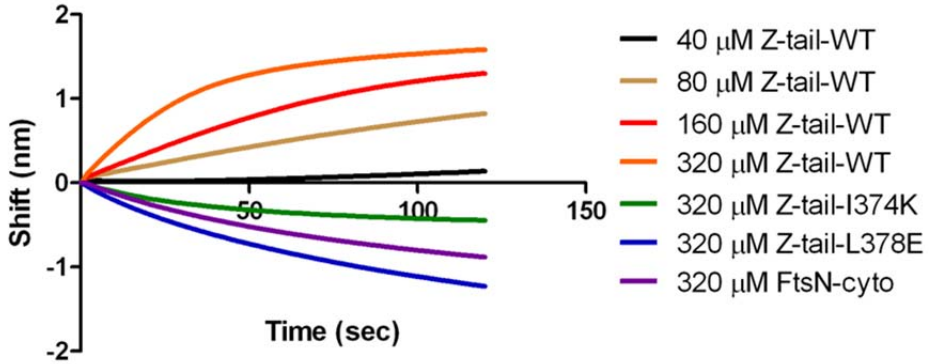
Shift (nm)
Time (sec)
40 μM Z-tail-WT
80 μM Z-tail-WT
160 μM Z-tail-WT
320 μM Z-tail-WT
320 μM Z-tail-I374K
320 μM Z-tail-L378E
320 μM FtsN-cyto

B.

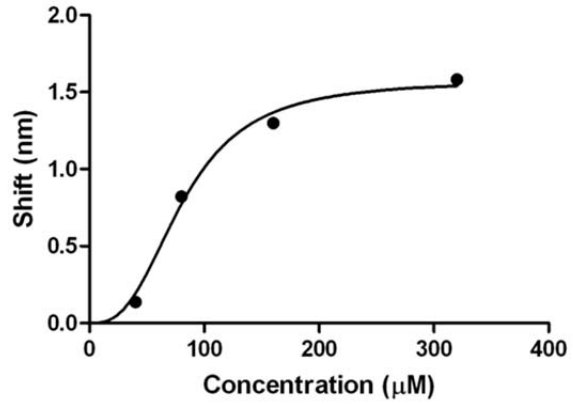
Shift (nm)
Concentration (μM)

C.

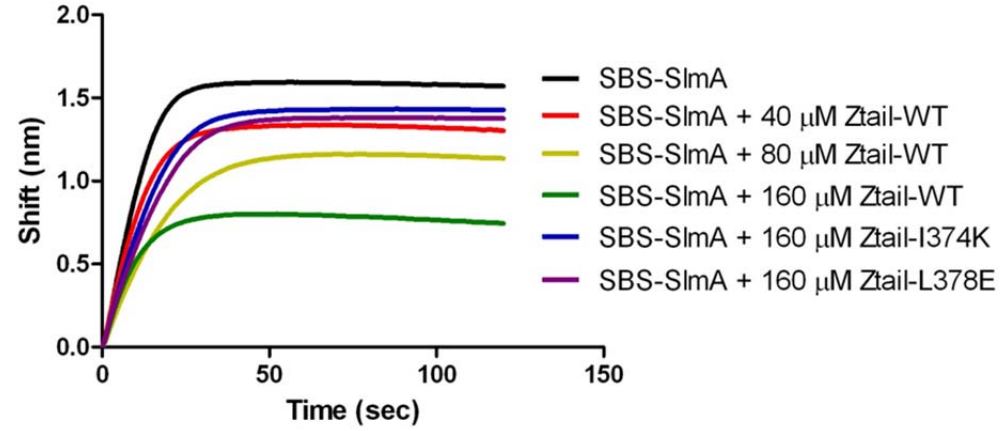
Shift (nm)
Time (sec)
SBS-SlmA
SBS-SlmA + 40 μM Ztail-WT
SBS-SlmA + 80 μM Ztail-WT
SBS-SlmA + 160 μM Ztail-WT
SBS-SlmA + 160 μM Ztail-I374K
SBS-SlmA + 160 μM Ztail-L378E

Fig. 31. $ZipA_{185-328}$ competes with SBS bound SlmA for the conserved C-terminal tail of FtsZ. Experiments were performed as in Fig. 23B. Streptavidin biosensor tips were loaded with 50 nM biotinylated SBS17-30mer for 5 minutes followed by a 10 second wash. SBS17-30mer-SlmA complexes were generated by moving the SBS17-30mer coated tips to tubes containing 4 μM SlmA. Two minutes after incubation, the tips with biotinylated SBS17-30mer and SlmA bound were washed for 10 seconds and then moved to tubes containing 4 μM FtsZ preincubated with $ZipA_{185-328}$ to measure the association for 1 minute. Dissociation was initiated by moving the tips into buffer lacking protein and dissociation followed for 2 minutes (dissociation step is not shown). Data were generated automatically by the BLItz™ software and then analyzed by GraphPad Prism 5.0.

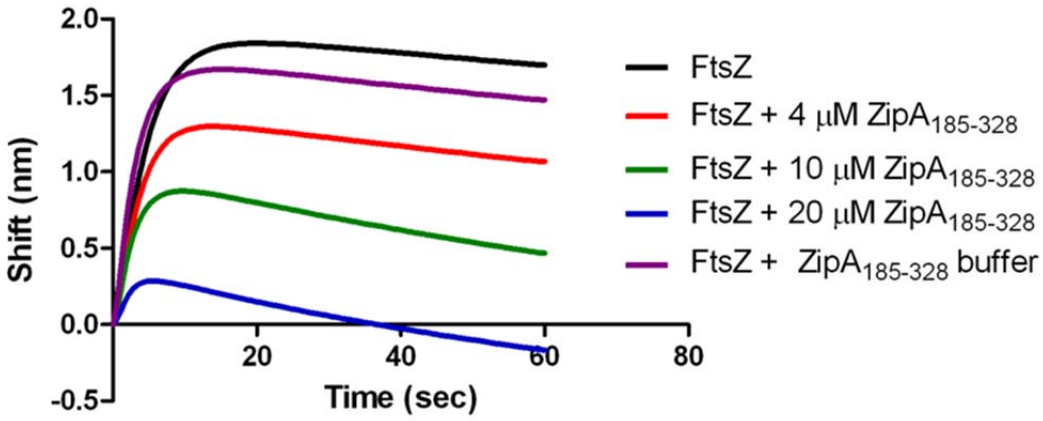
2.0
1.5
1.0
0.5
0.0
-0.5
Shift (nm)
20
40
60
80
Time (sec)
FtsZ
FtsZ + 4 μM ZipA185-328
FtsZ + 10 μM ZipA185-328
FtsZ + 20 μM ZipA185-328
FtsZ + ZipA185-328 buffer

However, this is not unusual because FtsZ tail peptides also display low binding affinity for ZipA (20 μM) and FtsA (50 μM) (Mosyak et al., 2000; Szwedziak et al., 2012). It is not clear why the full length FtsZ binds to these tail binding proteins with a Kd within the nM range while FtsZ tail peptides only bind weakly. Consistent with the results above, mutants of the Z tail peptides, Ztail-I374K and Ztail-L378E, did not bind to SBS17-30mer-SlmA even at the highest concentration tested 320 μM (Fig 30A). A peptide representing the cytoplasmic domain of FtsN also failed to bind SlmA, suggesting that the SlmA binding of the Ztail-WT peptide was specific. Thus, the C-terminal 14 amino acids of FtsZ are sufficient for SlmA binding.

As the Ztail-WT peptide binds to SlmA, preincubation of SBS bound SlmA with the Ztail-WT peptide should block or reduce the binding signal of SlmA with FtsZ because the FtsZ binding site has been occupied by the Ttail-WT peptide. To this end, we immobilized 6×His-FtsZ-FL on the surface of Ni-NTA biosensors and monitored the binding kinetics of SBS17-30mer-SlmA (His tag free) in the presence or absence of Ztail-WT peptide. As shown in Fig. 30C, SBS17-30mer-SlmA bound to immobilized 6×His-FtsZ-FL strongly and reached a plateau within 30 sec. Pre-incubation of SBS17-30mer-SlmA with the Ztail-WT peptide decreased the binding signal in the Ztail-WT concentration dependent manner. At 40 μM Ztail-WT peptide, the binding plateau decreased about 20%, while at 160 μM, the binding signal was reduced about 60%. More importantly, the mutant Ztail-I374K and Ztail-L378E peptides only slightly affected the binding signal of SBS17-30mer SlmA with 6×His-FtsZ-FL. These results confirm that the Z tail peptide specifically competes with full length FtsZ for binding to SBS17-30mer-SlmA.

SlmA competes with ZipA for the conserved C-terminal tail of FtsZ

Previous studies showed that although both ZipA and FtsA bind to the conserved C-terminal tail of FtsZ, there are subtle differences in the sequence specificity (Haney et al., 2001; Mosyak et al., 2000;

Szwedziak et al., 2012). ZipA interacts with the conserved C-terminal tail of FtsZ largely through hydrophobic interactions, while FtsA mainly forms salt bridges (Mosyak et al., 2000; Szwedziak et al., 2012). Furthermore, the tail adopts different conformations in the ZipA-Ztail and the FtsA-Ztail complexes (Mosyak et al., 2000; Szwedziak et al., 2012), suggesting that the tail of FtsZ cannot bind to ZipA and FtsA simultaneously. More importantly, MinC, the effector of the Min system, competes *in vivo* with ZipA and FtsA for the tail of FtsZ (Shen and Lutkenhaus, 2009). As SlmA also binds to the conserved C-terminal tail of FtsZ, we tested whether it competed for the tail or binds to the tail regardless of the presence of the other tail binding proteins. We thus purified $ZipA_{185-328}$, which binds to FtsZ with high affinity, and incubated it with FtsZ to see whether this pre-incubation would block FtsZ binding to SBS17-30mer bound SlmA. As shown in Fig. 31, $ZipA_{185-328}$ blocked FtsZ binding to SlmA bound with SBS17-30mer in a concentration dependent manner. At a 1:1 ratio with FtsZ (4 μM), $ZipA_{185-328}$ reduced the the binding signal of FtsZ with SBS17-30mer-SlmA about 30%, at 5:1 ratio, FtsZ shown almost no binding with SBS17-30mer-SlmA, suggesting that the FtsZ available to bind SlmA was dramatically reduced in the presence of excess $ZipA_{185-328}$. Thus, these data demonstrate that SlmA competes with ZipA for the conserved tail of of FtsZ.

SlmA and MinC bind to the conserved C-terminal tail of FtsZ differently

Shen and Lutkenhaus have isolated some FtsZ tail mutants that support normal division but become insensitive to the division inhibitory activity of $MinC^C$-MinD (Shen and Lutkenhaus, 2009). These FtsZ mutants, including D373E, I374V, A376P (unpublished data), L378V and K380M, likely eliminate or reduce the interaction between FtsZ and $MinC^C$ but retain interaction with ZipA and FtsA (Shen and Lutkenhaus, 2009). We would like to test whether these mutants were also insensitive to the division inhibitory activity of SlmA in the presence of extra copies of SBS in a plasmid, but we first had to make sure that these mutants complement the DU11/pKD3C strain [*W3110 ftsZ^0 recA::Tn10*

Fig. 32. FtsZ tail mutants resistant to MinC display differential sensitivity to de-localized SlmA. Experiments were done as in Fig. 13. Plasmids pSD133 (P*tac::slmA*) and p2SBSK (pUC18 with 2SBS sites) were introduced into the *ftsZ*⁻ strain DU11 (*ftsZ*^{0} *slmA<frt> recA::Tn10*) complemented with pBANG112 or its derivatives containing different *ftsZ* alleles. One colony of each resultant strain was resuspended in 1 ml LB medium, serially diluted by 10 and 3 µl from each dilution was then spotted on LB plates containing various concentration of IPTG and supplemented with Ampicillin, Spectinomycin and Kanamycin. The plates were incubated at 30°C for 30 hours before being photographed.

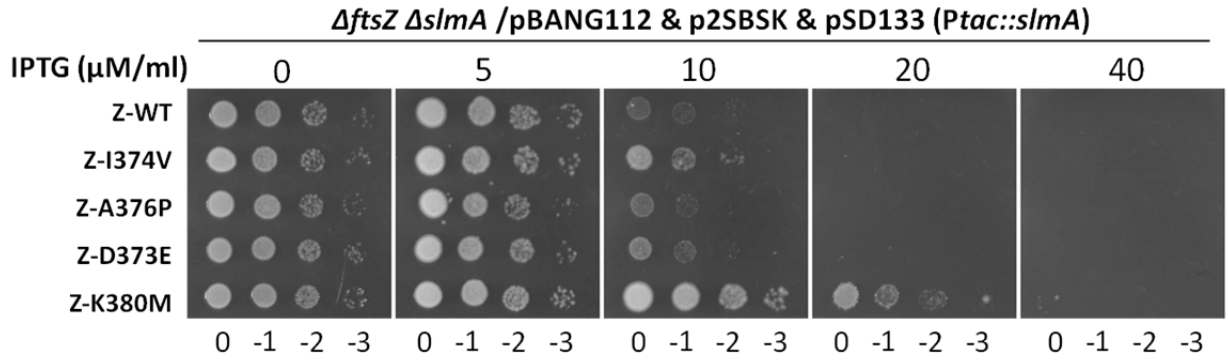
ΔftsZ ΔslmA /pBANG112 & p2SBSK & pSD133 (Ptac::slmA)
IPTG (µM/ml)
0
5
10
20
40
Z-WT
Z-I374V
Z-A376P
Z-D373E
Z-K380M
0 -1 -2 -3 0 -1 -2 -3 0 -1 -2 -3 0 -1 -2 -3 0 -1 -2 -3

slmA<frt>/pKD3C ftsZ^{+}*]*. All FtsZ mutants expressed from pBANG112 complemented DU11/pKD3C at 42°C, but the cells of DU11/pBANG112-L378V were a mixture of filaments and elongated cells. When restreaked on plates DU11/pBANG112-L378V cells did not grow at 30°C. Thus, the FtsZ-L378V was not tested for SlmA resistance. The I374V mutant which confers complete resistance to MinC^{C}-MinD, showed almost no effect on the growth of cells when SlmA was induced, indicating that although SlmA and MinC bind to the conserved C-teriminal tail of FtsZ, they interact with the tail in a different manner. Among the other three mutants, K380M showed some resistance to SlmA in the presence of extra SBS in a plasmid, providing *in vivo* support of our finding that the conserved C-terminal tail of FtsZ is required for SlmA binding.

Regulation of Z ring formation through competition for the conserved C-terminal tail of FtsZ

Both SlmA and MinC bind to the conserved C-terminal tail of FtsZ, but genetic screens for SlmA or MinC resistant mutants using the same approach generated completely different mutants. For MinC, some of the resistant mutations were located in the conserved C-terminal tail and some in the globular domain of FtsZ. When a second screen was carried out with MinC C terminal domain, only mutations in the tail region were obtained (Shen and Lutkenhaus, 2009). For SlmA, the resistant mutations K190V and D86N are located far away from the tail, raising a question why FtsZ tail mutants did not show up in the screen for SlmA resistant mutants. One possibility is that mutants resistant to SlmA were not generated by the error prone PCR mutagnesis because this approach normally introduces single nucleotide change to a codon, limiting the possible substitutions. Also, K190V dominated the screen even though MinC resistant mutants were isolated from the same library indicating there was diversity. Another possibility is that SlmA binds to the tail of FtsZ similarly as ZipA or FtsA. Mutations disrupting

the FtsZ-SlmA interaction would also destroy the FtsZ-ZipA or FtsZ-FtsA interaction such that the mutants would not show up in the screen because they are not viable.

As I374 is critical for FtsZ-SlmA interaction, we mutated it to Met, Leu, Phe, Tyr and Trp by site-directed mutagenesis to see whether these mutants would support growth and be completely resistant to the division inhibition by SlmA. All of these mutants expressed from pBANG112, except I374F, failed to complement the DU11(ftsZ^0, Δ*slmA*)/pKD3C strain at 42°C, suggesting that this position has limited tolerance for viable substitutions. This appears to be plausible because I374 is highly conserved and important for ZipA, FtsA and MinC binding and possibly ZapD and ClpX interaction. Further characterization of the I374F mutant found that it was cold sensitive, forming extremely long filaments at 30 °C (data not shown). This resulst suggested that although I374F was able to support division above 37°C, it must have some defect in binding the other tail binding proteins. In agreement with this, I374F containing cells were a mixture of filaments and normal cells even at 42°C. This phenotype prompted up to test whether this mutant could support division of the wild type strain S18/pKD3C because if I374F retains normal interaction with SlmA but has lower binding affinity for ZipA or FtsA, addition of SlmA may exacerbate the division defect due to the competition for the FtsZ tail. As shown in Table 4, I374F in pBANG112 failed to complement S18/pKD3C at 42°C, suggesting I374F likely still interacts with SlmA well. By analogy, if I374F retains interaction with MinC, deletion of MinC from the S18 strain should allow the growth of this mutant because more FtsZ would be available to bind ZipA and FtsA. We thus tested whether this mutant could complement the *min* system knockout strain S7/pKD3C. As expected, S7 cells carrying I374F grew as well as S7 cells carrying wild type FtsZ at temperatures from 30 to 42°C, suggesting I374F interacts with MinC. S7 cells carrying I374F showed no resistance to expression of MinC^C-MinD confirming I374F still interacts with MinC^C (data not shown). The complementation results of I374F in different strains implies that competition for the conserved C-terminal tail of FtsZ between the FtsZ membrane anchors and the FtsZ negative regulators is critical for Z ring formation and disruption of

Table 4. Complementation of an *ftsZ* null in different strains by FtsZ tail mutants. Plasmid pBANG112 or its variants carrying different *ftsZ* alleles was transformed into strains S18/pKD3C, S7/pKD3C or DU11/pKD3C by selection with ampicillin at 42°C. If there were transformants on the plates, single colonies were restreaked on plates with ampicillin and grew at 42°C, 37°C and 30°C to determine the cold sensitivity of the *ftsZ* alleles.

Strain	**Plasmid pBANG112 variants**								
	FtsZ-WT			**FtsZ-I374V**			**FtsZ-I374F**		
	42°C	**37°C**	**30°C**	**42°C**	**37°C**	**30°C**	**42°C**	**37°C**	**30°C**
S18 (WT)	+	+	+	+	+	+	-	**ND**	**ND**
S7 (*min*$^-$)	+	+	+	+	+	+	+	+	+
DU11 (*slmA*$^-$)	+	+	+	+	+	+	+	+	-

this balance affects Z ring formation and leads to cell death. In other words the weakened interaction between I374F and FtsA/ZipA can be compensated for by deleting one of the negative regulators, which retains the ability to interact with I374F, reducing the competition for FtsZ and making more available to interact with ZipA/FtsA to make a Z ring.

Discussion

In chapter III, we showed that the nucleoid occlusion protein SlmA actively disassembles FtsZ polymers in the presence of SBS DNA molecules longer than 20 bp, suggesting a model in which SlmA prevents Z ring formation by antagonizing FtsZ polymerization. However, as the SlmA binding site on FtsZ had not been identified, our understanding of SlmA was not complete and it was not clear whether the antagonization of FtsZ polymerization observed *in vitro* has any physiological significance *in vivo*. Here, we show that the conserved C-terminal tail of FtsZ is the primary binding site for SlmA *in vitro* and an FtsZ tail mutant, K380M, provides resistance to SlmA *in vivo*. We also show that the ability of SlmA to disassemble FtsZ polymers depends on upon the tail of FtsZ. As the tail of FtsZ is not required for polymerization, our results thus suggest that SlmA acts on FtsZ in two steps: first, SlmA binds to the conserved C-terminal tail of FtsZ, activating the FtsZ polymerization inhibitory activity of SlmA; second, disassembles FtsZ filaments. In addition, we show that SlmA competes with ZipA for the conserved C-terminal tail of FtsZ and isolated FtsZ mutants that only complement FtsZ null strain in the absence of the Min system or SlmA, suggesting that competition for the conserved C-terminal tail of FtsZ is critical for regulating Z ring formation.

SlmA binds to the conserved C-terminal tail of FtsZ

The conserved C-terminal tail of FtsZ was reported to be unnecessary for SlmA binding (Tonthat et al., 2011), but we show here that it is the primary binding site for SlmA *in vivo* and *in vitro*. In the *BLItz* system, C-terminal FtsZ truncations (FtsZ320 and FtsZ360) with or without the 6×His tag showed

no binding to SlmA bound to an SBS17-30mer immobilized on biosensors. Single amino acid substitutions of highly conserved residues in the tail of FtsZ (FtsZ-I374K and L378E) also abolished the FtsZ-SlmA interaction. Consistent with these results, a 14 amino acid peptide (Ztail-WT) but not mutant forms (Ztail-I374K and Ztail-L378E) bound to SlmA and blocked its binding to FtsZ, suggesting that the conserved C-terminal tail of FtsZ is absolutely required for SlmA binding. More importantly, SBS17-30mer bound SlmA has no effect on dynamic or stable polymers formed by 6×His-FtsZ360, revealing an important role for FtsZ tail binding in activating the FtsZ inhibitory activity of SlmA. In agreement with this, an FtsZ tail mutant, K380M, provides resistance to SlmA in the presence of extra SBS in a multi-copy plasmid. Taken together, our results argue that the conserved C-terminal tail of FtsZ is the primary binding site for SlmA and necessary for SlmA to exert its function *in vivo*.

Tonthat et. al observed that FtsZ360 bound to SBS activated SlmA with nearly wild type binding signal (Tonthat et al., 2011), but we observed no binding signal between FtsZ360 with SBS bound SlmA. It is not clear why they did not see a defect in FtsZ360 binding to SlmA, however, by using multiple approaches we are sure that SlmA binds the tail of FtsZ. One possibility is that the FtsZ360 they used for their assays was actually wild type FtsZ. FtsZ truncations without the conserved C-terminal tail are highly toxic and difficult to introduce into *E. coli* strains using vectors with leaky expression. In this study we used expression plasmids with the arabinose promoter, which are less leaky than vectors using the lac or T7 promoters (data not shown).

In Chapter III we isolated FtsZ mutants (FtsZ-K190V and FtsZ-D86N) resistant to SlmA in the presence of extra copies of SBS in a plasmid, but neither of them are FtsZ tail mutants. Using the same approach, Shen and Lutkenhaus isolated FtsZ tail mutants resistant to $MinC^{C}$-MinD (Shen and Lutkenhaus, 2009), raising a question why the approach did not lead to the isolation of FtsZ tail mutants resistant to SlmA. One possibility is that FtsZ tail mutants abolishing FtsZ-SlmA interaction are not

Fig. 33. A model for SlmA-FtsZ interaction. A) A bipartite binding model for SlmA-FtsZ interaction. The binding site for the FtsZ tail (colored brown) is fully exposed upon SlmA binding to the SBS DNA. Once the binding site is occupied by the FtsZ tail, SlmA binds to a secondary binding site in the globular domain of FtsZ so that it can break the FtsZ polymer. Mutations in D86 (red) and K190 (blue) provide resistance to the action of SlmA but do not affect FtsZ-SlmA binding. Note that each subunit of the SlmA dimer-of-dimer can bind to an FtsZ molecule, for simplicity only one FtsZ is shown. B) SlmA and MinC act in a similar manner to antagonize Z ring formation in their vicinity. First, SlmA and MinC bind to the conserved C-terminal tail of FtsZ. Binding to the tail of FtsZ on the one hand reduces the tail binding to the Z ring promoting factors, ZipA and FtsA, on the other hand it positions the N terminal domain of MinC or the SlmA-DNA complex in proximity to the FtsZ filament; the N terminal domain of MinC or SlmA (site has not been identified) breaks FtsZ polymers. Note that the mechanisms for MinC and SlmA to break the filaments may be different.

A.

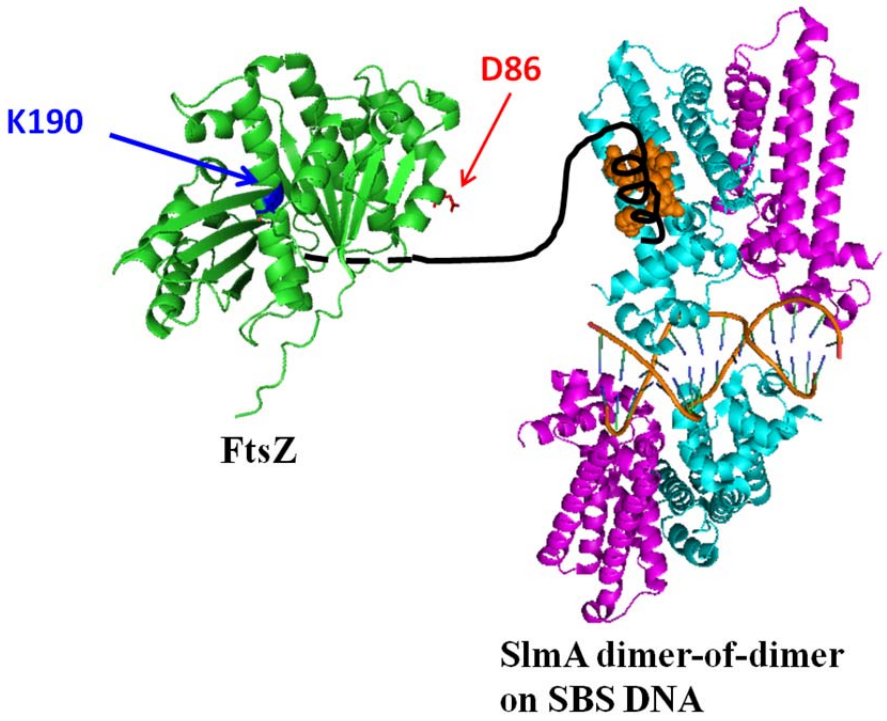
K190
D86
FtsZ
SlmA dimer-of-dimer
on SBS DNA

B.

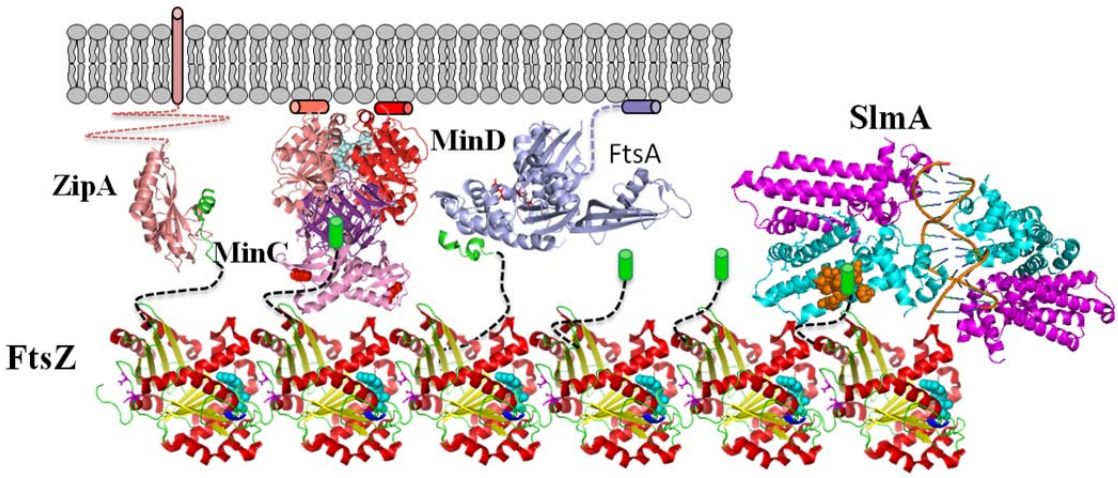
ZipA
MinC
MinD
FtsA
SlmA
FtsZ

viable while FtsZ tail mutants reducing or abolishing FtsZ-MinC^C interaction still support cell growth. Besides SlmA and MinC, the conserved C-terminal tail of FtsZ has been shown or suggested to be the binding sites for ZipA, FtsA, ZapD and ClpX. Accumulated evidence suggest that the FtsZ tail interacts with each tail binding protein differently and it can only engage with one tail binding protein at a time. For example, the tail interacts with ZipA tail through hydrophobic interactions while it forms salt bridges with FtsA (Mosyak et al., 2000; Szwedziak et al., 2012). Our results suggest that the tail also interacts with SlmA and MinC^C differently, since most MinC^C-MinD resistant FtsZ mutants (D373E, I374V, A375P, and L378V), display similar sensitivity to SlmA as wild type FtsZ. However, K380M did confer considerable resistance to SlmA providing evidence that the interaction between SlmA and the Z tail is important *in vivo*. Therefore, any perturbation to the sequence of the Z tail likely affects the interaction of the tail with many binding partners such that it is difficult to get an FtsZ tail mutant that only abolishes the FtsZ-SlmA interaction. It is likely that mutations in the tail of FtsZ disrupting FtsZ-SlmA interaction also abolish FtsZ interactions with ZipA or FtsA while mutations disrupting FtsZ-MinC^C interactions only slightly affect FtsZ interaction with ZipA and FtsA.

FtsZ-SlmA interaction

In the presence of SBS17-30mer, SlmA disassembles wild type FtsZ polymers but has no impact on polymers formed by FtsZ360. The primary binding site, the conserved C-terminal tail of FtsZ, is not necessary for FtsZ polymerization, so how does SlmA binding to the tail of FtsZ lead to FtsZ polymer disassembly? Our result showed that SlmA requires the presence of the conserved C-terminal tail of FtsZ to disassemble FtsZ polymers. One possibility is that SlmA binding to the tail transmits a signal to the globular domain of FtsZ, leading to GTP hydrolysis and filaments breakdown. However, in between the conserved C terminal tail and the globular domain of FtsZ is an intrinsic disordered linker more than 50

amino acids long and it is hard to imagine binding to the tail could initiate a signal that could be transmitted to the globular domain of FtsZ and lead to FtsZ disassembly. Another possibility is that there is a secondary SlmA binding site in the globular domain of FtsZ, which when bound with SlmA results in breakdown of FtsZ filaments. The isolation of FtsZ-K190V and FtsZ-D86N, which are located in the globular domain of FtsZ and show resistance to SlmA in the presence of extra copies of SBS in a plasmid, supports the second hypothesis. SAXS analysis of FtsZ316-GFP with SlmA also suggested that there is interaction between the globular domain of FtsZ with SlmA because FtsZ316-GFP and SlmA form a sandwich like complex with two FtsZ316-GFP molecules centering on a SlmA dimer (Tonthat et al., 2011). We did not detect an interaction between FtsZ360 with SlmA because it may be quite weak. Another possibility is that the secondary binding site on SlmA is not available unless the tail occupies the first binding site. However, adding the Z tail peptide and FtsZ360 together did not enhance binding (data not shown).

The FtsZ interaction interface on SlmA has been revealed by a recent elegant genetic study, and includes residues F65, R73, L94, G97, R101 and N102 (Cho and Bernhardt, 2013). All these residues are located in a cluster above the DNA binding domain in the SlmA structure. It is possible that these residues constitute the binding site for the conserved C-terminal tail of FtsZ as well as the secondary binding site for the globular domain of FtsZ (Fig 33A). Further investigations are required to pinpoint which residues are required for binding to the conserved C terminal tail and which residues are important for binding to the globular domain of FtsZ.

Formation of the Z ring requires FtsZ polymerizing into filaments of certain length that are tethered to the membrane by membrane anchors. Previous studies have shown that MinC prevents Z ring formation by competition with FtsA and ZipA for the conserved C-terminal tail of FtsZ and preventing FtsZ polymerization (Shen and Lutkenhaus, 2009, 2010). Here, we showed that SlmA also competes for

the conserved C terminal tail of FtsZ and antagonizes FtsZ polymerization (Fig 33B). This remarkable similarity between MinC and SlmA suggests that competition for the FtsZ tail and prevention of FtsZ polymerization may be a common mechanism for FtsZ spatial regulators to ensure Z ring formation does not occur at inappropriate places.

Competition for the conserved C-terminal tail of FtsZ is important for Z ring regulation

In an attempt to isolate an FtsZ tail mutant that still supports normal cell division but provides resistance to SlmA, we found one mutant, I374F, which has no resistance to SlmA, but does not support cell division unless the Min system or SlmA has been deleted. Further characterization showed that it is as sensitive as wild type FtsZ to $MinC^{C}$-MinD, suggesting that its inability to grow in the presence of the Min system and SlmA is due to a defect in interacting with the other tail binding proteins. It is possible that this mutant retains normal interaction with SlmA and MinC but interacts less well with ZipA and FtsA, both of which are essential for Z ring formation and thus cell survival. MinC and SlmA may outcompete ZipA or FtsA for this mutated FtsZ tail such that sufficient FtsZ-I374F filaments are not attached to the membrane to form the Z ring in their presence. When the Min system or SlmA is deleted, this deficiency may be compensated for by the loss of one of the negative regulators that detaches FtsZ polymers from the membrane, such that Z ring is formed. Although further studies are required to confirm that this mutant is impaired in interaction with ZipA or FtsA, this unexpected phenotype suggests that competition for the tail of FtsZ plays an underestimated role in regulating Z ring formation. In *E. coli*, the conserved C-terminal tail of FtsZ has been shown to be the binding site for many FtsZ binding proteins, including ZipA, FtsA, ZapD, MinC, SlmA and ClpX. These proteins could be divided into two different classes: proteins that promote Z ring formation (ZipA, FtsA and ZapD) and proteins that promote disassembly of Z rings (MinC/SlmA/ClpX). It is likely that successful Z ring formation requires a balance between the positive and negative interactions with the tail of FtsZ and any perturbation of the

balance interferes with Z ring formation and leads to cell death as shown for FtsZ-I374F. In *B. subtilis*, similarly, the conserved C-terminal tail of FtsZ has also been shown to be the binding site for many proteins, including FtsA, SepF, EzrA and MinC. The first two promote Z ring formation by tethering FtsZ filaments to the membrane while EzrA and MinC are negative regulators of FtsZ. It is possible that competition for the tail of FtsZ is also important for Z ring formation regulation in *B. subtilis*.

Chapter V Conclusion and discussion

The spatiotemporal regulation of Z ring formation in *E. coli* is largely dependent on two redundant negative regulatory systems, the Min system, which prevents Z ring formation near the cell poles and nucleoid occlusion, which prevents Z ring formation over the unsegregated nucleoid (Lutkenhaus, 2007). Accumulated evidence suggests that the effector of the Min system, MinC, in complex with its activator MinD, antagonizes Z ring formation by competing with FtsA and ZipA for the FtsZ tail and inhibiting FtsZ polymerization (Shen and Lutkenhaus, 2009, 2010). Although it has been well accepted that the effector of NO, SlmA, antagonizes Z ring formation through direct interaction with FtsZ, how its interaction with FtsZ prevents FtsZ from assembling into the Z ring is controversial. In this study we isolated FtsZ mutants resistant to the division inhibitory activity of SlmA. Through studies of these SlmA resistant FtsZ mutants we confirmed that SlmA prevents FtsZ polymerization, possibly by interfering with the communication between the N- and C-terminal sub-domains of the globular domain of FtsZ. We further showed that the conserved C-terminal tail of FtsZ is the primary binding site for SlmA and SlmA requires the presence of the conserved C-terminal tail of FtsZ to antagonize FtsZ polymerization. As the FtsZ tail is not required for FtsZ polymerization, our results therefore suggest that SlmA binding to the conserved C-terminal tail of FtsZ activates it to bind to a secondary binding site in the globular domain of FtsZ, resulting in the breakdown of FtsZ polymers. The mechanism of SlmA to antagonize Z ring formation thus appears to be similar to MinC: competing with FtsA and ZipA for the FtsZ tail and inhibiting FtsZ polymerization, the two steps required for the Z ring formation.

SlmA SBS binding and its NO function

The ability of SlmA to coordinate the Z ring formation and chromosome segregation depends on its interaction with DNA and its interaction with FtsZ. Disruption of either one would render SlmA deficient in NO. SlmA-DNA interaction contributes to the NO function of SlmA in two ways. First, the

asymmetric distribution of the SlmA binding sites (SBSs, with a consensus sequence of [**GTgAGtaCTcAC**]) in the *E. coli* chromosome provides a way to regulate the activity of SlmA temporally and spatially by the chromosome. There are about 24 to 52 SBSs in the *E. coli* chromosome, but most of them are distributed in the origin-proximal region of the chromosome such that the activity of SlmA is restricted to the locations occupied by the origin-proximal region (Cho et al., 2011; Tonthat et al., 2011). This asymmetric localization of SlmA allows Z ring formation at the midcell when the origin proximal region of chromosome is segregated away but not in new born cells in which the origin proximal region of the chromosome locates roughly at the midcell.

Another function of SlmA-DNA interaction is to activate the SlmA-FtsZ interaction. When SlmA is de-localized by mutation that disrupts the SlmA-DNA interaction, dramatic overexpression is required for SlmA to block the Z ring formation (Cho et al., 2011). However, in the presence of extra copies of SBS in a plasmid, which will delocalize SlmA from the chromosome to random locations occupied by the plasmid, SlmA blocks Z ring formation throughout the cell without dramatic overexpression (Cho et al., 2011), suggesting that SlmA SBS binding significantly increase its Z ring assembly antagonizing activity. Consistent with this, SlmA has minimal activity toward FtsZ polymerization in the absence of SBS DNA, but it disassembles FtsZ polymers actively in the presence of SBS DNA *in vitro* (Cho et al., 2011). It has been proposed that SBS DNA binding induces a conformational change in the SlmA dimers to fully expose its hidden FtsZ binding site such that it can bind to FtsZ with high affinity (Cho and Bernhardt, 2013). Structural analysis of SlmA with and without SBS DNA supports such a model. However, this model was questioned by a recent study, which showed that SlmA forms oriented dimer-of-dimers on SBS DNA, and which can spread on the DNA, but has no impact on FtsZ polymerization (Tonthat et al., 2013). These unexpected findings led to the assumption that the conformational change induced by SBS binding contributes little to the SlmA-FtsZ interaction. Oligomerization of SlmA upon SBS binding thus appears to be the main contribution of SlmA SBS binding because SlmA oligomers can sequester FtsZ filaments onto the SlmA-DNA complexes. We found that SlmA binds to FtsZ-GDP with a Kd about 20

μM, but the SBS17-30mer bound SlmA binds to FtsZ-GDP with a Kd about 200 nM. This 100 fold increase of affinity must be due to the conformational change induced by SBS binding because SlmA can form only one dimer-of-dimer on SBS17-30mer. Spreading of SlmA dimer-of-dimers on the DNA may further increase the SlmA-FtsZ interaction, but further investigation is required to explore the role of spreading.

Similar to SlmA, Noc coordinates the Z ring formation with chromosome segregation in *B. subtilis* (Wu and Errington, 2004). Previous studies have shown that Noc also binds to specific DNA sequences (NBSs) and spreads onto DNA adjacent to the NBSs (Wu et al., 2009). Even though the target of Noc has not been identified, we speculate that Noc NBS binding must contribute to its NO function similarly to SlmA SBS binding: spatiotemporally regulating its function and increasing its affinity for the target.

A bipartite module for SlmA-FtsZ interaction

Before this study, two different models have been proposed for how SlmA prevents FtsZ assembly into the Z ring. One model suggests that SlmA, once activated by its specific DNA sequences, prevents Z ring formation by antagonizing FtsZ polymerization, while another model suggests that SlmA oligomerized on the DNA sequesters FtsZ filaments onto the SlmA-DNA complexes (Cho et al., 2011; Tonthat et al., 2013). We found that SlmA indeed antagonizes FtsZ polymerization, but this inhibitory activity of SlmA correlates with the length of the bound SBS DNA molecules. SBS DNA molecules of 14 bp, 18 bp, 20 bp and 30 bp are able to stimulate SlmA to bind to FtsZ, but the ability of SlmA to prevent FtsZ polymerization decreases as the length of bound SBS DNA decreases. SlmA bound to SBS17-30mer disassembles FtsZ polymers efficeiently, but SlmA bound to SBS-14mer has less impact on FtsZ polymers. Previous studies showed that SlmA makes 6 additional contacts with the SBS-20mer than with SBS-12mer, displaying a 2-3 fold higher affinity for the longer SBS DNA (Tonthat et al., 2013). This reduced affinity for SlmA and the weaker ability of SlmA to antagonize FtsZ polymerization in Tonthat's

buffer explains the lack of effect on FtsZ polymerization observed by Schumacher's group (Tonthat et al., 2013).

As discussed above, SBS activated SlmA antagonizes FtsZ polymerization, but our results showed that it binds to FtsZ largely through the conserved C-terminal tail of FtsZ, which is not necessary for FtsZ polymerization. More importantly, SlmA requires the presence of the FtsZ tail to disassemble FtsZ polymers. Although it is possible that SlmA dimer-of-dimers sequesters FtsZ polymers, the fact that it bundles FtsZ polymers in the absence of GTP hydrolysis suggest that it is more likely that SlmA binds to a secondary binding site in the globular domain of FtsZ to prevent FtsZ polymerization. Either this secondary binding site is not available in the stable FtsZ polymers or SlmA binds to it but is not able to weaken the FtsZ-FtsZ interaction such that it cannot disassemble the stable FtsZ polymers. Consistent with this two binding site model, previous SAXS analysis of SlmA-FtsZ complex and SlmA-FtsZ316-GFP complex suggest that SlmA binds to the C-terminal sub-domain of the globular domain of FtsZ (Tonthat et al., 2011). In support of this model, we have isolated FtsZ mutations (FtsZ-K190V and FtsZ-D86N) in the globular domain that confer resistance to the action of SlmA *in vivo* and *in vitro*. The FtsZ-K190V mutant is especially interesting in that it locates in the H7 helix of FtsZ and binds to SBS bound SlmA with a different kinetics compared to the wild type FtsZ. The H7 helix mediates the conformational change between the two sub-domains of the globular domain of FtsZ during assembly (Elsen et al., 2012). The side chain of K190 in the FtsZ-GDP structure rotates about 90° compared to that in the FtsZ-GTP structure, suggesting that SBS bound SlmA may take advantage of this rotation to disassemble FtsZ polymers. In support of this idea, all substitutions of K190, except for K190R, confer resistance to SlmA.

The FtsZ interaction interface has been revealed by genetic study from the Bernhardt group, it is a region partially hidden by the DNA binding domain of SlmA (Cho and Bernhardt, 2013). We propose that once activated by SBS DNA, SlmA binds to the conserved C-terminal tail of FtsZ through this region

(Fig 33A). Once this region is occupied by the tail of FtsZ, SlmA binds to a secondary site in the globular domain of FtsZ and takes advantage of the positive K190 residue to disassemble FtsZ polymers.

A universal mechanism for FtsZ spatial regulators

The conserved C-terminal tail of FtsZ has been shown to be the binding site of MinC (Shen and Lutkenhaus, 2009). The unexpected finding that SlmA also binds to this tail indicates that the conserved C-terminal tail of FtsZ may be an important target for FtsZ spatial regulators. ZipA and FtsA also bind to the conserved C-terminal tail of FtsZ, but they promote Z ring formation by tethering FtsZ filaments to the membrane (Mosyak et al., 2000; Pichoff and Lutkenhaus, 2002; Szwedziak et al., 2012). MinC and SlmA bind to the conserved C-terminal tail of FtsZ, but they prevent Z ring formation in their vicinity. Binding to the tail of FtsZ on the one hand positions MinC and SlmA close to the FtsZ filaments so that they can attack FtsZ filaments, on the other hand reduces the conserved C-terminal tail of FtsZ binding to ZipA and FtsA. In an attempt to isolate FtsZ tail mutants resistant to SlmA, we isolated an FtsZ tail mutant (FtsZ-I374F) that only supports cell growth when the Min system or SlmA has been deleted. I374F retains normal interaction with MinC and SlmA, but only supports cell division in the absence of the Min system or SlmA but not when both are present. Although additional tests are necessary to prove I374F interacts with ZipA or FtsA less well, the phenotypes of I374F suggest that competition for the conserved C-terminal tail of FtsZ between the proteins that promote Z ring formation and proteins that prevent Z ring formation may be important for Z ring formation regulation.

Both MinC and SlmA have been proposed to sever FtsZ filaments, but they likely do it in different mechanisms (Cho et al., 2011; Shen and Lutkenhaus, 2010). Genetic studies suggest that the N terminal domain of MinC binds to the interfaces of two FtsZ subunits to disrupt FtsZ polymerization (Shen and Lutkenhaus, 2010), while our results suggest that SlmA disassembles FtsZ polymers by affecting the communication between the two sub-domains of FtsZ. Consistent with this, FtsZ mutants resistant to the N terminal domain of MinC have no resistance to SlmA and FtsZ mutants resistant to

SlmA confer no resistance to MinC. In addition, MinC has no impact on FtsZ GTPase activity, but SlmA stimulates the GTPase activity of FtsZ. Despite these differences, the remarkable similarity of these two FtsZ inhibitors suggests that competition for the conserved C-terminal tail of FtsZ and inhibition of FtsZ polymerization may be a universal mechanism for FtsZ spatial regulators.

References

Addinall, S.G., Bi, E., and Lutkenhaus, J. (1996). FtsZ ring formation in fts mutants. Journal of bacteriology *178*, 3877-3884.

Addinall, S.G., Cao, C., and Lutkenhaus, J. (1997). FtsN, a late recruit to the septum in Escherichia coli. Molecular microbiology *25*, 303-309.

Anderson, D.E., Gueiros-Filho, F.J., and Erickson, H.P. (2004). Assembly dynamics of FtsZ rings in Bacillus subtilis and Escherichia coli and effects of FtsZ-regulating proteins. Journal of bacteriology *186*, 5775-5781.

Begg, K.J., Dewar, S.J., and Donachie, W.D. (1995). A new Escherichia coli cell division gene, ftsK. Journal of bacteriology *177*, 6211-6222.

Begg, K.J., and Donachie, W.D. (1985). Cell shape and division in Escherichia coli: experiments with shape and division mutants. Journal of bacteriology *163*, 615-622.

Bernhardt, T.G., and de Boer, P.A. (2005). SlmA, a nucleoid-associated, FtsZ binding protein required for blocking septal ring assembly over Chromosomes in E. coli. Molecular cell *18*, 555-564.

Bi, E., and Lutkenhaus, J. (1990a). Analysis of ftsZ mutations that confer resistance to the cell division inhibitor SulA (SfiA). Journal of bacteriology *172*, 5602-5609.

Bi, E., and Lutkenhaus, J. (1990b). FtsZ regulates frequency of cell division in Escherichia coli. Journal of bacteriology *172*, 2765-2768.

Bi, E., and Lutkenhaus, J. (1990c). Interaction between the min locus and ftsZ. Journal of bacteriology *172*, 5610-5616.

Bi, E., and Lutkenhaus, J. (1993). Cell division inhibitors SulA and MinCD prevent formation of the FtsZ ring. Journal of bacteriology *175*, 1118-1125.

Bi, E.F., and Lutkenhaus, J. (1991). FtsZ ring structure associated with division in Escherichia coli. Nature *354*, 161-164.

Bigot, S., Saleh, O.A., Lesterlin, C., Pages, C., El Karoui, M., Dennis, C., Grigoriev, M., Allemand, J.F., Barre, F.X., and Cornet, F. (2005). KOPS: DNA motifs that control E. coli chromosome segregation by orienting the FtsK translocase. The EMBO journal *24*, 3770-3780.

Bowman, G.R., Comolli, L.R., Zhu, J., Eckart, M., Koenig, M., Downing, K.H., Moerner, W.E., Earnest, T., and Shapiro, L. (2008). A polymeric protein anchors the chromosomal origin/ParB complex at a bacterial cell pole. Cell *134*, 945-955.

Bramkamp, M., Emmins, R., Weston, L., Donovan, C., Daniel, R.A., and Errington, J. (2008). A novel component of the division-site selection system of Bacillus subtilis and a new mode of action for the division inhibitor MinCD. Molecular microbiology *70*, 1556-1569.

Buddelmeijer, N., Aarsman, M.E., Kolk, A.H., Vicente, M., and Nanninga, N. (1998). Localization of cell division protein FtsQ by immunofluorescence microscopy in dividing and nondividing cells of Escherichia coli. Journal of bacteriology *180*, 6107-6116.

Buddelmeijer, N., and Beckwith, J. (2004). A complex of the Escherichia coli cell division proteins FtsL, FtsB and FtsQ forms independently of its localization to the septal region. Molecular microbiology *52*, 1315-1327.

Busiek, K.K., Eraso, J.M., Wang, Y., and Margolin, W. (2012). The early divisome protein FtsA interacts directly through its 1c subdomain with the cytoplasmic domain of the late divisome protein FtsN. Journal of bacteriology *194*, 1989-2000.

Buske, P.J., and Levin, P.A. (2013). A flexible C-terminal linker is required for proper FtsZ assembly in vitro and cytokinetic ring formation in vivo. Molecular microbiology *89*, 249-263.

Buss, J., Coltharp, C., Huang, T., Pohlmeyer, C., Wang, S.C., Hatem, C., and Xiao, J. (2013). In vivo organization of the FtsZ-ring by ZapA and ZapB revealed by quantitative super-resolution microscopy. Molecular microbiology *89*, 1099-1120.

Camberg, J.L., Hoskins, J.R., and Wickner, S. (2009). ClpXP protease degrades the cytoskeletal protein, FtsZ, and modulates FtsZ polymer dynamics. Proceedings of the National Academy of Sciences of the United States of America *106*, 10614-10619.

Chen, J.C., and Beckwith, J. (2001). FtsQ, FtsL and FtsI require FtsK, but not FtsN, for co-localization with FtsZ during Escherichia coli cell division. Molecular microbiology *42*, 395-413.

Chen, Y., and Erickson, H.P. (2005). Rapid in vitro assembly dynamics and subunit turnover of FtsZ demonstrated by fluorescence resonance energy transfer. The Journal of biological chemistry *280*, 22549-22554.

Chen, Y., and Erickson, H.P. (2009). FtsZ filament dynamics at steady state: subunit exchange with and without nucleotide hydrolysis. Biochemistry *48*, 6664-6673.

Chien, A.C., Zareh, S.K., Wang, Y.M., and Levin, P.A. (2012). Changes in the oligomerization potential of the division inhibitor UgtP co-ordinate Bacillus subtilis cell size with nutrient availability. Molecular microbiology *86*, 594-610.

Cho, H., and Bernhardt, T.G. (2013). Identification of the SlmA active site responsible for blocking bacterial cytokinetic ring assembly over the chromosome. PLoS genetics *9*, e1003304.

Cho, H., McManus, H.R., Dove, S.L., and Bernhardt, T.G. (2011). Nucleoid occlusion factor SlmA is a DNA-activated FtsZ polymerization antagonist. Proceedings of the National Academy of Sciences of the United States of America *108*, 3773-3778.

Corbin, B.D., Geissler, B., Sadasivam, M., and Margolin, W. (2004). Z-ring-independent interaction between a subdomain of FtsA and late septation proteins as revealed by a polar recruitment assay. Journal of bacteriology *186*, 7736-7744.

Dai, K., and Lutkenhaus, J. (1991). ftsZ is an essential cell division gene in Escherichia coli. Journal of bacteriology *173*, 3500-3506.

Dai, K., Mukherjee, A., Xu, Y., and Lutkenhaus, J. (1994). Mutations in ftsZ that confer resistance to SulA affect the interaction of FtsZ with GTP. Journal of bacteriology *176*, 130-136.

Dai, K., Xu, Y., and Lutkenhaus, J. (1993). Cloning and characterization of ftsN, an essential cell division gene in Escherichia coli isolated as a multicopy suppressor of ftsA12(Ts). Journal of bacteriology *175*, 3790-3797.

Dajkovic, A., Lan, G., Sun, S.X., Wirtz, D., and Lutkenhaus, J. (2008a). MinC spatially controls bacterial cytokinesis by antagonizing the scaffolding function of FtsZ. Current biology : CB *18*, 235-244.

Dajkovic, A., Mukherjee, A., and Lutkenhaus, J. (2008b). Investigation of regulation of FtsZ assembly by SulA and development of a model for FtsZ polymerization. Journal of bacteriology *190*, 2513-2526.

Datsenko, K.A., and Wanner, B.L. (2000). One-step inactivation of chromosomal genes in Escherichia coli K-12 using PCR products. Proceedings of the National Academy of Sciences of the United States of America *97*, 6640-6645.

de Boer, P.A. (2010). Advances in understanding E. coli cell fission. Current opinion in microbiology *13*, 730-737.

de Boer, P.A., Crossley, R.E., Hand, A.R., and Rothfield, L.I. (1991). The MinD protein is a membrane ATPase required for the correct placement of the Escherichia coli division site. The EMBO journal *10*, 4371-4380.

de Boer, P.A., Crossley, R.E., and Rothfield, L.I. (1989). A division inhibitor and a topological specificity factor coded for by the minicell locus determine proper placement of the division septum in E. coli. Cell *56*, 641-649.

de Boer, P.A., Crossley, R.E., and Rothfield, L.I. (1990). Central role for the Escherichia coli minC gene product in two different cell division-inhibition systems. Proceedings of the National Academy of Sciences of the United States of America *87*, 1129-1133.

Din, N., Quardokus, E.M., Sackett, M.J., and Brun, Y.V. (1998). Dominant C-terminal deletions of FtsZ that affect its ability to localize in Caulobacter and its interaction with FtsA. Molecular microbiology *27*, 1051-1063.

Durand-Heredia, J., Rivkin, E., Fan, G., Morales, J., and Janakiraman, A. (2012). Identification of ZapD as a cell division factor that promotes the assembly of FtsZ in Escherichia coli. Journal of bacteriology *194*, 3189-3198.

Durand-Heredia, J.M., Yu, H.H., De Carlo, S., Lesser, C.F., and Janakiraman, A. (2011). Identification and characterization of ZapC, a stabilizer of the FtsZ ring in Escherichia coli. Journal of bacteriology *193*, 1405-1413.

Elsen, N.L., Lu, J., Parthasarathy, G., Reid, J.C., Sharma, S., Soisson, S.M., and Lumb, K.J. (2012). Mechanism of action of the cell-division inhibitor PC190723: modulation of FtsZ assembly cooperativity. Journal of the American Chemical Society *134*, 12342-12345.

Erickson, H.P. (2007). Evolution of the cytoskeleton. BioEssays : news and reviews in molecular, cellular and developmental biology *29*, 668-677.

Erickson, H.P., Anderson, D.E., and Osawa, M. (2010). FtsZ in bacterial cytokinesis: cytoskeleton and force generator all in one. Microbiology and molecular biology reviews : MMBR *74*, 504-528.

Erickson, H.P., Taylor, D.W., Taylor, K.A., and Bramhill, D. (1996). Bacterial cell division protein FtsZ assembles into protofilament sheets and minirings, structural homologs of tubulin polymers. Proceedings of the National Academy of Sciences of the United States of America *93*, 519-523.

Eswaramoorthy, P., Erb, M.L., Gregory, J.A., Silverman, J., Pogliano, K., Pogliano, J., and Ramamurthi, K.S. (2011). Cellular architecture mediates DivIVA ultrastructure and regulates min activity in Bacillus subtilis. mBio *2*.

Fenton, A.K., and Gerdes, K. (2013). Direct interaction of FtsZ and MreB is required for septum synthesis and cell division in Escherichia coli. The EMBO journal *32*, 1953-1965.

Fleming, T.C., Shin, J.Y., Lee, S.H., Becker, E., Huang, K.C., Bustamante, C., and Pogliano, K. (2010). Dynamic SpoIIIE assembly mediates septal membrane fission during Bacillus subtilis sporulation. Genes & development *24*, 1160-1172.

Fu, G., Huang, T., Buss, J., Coltharp, C., Hensel, Z., and Xiao, J. (2010). In vivo structure of the E. coli FtsZ-ring revealed by photoactivated localization microscopy (PALM). PloS one *5*, e12682.

Fu, X., Shih, Y.L., Zhang, Y., and Rothfield, L.I. (2001). The MinE ring required for proper placement of the division site is a mobile structure that changes its cellular location during the Escherichia coli division cycle. Proceedings of the National Academy of Sciences of the United States of America *98*, 980-985.

Gardner, K.A., Moore, D.A., and Erickson, H.P. (2013). The C-terminal linker of Escherichia coli FtsZ functions as an intrinsically disordered peptide. Molecular microbiology *89*, 264-275.

Geissler, B., Elraheb, D., and Margolin, W. (2003). A gain-of-function mutation in ftsA bypasses the requirement for the essential cell division gene zipA in Escherichia coli. Proceedings of the National Academy of Sciences of the United States of America *100*, 4197-4202.

Geissler, B., and Margolin, W. (2005). Evidence for functional overlap among multiple bacterial cell division proteins: compensating for the loss of FtsK. Molecular microbiology *58*, 596-612.

Geissler, B., Shiomi, D., and Margolin, W. (2007). The ftsA* gain-of-function allele of Escherichia coli and its effects on the stability and dynamics of the Z ring. Microbiology *153*, 814-825.

Gerding, M.A., Liu, B., Bendezu, F.O., Hale, C.A., Bernhardt, T.G., and de Boer, P.A. (2009). Self-enhanced accumulation of FtsN at Division Sites and Roles for Other Proteins with a SPOR domain (DamX, DedD, and RlpA) in Escherichia coli cell constriction. Journal of bacteriology *191*, 7383-7401.

Gerding, M.A., Ogata, Y., Pecora, N.D., Niki, H., and de Boer, P.A. (2007). The trans-envelope Tol-Pal complex is part of the cell division machinery and required for proper outer-membrane invagination during cell constriction in E. coli. Molecular microbiology *63*, 1008-1025.

Goehring, N.W., Gueiros-Filho, F., and Beckwith, J. (2005). Premature targeting of a cell division protein to midcell allows dissection of divisome assembly in Escherichia coli. Genes & development *19*, 127-137.

Gregory, J.A., Becker, E.C., and Pogliano, K. (2008). Bacillus subtilis MinC destabilizes FtsZ-rings at new cell poles and contributes to the timing of cell division. Genes & development *22*, 3475-3488.

Gueiros-Filho, F.J., and Losick, R. (2002). A widely conserved bacterial cell division protein that promotes assembly of the tubulin-like protein FtsZ. Genes & development *16*, 2544-2556.

Hale, C.A., and de Boer, P.A. (1997). Direct binding of FtsZ to ZipA, an essential component of the septal ring structure that mediates cell division in E. coli. Cell *88*, 175-185.

Hale, C.A., and de Boer, P.A. (2002). ZipA is required for recruitment of FtsK, FtsQ, FtsL, and FtsN to the septal ring in Escherichia coli. Journal of bacteriology *184*, 2552-2556.

Hale, C.A., Meinhardt, H., and de Boer, P.A. (2001). Dynamic localization cycle of the cell division regulator MinE in Escherichia coli. The EMBO journal *20*, 1563-1572.

Hale, C.A., Shiomi, D., Liu, B., Bernhardt, T.G., Margolin, W., Niki, H., and de Boer, P.A. (2011). Identification of Escherichia coli ZapC (YcbW) as a component of the division apparatus that binds and bundles FtsZ polymers. Journal of bacteriology *193*, 1393-1404.

Haney, S.A., Glasfeld, E., Hale, C., Keeney, D., He, Z., and de Boer, P. (2001). Genetic analysis of the Escherichia coli FtsZ.ZipA interaction in the yeast two-hybrid system. Characterization of FtsZ residues essential for the interactions with ZipA and with FtsA. The Journal of biological chemistry *276*, 11980-11987.

Haydon, D.J., Stokes, N.R., Ure, R., Galbraith, G., Bennett, J.M., Brown, D.R., Baker, P.J., Barynin, V.V., Rice, D.W., Sedelnikova, S.E.*, et al.* (2008). An inhibitor of FtsZ with potent and selective anti-staphylococcal activity. Science *321*, 1673-1675.

Hill, N.S., Buske, P.J., Shi, Y., and Levin, P.A. (2013). A moonlighting enzyme links Escherichia coli cell size with central metabolism. PLoS genetics *9*, e1003663.

Hill, N.S., Kadoya, R., Chattoraj, D.K., and Levin, P.A. (2012). Cell size and the initiation of DNA replication in bacteria. PLoS genetics *8*, e1002549.

Hirota, Y., Ryter, A., and Jacob, F. (1968). Thermosensitive mutants of E. coli affected in the processes of DNA synthesis and cellular division. Cold Spring Harbor symposia on quantitative biology *33*, 677-693.

Hu, Z., and Lutkenhaus, J. (1999). Topological regulation of cell division in Escherichia coli involves rapid pole to pole oscillation of the division inhibitor MinC under the control of MinD and MinE. Molecular microbiology *34*, 82-90.

Hu, Z., and Lutkenhaus, J. (2000). Analysis of MinC reveals two independent domains involved in interaction with MinD and FtsZ. Journal of bacteriology *182*, 3965-3971.

Hu, Z., and Lutkenhaus, J. (2001). Topological regulation of cell division in E. coli. spatiotemporal oscillation of MinD requires stimulation of its ATPase by MinE and phospholipid. Molecular cell *7*, 1337-1343.

Hu, Z., Mukherjee, A., Pichoff, S., and Lutkenhaus, J. (1999). The MinC component of the division site selection system in Escherichia coli interacts with FtsZ to prevent polymerization. Proceedings of the National Academy of Sciences of the United States of America *96*, 14819-14824.

Huecas, S., Llorca, O., Boskovic, J., Martin-Benito, J., Valpuesta, J.M., and Andreu, J.M. (2008). Energetics and geometry of FtsZ polymers: nucleated self-assembly of single protofilaments. Biophysical journal *94*, 1796-1806.

Huisman, O., and D'Ari, R. (1981). An inducible DNA replication-cell division coupling mechanism in E. coli. Nature *290*, 797-799.

Ingerman, E., and Nunnari, J. (2005). A continuous, regenerative coupled GTPase assay for dynamin-related proteins. Methods in enzymology *404*, 611-619.

Inoue, I., Ino, R., and Nishimura, A. (2009). New model for assembly dynamics of bacterial tubulin in relation to the stages of DNA replication. Genes to cells : devoted to molecular & cellular mechanisms *14*, 435-444.

Johnson, J.E., Lackner, L.L., and de Boer, P.A. (2002). Targeting of (D)MinC/MinD and (D)MinC/DicB complexes to septal rings in Escherichia coli suggests a multistep mechanism for MinC-mediated destruction of nascent FtsZ rings. Journal of bacteriology *184*, 2951-2962.

Karimova, G., Dautin, N., and Ladant, D. (2005). Interaction network among Escherichia coli membrane proteins involved in cell division as revealed by bacterial two-hybrid analysis. Journal of bacteriology *187*, 2233-2243.

Karimova, G., Pidoux, J., Ullmann, A., and Ladant, D. (1998). A bacterial two-hybrid system based on a reconstituted signal transduction pathway. Proceedings of the National Academy of Sciences of the United States of America *95*, 5752-5756.

Kiekebusch, D., Michie, K.A., Essen, L.O., Lowe, J., and Thanbichler, M. (2012). Localized dimerization and nucleoid binding drive gradient formation by the bacterial cell division inhibitor MipZ. Molecular cell *46*, 245-259.

Krol, E., van Kessel, S.P., van Bezouwen, L.S., Kumar, N., Boekema, E.J., and Scheffers, D.J. (2012). Bacillus subtilis SepF binds to the C-terminus of FtsZ. PloS one *7*, e43293.

Levin, P.A., Kurtser, I.G., and Grossman, A.D. (1999). Identification and characterization of a negative regulator of FtsZ ring formation in Bacillus subtilis. Proceedings of the National Academy of Sciences of the United States of America *96*, 9642-9647.

Levin, P.A., and Losick, R. (1996). Transcription factor Spo0A switches the localization of the cell division protein FtsZ from a medial to a bipolar pattern in Bacillus subtilis. Genes & development *10*, 478-488.

Li, Y., Hsin, J., Zhao, L., Cheng, Y., Shang, W., Huang, K.C., Wang, H.W., and Ye, S. (2013). FtsZ protofilaments use a hinge-opening mechanism for constrictive force generation. Science *341*, 392-395.

Liu, Z., Mukherjee, A., and Lutkenhaus, J. (1999). Recruitment of ZipA to the division site by interaction with FtsZ. Molecular microbiology *31*, 1853-1861.

Loose, M., Fischer-Friedrich, E., Ries, J., Kruse, K., and Schwille, P. (2008). Spatial regulators for bacterial cell division self-organize into surface waves in vitro. Science *320*, 789-792.

Lowe, J., and Amos, L.A. (1998). Crystal structure of the bacterial cell-division protein FtsZ. Nature *391*, 203-206.

Lowe, J., and Amos, L.A. (1999). Tubulin-like protofilaments in Ca2+-induced FtsZ sheets. The EMBO journal *18*, 2364-2371.

Lu, C., Reedy, M., and Erickson, H.P. (2000). Straight and curved conformations of FtsZ are regulated by GTP hydrolysis. Journal of bacteriology *182*, 164-170.

Lu, C., Stricker, J., and Erickson, H.P. (2001). Site-specific mutations of FtsZ--effects on GTPase and in vitro assembly. BMC microbiology *1*, 7.

Lu, M., and Kleckner, N. (1994). Molecular cloning and characterization of the pgm gene encoding phosphoglucomutase of Escherichia coli. Journal of bacteriology *176*, 5847-5851.

Lutkenhaus, J. (2007). Assembly dynamics of the bacterial MinCDE system and spatial regulation of the Z ring. Annual review of biochemistry *76*, 539-562.

Lutkenhaus, J., Pichoff, S., and Du, S. (2012). Bacterial cytokinesis: From Z ring to divisome. Cytoskeleton *69*, 778-790.

Lutkenhaus, J., Sanjanwala, B., and Lowe, M. (1986). Overproduction of FtsZ suppresses sensitivity of lon mutants to division inhibition. Journal of bacteriology *166*, 756-762.

Lutkenhaus, J.F. (1983). Coupling of DNA replication and cell division: sulB is an allele of ftsZ. Journal of bacteriology *154*, 1339-1346.

Lutkenhaus, J.F., Wolf-Watz, H., and Donachie, W.D. (1980). Organization of genes in the ftsA-envA region of the Escherichia coli genetic map and identification of a new fts locus (ftsZ). Journal of bacteriology *142*, 615-620.

Ma, X., Ehrhardt, D.W., and Margolin, W. (1996). Colocalization of cell division proteins FtsZ and FtsA to cytoskeletal structures in living Escherichia coli cells by using green fluorescent protein.

Proceedings of the National Academy of Sciences of the United States of America *93*, 12998-13003.
Ma, X., and Margolin, W. (1999). Genetic and functional analyses of the conserved C-terminal core domain of Escherichia coli FtsZ. Journal of bacteriology *181*, 7531-7544.
Maguin, E., Lutkenhaus, J., and D'Ari, R. (1986). Reversibility of SOS-associated division inhibition in Escherichia coli. Journal of bacteriology *166*, 733-738.
Marston, A.L., Thomaides, H.B., Edwards, D.H., Sharpe, M.E., and Errington, J. (1998). Polar localization of the MinD protein of Bacillus subtilis and its role in selection of the mid-cell division site. Genes & development *12*, 3419-3430.
Matsui, T., Yamane, J., Mogi, N., Yamaguchi, H., Takemoto, H., Yao, M., and Tanaka, I. (2012). Structural reorganization of the bacterial cell-division protein FtsZ from Staphylococcus aureus. Acta crystallographica. Section D, Biological crystallography *68*, 1175-1188.
Michie, K.A., and Lowe, J. (2006). Dynamic filaments of the bacterial cytoskeleton. Annual review of biochemistry *75*, 467-492.
Milam, S.L., Osawa, M., and Erickson, H.P. (2012). Negative-stain electron microscopy of inside-out FtsZ rings reconstituted on artificial membrane tubules show ribbons of protofilaments. Biophysical journal *103*, 59-68.
Mingorance, J., Tadros, M., Vicente, M., Gonzalez, J.M., Rivas, G., and Velez, M. (2005). Visualization of single Escherichia coli FtsZ filament dynamics with atomic force microscopy. The Journal of biological chemistry *280*, 20909-20914.
Miraldi, E.R., Thomas, P.J., and Romberg, L. (2008). Allosteric models for cooperative polymerization of linear polymers. Biophysical journal *95*, 2470-2486.
Mohammadi, T., van Dam, V., Sijbrandi, R., Vernet, T., Zapun, A., Bouhss, A., Diepeveen-de Bruin, M., Nguyen-Disteche, M., de Kruijff, B., and Breukink, E. (2011). Identification of FtsW as a transporter of lipid-linked cell wall precursors across the membrane. The EMBO journal *30*, 1425-1432.
Mosyak, L., Zhang, Y., Glasfeld, E., Haney, S., Stahl, M., Seehra, J., and Somers, W.S. (2000). The bacterial cell-division protein ZipA and its interaction with an FtsZ fragment revealed by X-ray crystallography. The EMBO journal *19*, 3179-3191.
Mukherjee, A., and Lutkenhaus, J. (1994). Guanine nucleotide-dependent assembly of FtsZ into filaments. Journal of bacteriology *176*, 2754-2758.
Mukherjee, A., and Lutkenhaus, J. (1998a). Dynamic assembly of FtsZ regulated by GTP hydrolysis. The EMBO journal *17*, 462-469.
Mukherjee, A., and Lutkenhaus, J. (1998b). Purification, assembly, and localization of FtsZ. Methods in enzymology *298*, 296-305.
Mulder, E., and Woldringh, C.L. (1989). Actively replicating nucleoids influence positioning of division sites in Escherichia coli filaments forming cells lacking DNA. Journal of bacteriology *171*, 4303-4314.
Nogales, E., Downing, K.H., Amos, L.A., and Lowe, J. (1998a). Tubulin and FtsZ form a distinct family of GTPases. Nature structural biology *5*, 451-458.
Nogales, E., Wolf, S.G., and Downing, K.H. (1998b). Structure of the alpha beta tubulin dimer by electron crystallography. Nature *391*, 199-203.
Oliva, M.A., Cordell, S.C., and Lowe, J. (2004). Structural insights into FtsZ protofilament formation. Nature structural & molecular biology *11*, 1243-1250.
Osawa, M., Anderson, D.E., and Erickson, H.P. (2008). Reconstitution of contractile FtsZ rings in liposomes. Science *320*, 792-794.
Osawa, M., and Erickson, H.P. (2005). Probing the domain structure of FtsZ by random truncation and insertion of GFP. Microbiology *151*, 4033-4043.

Osawa, M., and Erickson, H.P. (2013). Liposome division by a simple bacterial division machinery. Proceedings of the National Academy of Sciences of the United States of America *110*, 11000-11004.
Park, K.T., Wu, W., Battaile, K.P., Lovell, S., Holyoak, T., and Lutkenhaus, J. (2011). The Min oscillator uses MinD-dependent conformational changes in MinE to spatially regulate cytokinesis. Cell *146*, 396-407.
Patrick, J.E., and Kearns, D.B. (2008). MinJ (YvjD) is a topological determinant of cell division in Bacillus subtilis. Molecular microbiology *70*, 1166-1179.
Peters, N.T., Dinh, T., and Bernhardt, T.G. (2011). A fail-safe mechanism in the septal ring assembly pathway generated by the sequential recruitment of cell separation amidases and their activators. Journal of bacteriology *193*, 4973-4983.
Pichoff, S., and Lutkenhaus, J. (2001). Escherichia coli division inhibitor MinCD blocks septation by preventing Z-ring formation. Journal of bacteriology *183*, 6630-6635.
Pichoff, S., and Lutkenhaus, J. (2002). Unique and overlapping roles for ZipA and FtsA in septal ring assembly in Escherichia coli. The EMBO journal *21*, 685-693.
Pichoff, S., and Lutkenhaus, J. (2005). Tethering the Z ring to the membrane through a conserved membrane targeting sequence in FtsA. Molecular microbiology *55*, 1722-1734.
Pichoff, S., Shen, B., Sullivan, B., and Lutkenhaus, J. (2012). FtsA mutants impaired for self-interaction bypass ZipA suggesting a model in which FtsA's self-interaction competes with its ability to recruit downstream division proteins. Molecular microbiology *83*, 151-167.
Quardokus, E., Din, N., and Brun, Y.V. (1996). Cell cycle regulation and cell type-specific localization of the FtsZ division initiation protein in Caulobacter. Proceedings of the National Academy of Sciences of the United States of America *93*, 6314-6319.
Quardokus, E.M., Din, N., and Brun, Y.V. (2001). Cell cycle and positional constraints on FtsZ localization and the initiation of cell division in Caulobacter crescentus. Molecular microbiology *39*, 949-959.
Raskin, D.M., and de Boer, P.A. (1999a). MinDE-dependent pole-to-pole oscillation of division inhibitor MinC in Escherichia coli. Journal of bacteriology *181*, 6419-6424.
Raskin, D.M., and de Boer, P.A. (1999b). Rapid pole-to-pole oscillation of a protein required for directing division to the middle of Escherichia coli. Proceedings of the National Academy of Sciences of the United States of America *96*, 4971-4976.
Reddy, M. (2007). Role of FtsEX in cell division of Escherichia coli: viability of ftsEX mutants is dependent on functional SufI or high osmotic strength. Journal of bacteriology *189*, 98-108.
Schmidt, K.L., Peterson, N.D., Kustusch, R.J., Wissel, M.C., Graham, B., Phillips, G.J., and Weiss, D.S. (2004). A predicted ABC transporter, FtsEX, is needed for cell division in Escherichia coli. Journal of bacteriology *186*, 785-793.
Schumacher, M.A., Miller, M.C., Grkovic, S., Brown, M.H., Skurray, R.A., and Brennan, R.G. (2002). Structural basis for cooperative DNA binding by two dimers of the multidrug-binding protein QacR. The EMBO journal *21*, 1210-1218.
Schweizer, J., Loose, M., Bonny, M., Kruse, K., Monch, I., and Schwille, P. (2012). Geometry sensing by self-organized protein patterns. Proceedings of the National Academy of Sciences of the United States of America *109*, 15283-15288.
Shen, B., and Lutkenhaus, J. (2009). The conserved C-terminal tail of FtsZ is required for the septal localization and division inhibitory activity of MinC(C)/MinD. Molecular microbiology *72*, 410-424.
Shen, B., and Lutkenhaus, J. (2010). Examination of the interaction between FtsZ and MinCN in E. coli suggests how MinC disrupts Z rings. Molecular microbiology *75*, 1285-1298.
Shin, J.Y., Vollmer, W., Lagos, R., and Monasterio, O. (2013). Glutamate 83 and arginine 85 of helix H3 bend are key residues for FtsZ polymerization, GTPase activity and cellular viability of

Escherichia coli: lateral mutations affect FtsZ polymerization and E. coli viability. BMC microbiology *13*, 26.
Shiomi, D., and Margolin, W. (2007). The C-terminal domain of MinC inhibits assembly of the Z ring in Escherichia coli. Journal of bacteriology *189*, 236-243.
Singh, J.K., Makde, R.D., Kumar, V., and Panda, D. (2007). A membrane protein, EzrA, regulates assembly dynamics of FtsZ by interacting with the C-terminal tail of FtsZ. Biochemistry *46*, 11013-11022.
Singh, J.K., Makde, R.D., Kumar, V., and Panda, D. (2008). SepF increases the assembly and bundling of FtsZ polymers and stabilizes FtsZ protofilaments by binding along its length. The Journal of biological chemistry *283*, 31116-31124.
Strauss, M.P., Liew, A.T., Turnbull, L., Whitchurch, C.B., Monahan, L.G., and Harry, E.J. (2012). 3D-SIM super resolution microscopy reveals a bead-like arrangement for FtsZ and the division machinery: implications for triggering cytokinesis. PLoS biology *10*, e1001389.
Stricker, J., and Erickson, H.P. (2003). In vivo characterization of Escherichia coli ftsZ mutants: effects on Z-ring structure and function. Journal of bacteriology *185*, 4796-4805.
Stricker, J., Maddox, P., Salmon, E.D., and Erickson, H.P. (2002). Rapid assembly dynamics of the Escherichia coli FtsZ-ring demonstrated by fluorescence recovery after photobleaching. Proceedings of the National Academy of Sciences of the United States of America *99*, 3171-3175.
Szwedziak, P., Wang, Q., Freund, S.M., and Lowe, J. (2012). FtsA forms actin-like protofilaments. The EMBO journal *31*, 2249-2260.
Taschner, P.E., Huls, P.G., Pas, E., and Woldringh, C.L. (1988). Division behavior and shape changes in isogenic ftsZ, ftsQ, ftsA, pbpB, and ftsE cell division mutants of Escherichia coli during temperature shift experiments. Journal of bacteriology *170*, 1533-1540.
Thanbichler, M., and Shapiro, L. (2006). MipZ, a spatial regulator coordinating chromosome segregation with cell division in Caulobacter. Cell *126*, 147-162.
Tonthat, N.K., Arold, S.T., Pickering, B.F., Van Dyke, M.W., Liang, S., Lu, Y., Beuria, T.K., Margolin, W., and Schumacher, M.A. (2011). Molecular mechanism by which the nucleoid occlusion factor, SlmA, keeps cytokinesis in check. The EMBO journal *30*, 154-164.
Tonthat, N.K., Milam, S.L., Chinnam, N., Whitfill, T., Margolin, W., and Schumacher, M.A. (2013). SlmA forms a higher-order structure on DNA that inhibits cytokinetic Z-ring formation over the nucleoid. Proceedings of the National Academy of Sciences of the United States of America *110*, 10586-10591.
Treuner-Lange, A., Aguiluz, K., van der Does, C., Gomez-Santos, N., Harms, A., Schumacher, D., Lenz, P., Hoppert, M., Kahnt, J., Munoz-Dorado, J.*, et al.* (2013). PomZ, a ParA-like protein, regulates Z-ring formation and cell division in Myxococcus xanthus. Molecular microbiology *87*, 235-253.
Uehara, T., and Bernhardt, T.G. (2011). More than just lysins: peptidoglycan hydrolases tailor the cell wall. Current opinion in microbiology *14*, 698-703.
Van De Putte, P., Van, D., and Roersch, A. (1964). The Selection of Mutants of Escherichia Coli with Impaired Cell Division at Elevated Temperature. Mutation research *106*, 121-128.
Wang, L., Khattar, M.K., Donachie, W.D., and Lutkenhaus, J. (1998). FtsI and FtsW are localized to the septum in Escherichia coli. Journal of bacteriology *180*, 2810-2816.
Wang, L., and Lutkenhaus, J. (1998). FtsK is an essential cell division protein that is localized to the septum and induced as part of the SOS response. Molecular microbiology *29*, 731-740.
Wang, X., Huang, J., Mukherjee, A., Cao, C., and Lutkenhaus, J. (1997). Analysis of the interaction of FtsZ with itself, GTP, and FtsA. Journal of bacteriology *179*, 5551-5559.
Wang, X., and Lutkenhaus, J. (1993). The FtsZ protein of Bacillus subtilis is localized at the division site and has GTPase activity that is dependent upon FtsZ concentration. Molecular microbiology *9*, 435-442.

Ward, J.E., Jr., and Lutkenhaus, J. (1985). Overproduction of FtsZ induces minicell formation in E. coli. Cell *42*, 941-949.
Weart, R.B., Lee, A.H., Chien, A.C., Haeusser, D.P., Hill, N.S., and Levin, P.A. (2007). A metabolic sensor governing cell size in bacteria. Cell *130*, 335-347.
Weart, R.B., and Levin, P.A. (2003). Growth rate-dependent regulation of medial FtsZ ring formation. Journal of bacteriology *185*, 2826-2834.
Willemse, J., Borst, J.W., de Waal, E., Bisseling, T., and van Wezel, G.P. (2011). Positive control of cell division: FtsZ is recruited by SsgB during sporulation of Streptomyces. Genes & development *25*, 89-99.
Woldringh, C.L., Mulder, E., Valkenburg, J.A., Wientjes, F.B., Zaritsky, A., and Nanninga, N. (1990). Role of the nucleoid in the toporegulation of division. Research in microbiology *141*, 39-49.
Wu, L.J., and Errington, J. (2004). Coordination of cell division and chromosome segregation by a nucleoid occlusion protein in Bacillus subtilis. Cell *117*, 915-925.
Wu, L.J., Ishikawa, S., Kawai, Y., Oshima, T., Ogasawara, N., and Errington, J. (2009). Noc protein binds to specific DNA sequences to coordinate cell division with chromosome segregation. The EMBO journal *28*, 1940-1952.
Yang, D.C., Peters, N.T., Parzych, K.R., Uehara, T., Markovski, M., and Bernhardt, T.G. (2011). An ATP-binding cassette transporter-like complex governs cell-wall hydrolysis at the bacterial cytokinetic ring. Proceedings of the National Academy of Sciences of the United States of America *108*, E1052-1060.
Yang, D.C., Tan, K., Joachimiak, A., and Bernhardt, T.G. (2012). A conformational switch controls cell wall-remodelling enzymes required for bacterial cell division. Molecular microbiology *85*, 768-781.
Yu, X.C., and Margolin, W. (1997). Ca2+-mediated GTP-dependent dynamic assembly of bacterial cell division protein FtsZ into asters and polymer networks in vitro. The EMBO journal *16*, 5455-5463.
Yu, X.C., and Margolin, W. (1999). FtsZ ring clusters in min and partition mutants: role of both the Min system and the nucleoid in regulating FtsZ ring localization. Molecular microbiology *32*, 315-326.
Zupan, J.R., Cameron, T.A., Anderson-Furgeson, J., and Zambryski, P.C. (2013). Dynamic FtsA and FtsZ localization and outer membrane alterations during polar growth and cell division in Agrobacterium tumefaciens. Proceedings of the National Academy of Sciences of the United States of America *110*, 9060-9065.